Wood Cell Wall Modification
With Hydrophobic Molecules

von
Mahmut Ali Ermeydan

Dissertation
zur Erlangung des akademischen Grades
„doctor rerum naturalium"
(Dr. rer. nat.)
in der Wissenschaftsdisziplin „Kolloid- und Polymerchemie"

eingereicht an der
Mathematisch-Naturwissenschaftlichen Fakultät
der Universität Potsdam

Potsdam, Mai 2014

Abstract

Wood is used for many applications because of its excellent mechanical properties, relative abundance and as it is a renewable resource. However, its wider utilization as an engineering material is limited because it swells and shrinks upon moisture changes and is susceptible to degradation by microorganisms and/or insects. Chemical modifications of wood have been shown to improve dimensional stability, water repellence and/or durability, thus increasing potential service-life of wood materials. However current treatments are limited because it is difficult to introduce and fix such modifications deep inside the tissue and cell wall. Within the scope of this thesis, novel chemical modification methods of wood cell walls were developed to improve both dimensional stability and water repellence of wood material. These methods were partly inspired by the heartwood formation in living trees, a process, that for some species results in an insertion of hydrophobic chemical substances into the cell walls of already dead wood cells,

In the first part of this thesis a chemistry to modify wood cell walls was used, which was inspired by the natural process of heartwood formation. Commercially available hydrophobic flavonoid molecules were effectively inserted in the cell walls of spruce, a softwood species with low natural durability, after a tosylation treatment to obtain "artificial heartwood". Flavonoid inserted cell walls show a reduced moisture absorption, resulting in better dimensional stability, water repellency and increased hardness. This approach was quite different compared to established modifications which mainly address hydroxyl groups of cell wall polymers with hydrophilic substances. In the second part of the work in-situ styrene polymerization inside the tosylated cell walls was studied. It is known that there is a weak adhesion between hydrophobic polymers and hydrophilic cell wall components. The hydrophobic styrene monomers were inserted into the tosylated wood cell walls for further polymerization to form polystyrene in the cell walls, which increased the dimensional stability of the bulk wood material and reduced water uptake of the cell walls considerably when compared to controls. In the third part of the work, grafting of another hydrophobic and also biodegradable polymer, poly(ε-caprolactone) in the wood cell walls by ring opening polymerization of ε-caprolactone was studied at mild temperatures. Results indicated that polycaprolactone attached into the cell walls, caused permanent swelling of the cell walls up to 5%. Dimensional stability of the bulk wood material increased 40% and water absorption reduced more than 35%. A fully biodegradable and hydrophobized wood material was

obtained with this method which reduces disposal problem of the modified wood materials and has improved properties to extend the material's service-life.

Starting from a bio-inspired approach which showed great promise as an alternative to standard cell wall modifications we showed the possibility of inserting hydrophobic molecules in the cell walls and supported this fact with in-situ styrene and ε-caprolactone polymerization into the cell walls. It was shown in this thesis that despite the extensive knowledge and long history of using wood as a material there is still room for novel chemical modifications which could have a high impact on improving wood properties.

Zusammenfassung

Der nachwachsende Rohstoff Holz wird aufgrund seiner guten mechanischen Eigenschaften und der leichten Verfügbarkeit für viele Anwendungszwecke genutzt. Quellen und Schrumpfen bei Feuchtigkeitsänderungen des hygroskopischen Werkstoffs Holz limitieren jedoch die Einsatzmöglichkeiten. Ein weiteres Problem stellt der mitunter leichte Abbau – u.a. bei feuchtem Holz - durch Mikroorganismen und/oder Insekten dar. Durch chemische Modifizierungen können die Dimensionsstabilität, die Hydrophobizität und die Dauerhaftigkeit verbessert und damit die potentielle Lebensdauer des Werkstoffes erhöht werden. Dabei ist die dauerhafte Modifikation der Zellwand nur äußerst schwer realisierbar. Inspiriert von der Kernholzbildung in lebenden Bäumen, ein zellwandverändernder Prozess, der Jahre nach der Holzbildung erfolgt, wurden im Rahmen dieser Arbeit neue Ansätze zur chemischen Modifizierung der Zellwände entwickelt, um die Dimensionsstabilität und Hydrophobizität zu erhöhen.

Der erste Teil der Arbeit ist stark vom Prozess der Kernholzbildung inspiriert, eine abgeleitete Chemie wurde verwendet, um die Zellwände von Fichte, einem Nadelholz von geringer natürlicher Dauerhaftigkeit, zu modifizieren. Kommerziell verfügbare hydrophobe Flavonoide wurden nach einem Tosylierungsschritt erfolgreich in die Zellwand eingebracht, um so „artifizielles Kernholz" zu erzeugen. Die modifizierten Holzproben zeigten eine verringerte Wasseraufnahme, die zu erhöhter Dimensionsstabilität und Härte führte. Dieser Ansatz unterscheidet sich grundlegend von bereits etablierten Modifikationen, die hauptsächlich hypdrophile Substanzen an die Hydroxylgruppen der Zellwand anlagern. Der zweite Teil der Arbeit beschäftigt sich mit der Polymerisation von Styren in tosylierten Zellwänden. Es ist bekannt, dass es nur eine schwache Adhäsion zwischen den hydrophoben Polymeren und den hydrophilen Zellwandkomponenten gibt. Die hydrophoben Styren-Monomere wurden in die tosylierte Zellwand eingebracht und zu Polystyren polymerisiert. Wie bei der Modifikation mit Flavonoiden konnte eine erhöhte Dimensionsstabilität und reduzierte Wasseraufnahme der Zellwände beobachtet werden. Im dritten Teil der Arbeit wurde das biologisch abbaubare, hydrophobe poly(ε-caprolacton) in der Zellwand aufpolymerisiert. Die Ergebnisse deuten darauf hin, dass Polycaprolacton in der Zellwand gebunden ist und zu einer permanenten Quellung führt (bis zu 5 %). Die Dimensionsstabilität nahm um 40 % zu und die Wasseraufnahmerate konnte um mehr als 35 % reduziert werden. Mit dieser Methode kann nicht nur dimensionsstabileres Holz realisiert werden, auch biologische Abbaubarkeit und damit eine einfache Entsorgung sind gewährleistest.

Table of Contents

Chapter 1. Introduction

Motivation and Objectives

As a raw material wood is attracting more and more attention in modern societies because it is a material which is entirely derived from a renewable resource[1] and might become highly sustainable with an efficient forestry.[2, 3] The environmental benefits (low energy consumption and low carbon impact) of using wood rather than man-made materials are attracting increasing public interest[4-8] and have been documented in numerous peer reviewed papers.[9-12] Wood has excellent properties such as a good strength to weight ratio, it is easy to process, it is environmentally safe, and has an aesthetic appearance, etc.[13] Wood products can be processed to different extents. Minimally processed logs are often used in construction of houses or bridges, as alternative, to steel, which is heavy and more expensive. Highly processed and engineered wood composites can be manufactured for furniture, flooring, decking, wood structural panels, boards, joints, etc.[5] However, certain disadvantages limit wood usage such as dimensional instability and low durability.[14, 15] Due to the structure and chemistry of the cell wall, wood adsorbs and desorbs humidity/water with changing environmental conditions.[16] This leads to dimensional changes and may cause crack formation.[17] Besides, a high moisture content provides the environment for degradation by microorganisms. A summary of advantages and disadvantages can be found in Table 1-1.

Table 1-1. Some of the advantages and disadvantages of wood.

Advantages	Disadvantages
low cost and low energy need for production	susceptible to bio-degradation (fungi, insects, etc.)
environmentally friendly and a renewable resource	large biological variability
low thermal conductivity and no electrical conductivity	low flame retardency
low thermal conductivity provides good mechanical performance during fires	thermal and electrical conductivity strongly dependent on the moisture content
most woods are non-toxic	modifications, preservatives, coatings etc. generally create difficulties to recycling of wood
transport and disposal of wood are very low costs among other engineering materials	tropical woods are generally expensive and some of them are toxic
has a very high specific strength	dimensionally unstable and its strength decreases in wet conditions
good fracture properties	time-dependent deformations such as creep and viscoelasticity occur

To eliminate or reduce humidity/water absorption of the cell wall and to obtain dimensional stability of the material various chemical modification treatments have been applied so far. [14, 15, 18-21] The term "chemical modification of wood" was first used by Tarkow et al. (1946) who worked on acetylation of wood. However, the chemical modification to reduce swelling and

shrinking of cell walls is very difficult to achieve. In contrast, Nature has its own solution to improve durability of trees by inserting mainly phenolic substances into the cell walls. This natural process is called heartwood formation which often leads to a different color of the inner part of a tree trunk.[22, 23] Years after sapwood formation, the cell walls of some tree species are modified.[24-27] During this process, some phenolic materials (extractives) are synthesized at the transition of sapwood to heartwood and are accumulated in the cell walls.[22] The durability of heartwood is strongly dependent on the tree species, e.g. many tropical hardwood trees are known for their highly durable heartwood such as mahogany(*Swietenia macrophylla*)[28], teak (*Tectona grandis*)[29] or jatoba (*Hymenaea courbaril*)[30].

However, in the long term, deforestation of tropical trees creates a depletion risk of rain forests which also increases prices of qualitative hardwood timber every year.[14, 31-33] Sustainability of tropical hardwood trees is essential for the life on earth in terms of oxygen production and variability of species.[34] Meanwhile a sustainable forestation of softwoods has been developed but the heartwood of many softwoods is less durable. Therefore with an environmental consciousness, obtaining dimensionally stable and durable wood timber by chemical modification of softwood is necessary.

This work is inspired by the heartwood formation and aims to develop routines for alternative modifications of spruce wood cell walls (Picea abies – a softwood species) to decrease water absorption and to increase dimensional stability of the wood material and then to test such chemical modifications using physical and advanced chemical characterization methods.

Wood structure, Chemical Composition and Reactivity

Wood structure
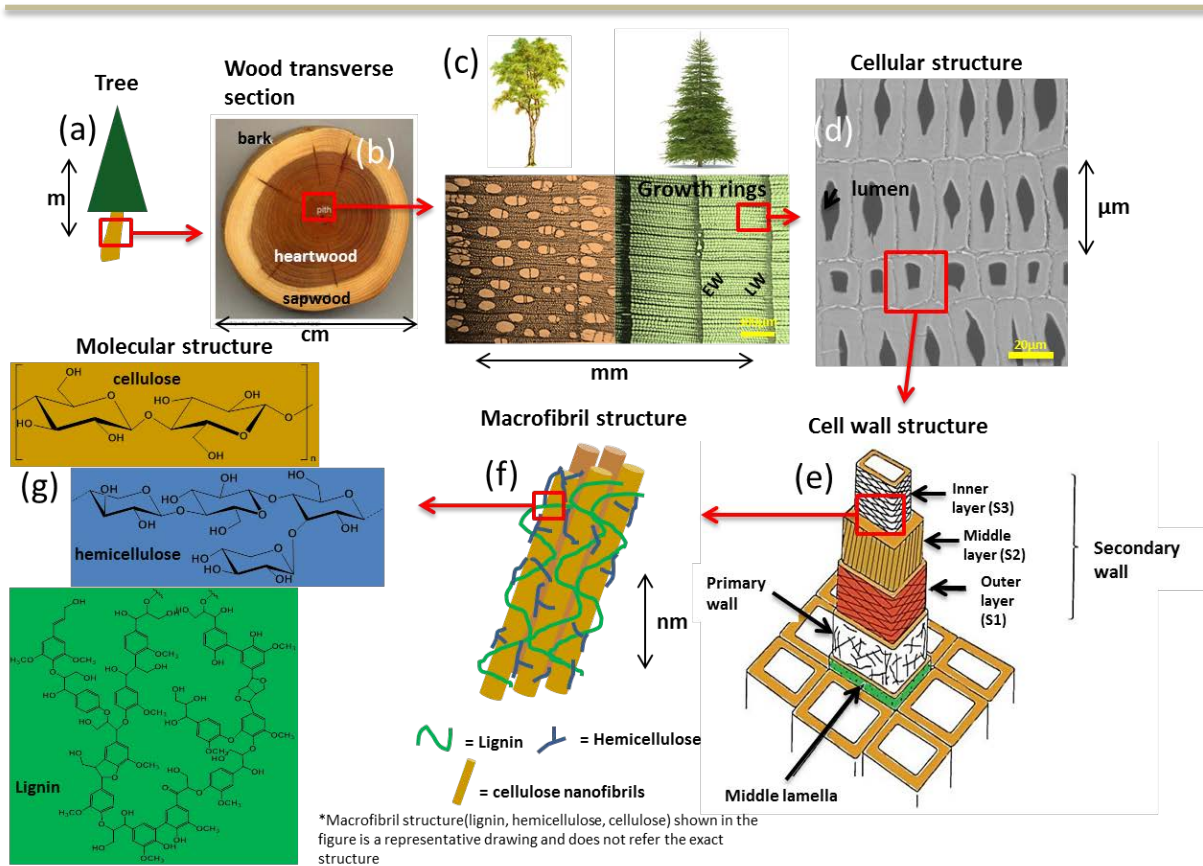
Figure 1-1. Cell wall polymers' structure in trees from tree to molecules. (a) A tree with an elongated stem with supporting branches (b) Transverse section of a softwood tree indicating heartwood, sapwood and bark (c) Left: Birch, a hardwood tree and light microscope image of its cellular structure with vessels. Right: Spruce (*Picea abies*) a softwood tree and light microscope image of the wood tissue indicating growth rings, earlywood and latewood cells (d) SEM image of several latewood cell walls of spruce wood in micron range (e) Structure of a single cell wall including primary and secondary cell wall layers (f) Microfibril structure of crystalline cellulose bundles surrounded with lignin and hemicellulose matrices (g) Molecular structures of cellulose, hemicellulose and lignin polymers.

Trees are perennial woody plants with an elongated main trunk, branches and roots.[16] The roots are subterranean structures for providing water and minerals from soil, providing biochemical storage and mechanical support to the trunk.[16] The trunk is the part of a tree that connects leaves to roots to carry and transport water and nutrients (**Figure 1-1a**). The trunk is the part where wood is obtained for utilization. **Figure 1-1b** shows the transverse section of a trunk**.**

The bark on the outside protects the tree from weather, fire, insects or mechanical injury.[35], followed by the phloem a thin layer of living cells for nutrient transport. Adjacent is the thin layer of vascular cambium, the living tissue which produces new phloem cells to the outside and xylem cells to the inside. Typically the xylem (wood) is the largest part of the trunk and

for some trees a distinction between sapwood and heartwood can be made (**Figure 1-1b**). Sapwood (the outer part) still contains some living cells while in heartwood even the parenchymatic tissue has died. Often heartwood is darker than sapwood. When we look closer to the cross-section of xylem annual growth rings consisting of earlywood (EW) and latewood (LW) can easily be seen as shown in **Figure 1-1c**. Latewood tissue of softwoods is denser than earlywood. This may not be the case in hardwoods. The cells of latewood which formed late in the growth season have very thick walls with small cell cavities (lumen) (**Figure 1-1d**), while those formed first in the season have thinner cell walls with large lumina. At this point, it is essential to mention the difference of hardwood and softwood trees (**Figure 1-1c**). The terms 'hardwood' and 'softwood' does not mean hardness or softness of wood. In fact, some softwood species are harder and heavier than hardwoods. For example, a well-known balsa tree is a hardwood and it is softer than any commercial softwood. The main differences between hardwoods, which belong to the angiosperms (flowering plants) and softwoods (gymnosperms) are related to the microstructure. The cells of the evolutionary younger hardwoods are more specialized. Softwood trees (e.g. pine (*Pinus*) or spruce (*Picea*) have generally evergreen needle-like leaves. [15, 16] Basic structural differences between hardwoods and softwoods are shown in **Figure 1-1c**.

As one can see in **Figure 1-1d** the cells are held together by the highly lignified middle lamella. The cell walls themselves (**Figure 1-1e**) consist of primary cell walls and secondary cells walls.[16] One of the building blocks of the wood cell wall is the cellulose microfibril. It consists of bundles of cellulose polymer chains in partly highly ordered crystalline lattices oriented with an angle to the longitudinal cell axis which is called microfibril angle (MFA).[36] Those partly crystalline cellulose fibrils are embedded in an amorphous lignin and hemicellulose matrix (**Figure 1-1f**).[16, 37, 38] The primary cell wall is the first layer to be formed after the cell division and is composed of less oriented microfibrils that allow expansion of the cell. [39, 40] The subsequently formed layer is the secondary cell wall having sub-layers exhibiting different patterns in the orientation of microfibrils with a helical winding pattern (S1, S2, S3) (**Figure 1-1e**).[41, 42] S1 is a thin layer with microfibril angles between 50-70 degrees.[16] The S2 layer has the largest volume of the wall with microfibril angles between ~5-45 degrees. Thus the S2 layer has the greatest influence on the wood properties (i.e. mechanical, stability). The S3 layer is very thin and has a microfibril angle similar to the S1 layer. Micro- or nano-pores are also present in cell walls which are accessible under certain conditions.[43] The cell wall polymers: cellulose, hemicellulose and lignin and their interrelations are described in the next section.

Chemical composition

Cellulose, hemicellulose and lignin are the three major polymeric materials that make up the heterogeneous structure of the cell walls. All the other wood components which are also known as non-structural cell wall components are called extractives.

Cellulose. Cellulose is a polymer of D-glucopyranose units. These monomeric units (anhydroglucose units, AGU) are alternately inverted in the plane of the ring. AGU are linked together by β(1→4) glycosidic bonds forming the linear polymer cellulose. The average degree of polymerization (DP) of cellulose in native wood is about 10.000.[16] The cellulose content of wood varies from about 40% to 50%.[16] Cellulose molecules form intra- and intermolecular hydrogen bonds which results in the formation of microfibrils which are reinforcing the cell wall structure. As the density of cellulose microfibrils increases, crystalline regions are formed. Wood derived cellulose generally contains about 65% crystalline regions.[16]

Hemicellulose. Hemicelluloses are heterogeneous polymers constructed with C5 and C6 sugars (such as xylose, arabinose, glucose, galactose, mannose, etc.) as shown in **Figure 1-1g** and besides cellulose, hemicellulose is one of the most abundant components of biomass.[44, 45] The chemical structure and the amount of hemicelluloses vary between species and type of the cells.[46] Hemicelluloses are thought to be the links between cellulose and lignin.[16, 38, 46, 47]

Lignin. Lignin is an amorphous phenolic polymer with intermediate molecular weight (see **Figure 1-1g**). It is responsible for providing additional stiffness to the cell wall and also functions to bond individual cells together in the middle lamella region. There is a wide variation of lignin structures within different wood species. The lignin content of hardwoods is usually in the range of 18-25%, whereas in softwoods its content varies between 25-35%. Lignin is associated by covalent bonding (ester and ether) with hemicelluloses forming lignin-carbohydrate complexes. There is no evidence that lignin is associated with cellulose but hydrogen bonds and even covalent bonds are established with hemicelluloses.[44]

Extractives. These small molecular weight organic materials (nonstructural wood components) can be extracted with neutral solvents. The amount of extractives varies between species up to 0,5-20%. Tropical woods can have relatively high amounts of extractives. Some extractives contribute to some wood characteristics such as color, durability, etc.[48] Aromatic (phenolic) compounds (e.g. flavonoids), terpenes, aliphatic acids, alcohols, inorganic substances are some examples to extractive materials.[16]

Reactivity of components

Because of the intermolecular hydrogen bonds cellulose forms a compact structure. For this reason reactants can hardly reach the crystalline regions of cellulose polymer, which decreases its reactivity. Hemicelluloses on the other hand contain side chains which hinder the formation of intermolecular hydrogen bonds and the stacking conformation. Therefore hemicelluloses are more reactive compared to cellulose. Although lignin is a randomly branched polymer, it has limited reactivity due to aromatic groups in its structure. The possibility to form intramolecular hydrogen bonds increases the stability even further.

Chemical modification of wood cell walls

State of the art

Chemical modification of wood includes various techniques to reduce water absorption of wood material, in order to increase durability and dimensional stability. These techniques can be classified via the method in which chemicals are introduced into the wood structure. [14, 15, 49, 50] There are several possibilities as shown in **Figure 1-2**. Establishing single covalent bonds with one – OH group or cross-linking between two or more -OH groups of cell wall polymers is one of those techniques (e.g. esterification, etherification or silylation).[14, 15, 51-56] Chemicals that have been used and covalently bonded to wood hydroxyl groups include anhydrides, acid chlorides, carboxylic acids, isocyanates, aldehydes, alkyl chlorides, lactones, nitriles, or epoxides. In those approaches highly active chemicals (e.g. anhydrides) can penetrate the cell walls and react with hydroxyl groups of the cell wall components (hemicellulose, lignin, cellulose)[57-60] and consequently wood products may have good dimensional stability.[14, 61] Shielding hydroxyl groups with those reagents provides an additional mass inside the cell wall (bulking) and creates a hydrophobic surface in the cell walls that increases water repellence.[14, 15, 62] In addition, the filling of micro- and nanopores in the cell walls prevents entrance of the water, thus hindering attack by micro-organisms.[14, 21]

 Another technique which has been used so far is generally called impregnation modification which is based on impregnation of various monomers into wood and further polymerization. These monomers can either enter the cell wall if they are hydrophilic (dimethyloldihydroxyethyleneurea (DMDHEU), furfuryl alcohol)[14, 15] or can only polymerize in the lumen area. Hydrophilic monomers can either homopolymerize inside the cell wall or can react and cross link through hydroxyl groups of the cell walls.[14, 15] In the case of lumen modifications hydrophobic monomers are used such as acrylic monomers or styrene (**Figure 1-2**, lumen modification). [20] Hydrophobicity of those monomers hinders their migration into

the cell wall meaning polymerization takes place only in the lumen. In this technique, water repellency of the final material improves with increasing polymer content. Such modifications, however still have little effect on dimensional stability of the wood material due to the absence of additional polymer in the cell walls.[15, 63] The last chemical modification technique is impregnation of hydrophilic polymers or molecules inside the cell wall (e.g. Polyethylene glycol (PEG)[64], and some flavonoids[65, 66]) which make a bulking effect inside the cell walls and improves some properties such as dimensional stability (**Figure 1-2**, cell wall bulking). However, wood should be sealed by coatings afterwards in those cases because inserted materials are still water soluble and can be removed by washing.
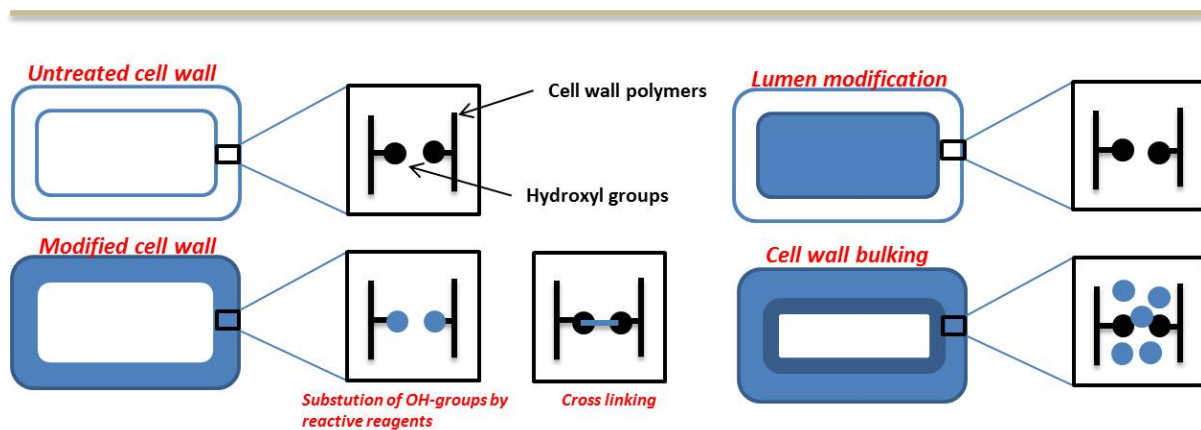
Figure 1-2. Cell and sub-cell level illustration of different chemical treatments for wood modification.

To make an efficient modification in terms of water repellence and dimensional stability, it is essential that the solvent or chemicals used for modification are able to swell wood to provide penetration of the reactive reagents into the cell walls.[15, 67] The substitution or polymerization reactions should take place under neutral or mild alkaline conditions at temperatures below 120°C.[15] Otherwise, the structure of the cell walls might be altered due to chemical deformations of cell wall polymers. The consequence of modifications applied at high temperature or high acidic/basic conditions are reduced mechanical properties. Another issue is to fix chemicals inside the cell walls so that they cannot be removed by water. This requires either a reaction with hydroxyl groups to establish stable chemical bonds or the filling of cell wall nanovoids with hydrophobic molecules.[14] Avoiding byproducts is a further demand for wood modification and the modified wood should still possess the aesthetic appearance of untreated wood.

Today, although some restrictions are applied based on environmental consciousness, in fact there are still wood preserving treatments in use by impregnating toxic chemicals (such as chromated copper arsenate (CCA), oils, ammonia or metal compounds) into the cell walls of the wood to improve durability of bulk wood material. Many of those substances are filling the voids but do not change the main chemistry of the wood. Inhospitable environments created by toxic chemicals repulse the unwanted organisms, such as fungi or insects. However, the toxicity of such products has environmental influence, both during the service-life of the wood and for its safe disposal. Additionally, those treatments don't have positive contributions to other critical properties of wood such as dimensional stability or water absorption.

By contrast, several chemical modification methods allow for producing both durable and dimensionally stable wood timber by using non-toxic chemicals and are highly recyclable. Those methods have already been industrialized in the last decade: Acetylation (e.g. Accoya), DMDHEU (e.g. Belmadur), and Furfurylation (e.g. Kebony) are on the market.[14] Melamine resin and silocone/silane treatments are also promising methods which may soon be used for mass production.[14]

Currently successful products on the market are produced at comparably low cost. The marketing of those products is based on their improved properties (dimensional stability, water repellency and durability) and environmental issues (safety, renewability, sustainability, etc.). Also, chemically modified materials can be disposed of as untreated wood or recycled as it is done with WPCs (DMDHEU treatment).[14] But the best strategy would be to develop a materials cascade. Cascading is the optimal use of all components of the materials, including multiple usages of chemical resources, before they are used to generate power at the end of their life cycles. An example is the use of lignocellulosics: Wood material used to produce fibreboard, can be followed by chemical use in the pulp and paper industry and finally the fibres can be burnt for energy. This is also essential for chemically modified wood because carbon and improved properties of cell walls can still be carried on to different products such as fiberboards. Thus, disposal problem and toxicity (of both wood and by-products) should be considered during the invention of chemical method for wood modifications. Furthermore, the chemicals during manufacturing should be "green" which means environmentally safe. In that context, "*Green*" modifications would be increasingly an important concept in the future for this bioresource derived material. On the other hand, with improving technology, targeted products could be produced for high-tech purposes such as electric conducting wood

materials[68], or organic-inorganic hybrid wood materials by nanomaterial insertion into or nanomaterial formation inside the wood or cell walls,[69-71] etc.

Chapter 2. Characterization methods

In this session a brief introduction will be given about some of the characterization methods which are specifically important and were used for the purpose of this thesis. Apart from the below mentioned analysis methods, Scanning Electron Microscopy (SEM), Attenuated Total Reflectance Fourier Transform Infrared Spectroscopy (ATR-FTIR), powder X-Ray Diffraction and Differential Scanning Calorimetry (DSC) were used.

Raman Imaging and Spectroscopy
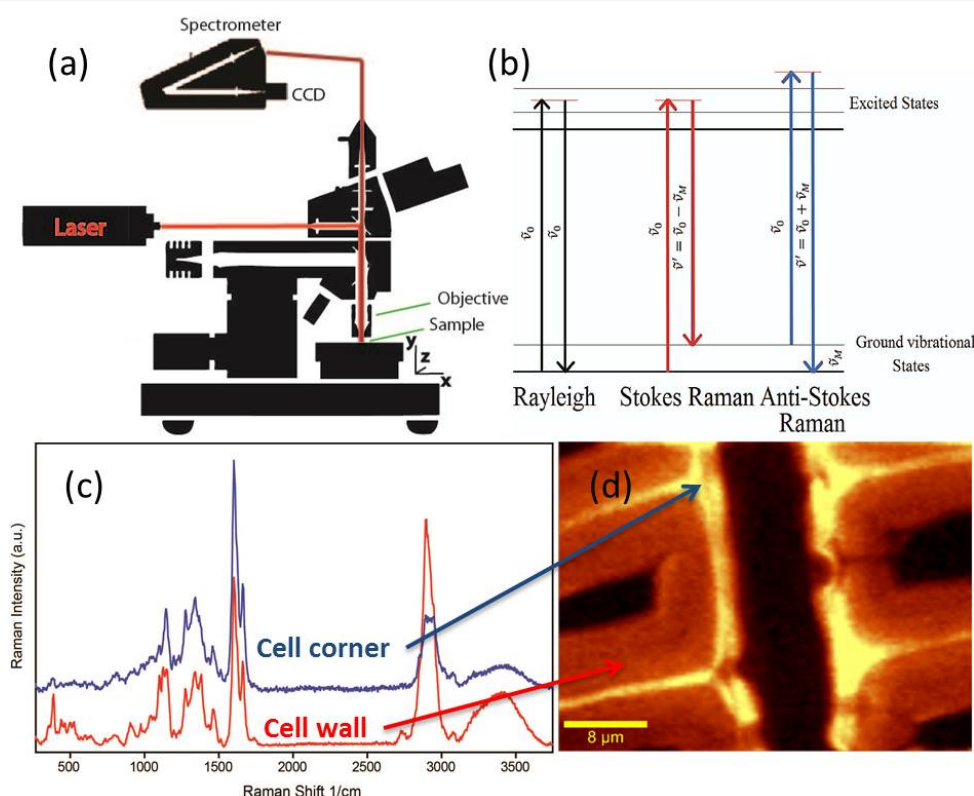
Figure 2-1. (a) Typical set up of a confocal Raman microscope (b) Diagrammatic representation of an energy transfer model of Rayleigh scattering, Stokes Raman and anti-Stokes Raman scattering (c) Typical Raman spectrum of wood cell wall and cell corner derived from image c. (c) Raman image of spruce cell walls integration from 250-3100 cm-1.

Raman spectroscopy measures basically the excitation of molecular vibrations. The Raman effect is based on an inelastic scattering of a photon from a laser light source with the molecule excited to a higher vibrational energy level.[72] When the light interacts with the molecule and distorts (polarizes) the electron cloud, a short-lived 'virtual state' is formed. The photons will be scattered with small frequency changes if electron cloud distortion is involved in scattering.[73] This elastic scattering process is the dominant process and called Rayleigh scattering. However, the light photons may lose or gain energy during the scattering process if

the energy is transferred from the incident photon to the molecule, it is called Stokes scattering or if the energy may be transferred from the molecule to the scattered photon which is called Anti-Stokes scattering(see **Figure 2-1b**).[74] The Raman-shift is the energy difference of the scattered photon and that of the incident photon which depends on the polarizability changes due to molecular vibrations. Additionally, water gives only weak Raman scattering which makes the Raman technique very suitable for in-situ studies of biological material.

Raman microscopy is the combination of a Raman spectrometer with a standard optical microscope, allowing high magnified visualization of a sample and Raman analysis with a microscopic laser spot. A typical confocal Raman microscope setup is shown in **Figure 2-1a**.[73] The excitation laser is focused via an optical fibre and a microscope objective onto the sample. The backscattered light is coupled out into a fibre, which acts as a pinhole. After passing the spectrometer the signal is detected by a CCD camera. For visual inspection of the sample usually a white light source and for picture capturing a camera is used. A piezo-driven XY- stage and a Z-stage is used scanning and mapping the sample.[73]

Raman microscopy is a chemical imaging technique that has been used for analysis of several materials including biomaterials.[75-80] These imaging techniques provide spatially resolved chemical information without destructing the material. In this thesis Raman imaging was used for detailed chemical characterization of the modified wood cell walls, because of its high spatial resolution (< 0.5 µm). Raman imaging is an established technique for generating detailed chemical images based on a set of Raman spectra (**Figure 2-1c**).[81, 82] A set of spectra is acquired at each pixel of the image, and then implemented to generate false color images based on material composition and structure (**Figure 2-1d**).[82, 83]

Nanoindentation

Nanoindentation is used for mechanical characterization of different materials at small length scales. It has also been used to study mechanical properties of wood cell walls for several years. [84-86] A probe tip, in this case a three-sided, pyramid-shaped Berkovich indenter, is pushed into the cell wall at a given speed until a defined maximum force is reached. Two materials parameters can be extracted from such experiments, the Hardness and (indentation) modulus. Hardness (H) is the measure of the resistance of a material to indentation because of a constant compression load from a sharp object with a known shape. The indentation modulus is related to the Young's modulus and gives information about the resistance of a material to elastic (recoverable) deformation under load.[87]
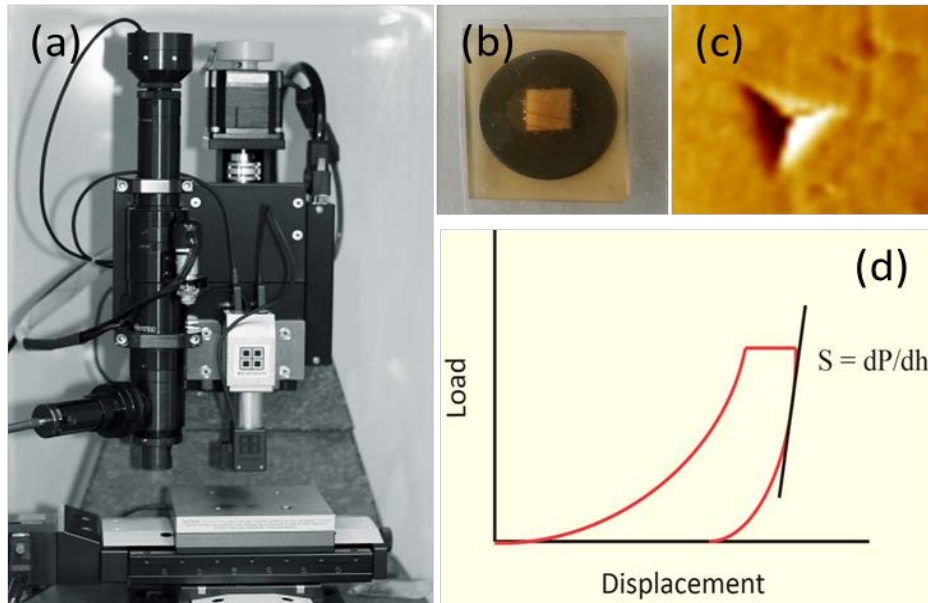
Figure 2-2. (a)Hystron nanoindeter (b) Wood sample for nanoindentation embedded in agar resin (c) Image of a nanoindented and deformed wood surface (d) Load-Displacement curve.

The load–displacement data from the nanoindentation tests were used to calculate hardness and elastic modulus. The hardness (H) of the samples for an indentation depth (h) can be calculated from the following equation: $H = \frac{P_{max}}{A}$, where P_{max} refers to the load measured at a maximum depth of penetration (h) in an indentation cycle, while *A* refers to the projected area of contact between the indenter and sample at P_{max}. The reduced indentation modulus (E_r) was determined from the following expression[84, 88]: $E_r = \frac{1}{2}\sqrt{\pi}\frac{S}{\sqrt{A}}$, where S (dP/dh) is the slope of the line in tangent to the initial unloading curve in the load–displacement plot (**Figure 2-2d**).

Equilibrium Moisture Content (EMC)

Moisture content of the wood depends on the relative humidity and temperature of the surrounding environment. The equilibrium moisture content (EMC) is the moisture content at which the wood is neither gaining nor losing moisture.

Moisture content (EMC) at equilibrium is calculated as follows: $EMC = \frac{(m - m_{od})}{m_{od}}$, where m is the mass of the wood (with moisture) and m_{od} is the oven-dry mass of wood (i.e. no moisture).

Anti-swelling Efficiency (ASE)

The ASE (anti-swelling efficiency) is the most known and straightforward method for evaluation of dimensional stability of modified wood. Dimensions of the wood blocks are

measured after water immersion and oven-drying cycle. First the swelling percentage of the wood is calculated: $(\%) = \frac{V_i - V_{ii}}{V_{ii}} \times 100$, where S(%): volumetric swelling; V_i: wood volume after wetting with liquid water; V_{ii}: wood volume of oven-dried sample before wetting.

$ASE(\%) = \frac{S_{um} - S_m}{S_{um}} \times 100$, where ASE(%): antishrinking/antiswelling efficiency resulting from the modification; S_m: modified volumetric swelling coefficient; S_{um}: unmodified volumetric swelling coefficient.

Author's Contribution to the Publications

The author performed all the experiments, physical and chemical analysis and wrote the first draft of manuscript.

The author performed all the experiments, physical and chemical analysis and wrote the first draft of manuscript.

Except for the contact angle measurements, the author performed all the experiments, physical and chemical analysis and wrote the first draft of manuscript.

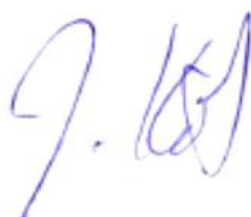# Chapter 3. Flavonoid Insertion into Cell Walls Improves Wood Properties

Mahmut A. Ermeydan[1], Etienne Cabane[2,3], Admir Masic[1], Joachim Koetz[4] and Ingo Burgert[1,2,3*]

[1]*Max Planck Institute of Colloids and Interfaces, Department of Biomaterials, Potsdam, Germany*

[2]*ETH Zurich, Institute for Building Materials, Zurich, Switzerland*

[3]*Empa - Swiss Federal Laboratories for Material Testing and Research, Applied Wood Research Laboratory, Dübendorf, Switzerland*

[4]*University of Potsdam, Institute of Chemistry, Potsdam, Germany*

*Corresponding author

Abstract

Wood has an excellent mechanical performance, but wider utilization of this renewable resource as an engineering material is limited by unfavorable properties such as low dimensional stability upon moisture changes and a low durability. However, some wood species are known to produce a wood of higher quality by inserting mainly phenolic substances in the already formed cell walls − a process so called heartwood formation. In the present study, we used the heartwood formation in black locust (Robinia pseudoacacia) as a source of bioinspiration and transferred principles of the modification in order to improve spruce wood properties (Picea abies) by a chemical treatment with commercially available flavonoids. We were able to effectively insert hydrophobic flavonoids in the cell wall after a tosylation treatment for activation. The chemical treatment reduced the water uptake of the wood cell walls and increased the dimensional stability of the bulk spruce wood. Further analysis of the chemical interaction of the flavonoid with the structural cell wall components revealed the basic principle of this bioinspired modification. Contrary to established modification treatments, which mainly address the hydroxyl groups of the carbohydrates with hydrophilic substances, the hydrophobic flavonoids are effective by a physical bulking in the cell wall most probably stabilized by $\pi-\pi$ interactions. A biomimetic transfer of the

underlying principle may lead to alternative cell wall modification procedures and improve the performance of wood as an engineering material.

Introduction

Wood is known for its excellent mechanical properties in view of a low density. However, wood also possesses some intrinsic features such as a low dimensional stability and durability that restrict its wider utilization in common applications.[1,2] The relevant structural unit which strongly determines the property profile of wood is the cell wall of the wood fibers. Wood cell walls are naturally fiber composites consisting of parallel aligned cellulose fibrils embedded in a matrix made of hemicelluloses and lignin.[3,4] Because of the hygroscopic nature of amorphous cellulose and hemicelluloses wood cell walls shrink or swell upon changes in relative humidity which can lead to substantial deformations of construction elements.[5] Application of unprotected wood in the presence of high moisture almost inevitably results in degradation of cell walls by fungi and in consequence in a low durability.

Accordingly, there is a long history of research activities aiming at producing durable and stable wood timber by cell wall modification. Several reactive chemicals have been used so far such as; anhydrides, carboxylic acids, acid chlorides, isocyanides, epoxides, aldehydes, silicon-containing compounds, etc.[1,2,6,7] These chemical applications are mainly targeting to establish a single covalent bond with the hydroxyl groups of cell wall polymers or cross-links between several hydroxyl groups. The reduced availability of hydroxyl groups increases wood repellency against water and therefore such modifying treatments usually reduce equilibrium moisture content and increase dimensional stability. Besides this mode of action, an alternative treatment is to bulk the cell wall, i.e., to fill microvoids within the cell wall by incorporating materials, which may interact with cell wall components via weak hydrogen bonding or other physical interactions.[1]

Interestingly some tree species invented a process to subsequently modify the cell walls of dead wood fibers after they have been in function in the wood body for a few years. This so-called heartwood formation is a natural process that is driven by a variety of metabolic alterations in parenchyma cells at the sapwood−heartwood transition zone which lead to an insertion of heartwood substances into the cell walls.[8−14] Characteristics of heartwood tissue are determined by greater content of various organic substances classified as extractives,[9,10] thereof a major group are phenolic compounds.[8] Flavonoids belong to this class of phenolic compounds and can considerably affect wood quality and characteristics, such as durability and color in the course of heartwood formation.[9−11,15] A central-European wood species with

a heartwood of high durability is black locust (Robinia pseudoacia) due to the insertion of flavonoids such as dihydrorobinetin, robinetin, etc.[15] Although the biochemical pathways that play a role during formation of flavonoids from storage materials such as starch have been investigated,[10−14] it is still not fully understood how flavonoids are deposited into the cell wall and how they interact with the cell wall components.[11]

In this study, we are using the heartwood formation in black locust as source of bioinspiration in order to improve the property profile of spruce wood (Picea abies), an extensively utilized wood species, which possesses a low dimensional stability and durability. By insertion of commercially available flavonoids into the cell walls we aimed at producing "artificial heartwood" with improved dimensional stability and at unraveling the basic principles of chemical and physical polymer interactions in order to derive general principles of bioinspired wood modification processes. A similar wood modification approach has been reported with different molecules such as simple or polycyclic phenolic compounds.[16−19] Using natural hydrophilic extractives (hematoxylin and catechin) Sakai and co-workers found that the dimensional stabilizing effect was hardly improved.[16]

Experimental Section

Para toluene sulfonyl chloride, dry pyridine, 3-hydroxy flavone (3-HF), organosolvent lignin, D-xylose, acetone (dried with 3-Å molecular sieves) were bought from Sigma-Aldrich and used as received. Cellulose fibers kindly provided by Borregaard company were used as received. Norway spruce wood samples (Picea abies) were cut parallel to grain direction and sawn into blocks of $1.0 \times 0.5 \times 0.5$ cm^3 (tangential x radial x longitudinal).

Tosylation Reaction of Spruce Cell Walls. The Norway spruce (Picea abies) sapwood blocks were dried at 60 °C for 1 day and kept under vacuum for 1 more day in a round-bottom flask. Samples were weighed (0,78 g, 4,33 mmol, calculated as a glucopyranose equivalent). 40 mL of dry pyridine was added to the samples in the flask for swelling for 1 day. The flask was stored in an ice bath with the reactants. p-Toluenesulfonyl chloride (0,82 g, 4,33 mmol) was added to the solution and reacted for 1 day at 5 °C.

Impregnation of 3-Hydroxyflavone in the Cell Wall. Tosylated spruce wood blocks were washed with dry pyridine for 3h to get rid of unreacted tosylates. 3-Hydroxyflavone (1,03 g, 4.33 mmol) dissolved in minimum amount of dry acetone (40 mL, dried over 3-Å molecular sieves) was added dropwise to the swollen and tosylated samples. Acetone was evaporated slowly by heating the flask to 45 °C to keep and precipitate the dissolved flavonoid molecules inside the cell wall. This temperature was used in order to avoid wood cell wall damage due

to too high temperatures. After evaporation of acetone, samples were washed in a flask with distilled water while stirring to get rid of pyridine and flavonoid molecules that had not been impregnated in the cell walls but precipitated in the lumen.

Tosylation of Cellulose Fibers. Previously dried cellulose fibers (60 °C, 24 h) (0.23 g, 3.64 mmol of active OH-groups) were dispersed in 20 mL of dry pyridine and 2.35 g of p-toluene sulfonyl chloride (12.33 mmol, 3 equiv.) was added. The reaction mixture was stirred overnight at 5 °C. The reaction was stopped by the addition of an acetone/H2O mixture (20 mL, 1:1), and the product was washed thoroughly with distilled water. Raman spectroscopy was used for characterization and band assignments of tosylated fibers (**Figure 3-4A**).

Tosylation of Lignin. Organosolvent lignin (0,5 g, 2,78 mmol − calculated as a coniferyl alcohol equivalent) was dispersed in 40 mL of dry pyridine and 1.06 g p-toluene sulfonic acid chloride (5,56 mmol, 2 equiv) was added. The reaction mixture was stirred overnight at 5 °C, stopped with 40 mL and washed with distilled water. ATR FT-IR spectroscopy was used for characterization and band assignments of tosylated lignin (**Figure 3-4B**).

Tosylation of D-Xylopyranoside. D-Xylose was methylated anomericly and tosylated as reported elsewhere.[20] Methyl β-Dxylopyranoside was prepared by refluxing D-xylose in anhydrous methanol, in the presence of acidic ion-exchange resin. The pure β-anomer was obtained by recrystallization in ethanol. Tosylation of the secondary hydroxyl groups in pyridine at 5 °C give the tritosylate. Raman spectrometry was used for characterization (**Figure 3-4C**).

Reaction of 3-HF and Individual Tosylated Cell Wall Polymers. Tosylated cellulose fibers, organosolvent lignin and D-xylopyranoside were reacted with 3-HF (1:1 ratio) in dry acetone at 45°C in separate flasks. Isolated reaction products were characterized by Raman and ATR FTIR spectroscopies (**Figure 3-4A-C**).

Raman Spectroscopy and Imaging. For sample preparation (reference, tosylated, and modified spruce wood blocks), 40 μm thick slices were cut on a rotary microtome (LEICA RM2255, Germany) and kept between microscope slide and coverslip with a drop of water to maintain cell walls in wet condition. The modified spruce cell wall assembly was analyzed using confocal Raman microscopy. Spectra were acquired with a confocal Raman microscope (alpha300, WITec GmbH, Ulm, Germany) equipped with an objective (60X, NA = 0.8, 0.17 mm coverslip correction from Nikon Instruments, Amstelveen, The Netherlands). A 532 nm laser with k = 532 nm (Crysta Laser, Reno, NV, USA) was focused with a diffraction limited spot size of 0.61 λ/NA and the Raman light detected with an air cooled backilluminated CCD (DV401-BV, Andor, Belfast, North Ireland) behind a spectrograph (UHTS 300, WITec) with

a spectral resolution of 1 cm^{-1}. For mapping, an integration time of 0.2 s was chosen and every pixel corresponded to one scan and a spectrum (scan) acquired every 0.5 μm. Two-dimensional chemical images were measured by WitecProject software using the "basis analysis function". The algorithm of basis function fits each spectrum of the multispectral data set with a linear combination of the basis single spectra (four reference spectra; cellulose fibers, lignin, 3-hydroxyflavone, tosyl chloride) using the least-squares method. To solve the problem of variations in fluorescence background in various parts of the sample, the first derivative of both multispectral data set and basis single spectra was calculated and the distribution of various components (cellulose fibers, lignin, flavonoids, tosylated components) obtained from Raman spectral features were plotted.

Attenuated Total Reflection Fourier-Transform Infrared Spectroscopy (ATR FT-IR). To record attenuated total reflection (ATR) FT-IR spectra a FT-IR microscope (Hyperion 2000, Bruker Optics, Germany) equipped with a liquid nitrogen cooled MCT detector and connected to a Vertex 70 FT-IR spectrometer (Bruker GmbH, Germany) was used. The IR beam was focused to the sample surface through an ATR objective (Bruker Optics, Germany) characterized by the Ge internal reflection element with tip of 100 μm.

Thermal Analysis. Differential scanning calorimetry (DSC) was carried out on 10 mg samples using a Setaram TG/DSC Sensys Evo thermobalance equipment in the range 20−600 °C, with the temperature being increased at a rate of 5 °C/min.

XRD Analysis. The powder XRD patterns of all samples were measured in reflection mode (CuKα radiation) on a Bruker D8 diffractometer equipped with a scintillation counter.

Equilibrium Moisture Content (EMC). The modified and reference samples were equilibrated in a sealed system with a relative humidity (∼80%) obtained with saturated solution of NaCl at room temperature. For the reference and each treatment 5 samples were measured. Weight equilibrium of the samples was recorded by weighing samples until constant weight. Afterward samples were ovendried at 103 ± 2 °C and reweighed to determine final moisture content.

Cell Wall Shrinkage. Microtomed slices with a 40 μm thickness were observed under a Leica fluorescence microscope and photographed at wet (swollen) and dried (at room temperature for 1 day) conditions. Mean shrinkage of tangential cell walls was calculated by measuring radial dimensions of the same 40 cell walls (see **Figure 3-S2** in the Supporting Information).

Nanoindentation. The mechanical characterization of tracheid cell walls was carried out on a Dimension DI-3100 atomic force microscope (Digital Instruments, Veeco Metrology Group, Santa Barbara, CA) equipped with a Hysitron add-on force transducer for nanoindentation (Surface, Hueckelhoven, Germany). For this purpose, samples were dried overnight in an oven at 60 °C and subsequently immersed in AGAR resin (AGAR low viscosity resin kit, AGAR Scientific Ltd., Stansted, UK) to enable the resin to penetrate the wood samples. The impregnated specimens were glued onto metal discs (15 mm AFM specimen discs). Specimens impregnated with the embedding resin cured overnight in an oven at 60 °C. Then the samples surface was smoothed by polishing. Quasi-static indentation tests were performed in a force-controlled mode, the indenter tip (Berkovich-type triangular pyramid, radius of curvature ~150 nm) was loaded to a peak force of 250 µN at a loading rate of 100 µN/s, held at constant load for 15 s, and unloaded at a rate of 100 µN/s.[21] Middle regions of secondary cell walls of reference, activated (tosylated), and modified samples were chosen for nanoindentation (see **Figure 3-S3** in the Supporting Information). A minimum of 20 indents were made on a group of cell walls.

Results and Discussion

Flavonoid Loading of Spruce Cell Walls

Small spruce wood samples were first activated by tosylation and then impregnated by 3-hydroxyflavone (3-HF) (see methods part). To gain detailed understanding of possible changes in the chemical structure after modification of spruce wood blocks, we applied confocal Raman imaging[22] on cross-sections of cell walls. Images A and B in **Figure 3-1** highlight the distribution of cellulose and lignin in the cell wall and further show that the chemical treatments did not result in cell wall degradation. Apart from the fiber-to-fiber interfaces, a homogeneous distribution of cellulose can be found (**Figure 3-1A**). In **Figure 3-1B**, cell corners (CC) and compound middle lamella (CML) are visible in brighter red color representing highly lignified regions.[23] The distribution of 3-hydroxyflavone impregnated into the cell walls is shown in the **Figure 3-1C**. Clearly this process takes place from the lumen side of the cells because the inner cell wall region shows the major 3-hydroxyflavone loading. Careful analysis of Raman spectra indicates no reaction or impregnation in CC and CML regions. Interestingly impregnated flavonoid molecules were found exactly in the same region
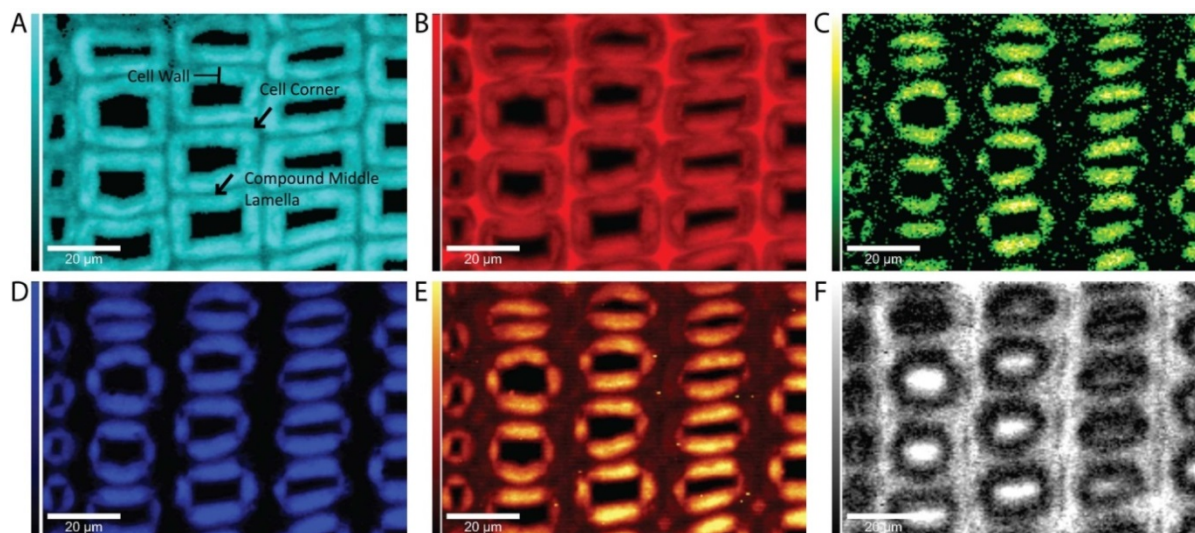
Figure 3-1. Confocal Raman microscopic images (100 × 70 μm2) of of latewood cell wall tissue. (A–D) Plotted by fitting multispectral Raman data set with reference spectra of (A) cellulose fibers, (B) lignin, (C) flavonoid, and (D) tosyl chloride. (E) Basis analysis error indicating parts of the sample where the set of reference spectra was unsuccessful to fit original data set. (F) Water distribution (calculated by integrating from 3135 to 3735 cm^{-1} which is specific for hydroxyl stretching mode).

of tosylated tissue (**Figure 3-1D**). **Figure 3-1E** shows the error from the basis analysis of the fitting procedure. Normally the basis analysis error should be almost constant for all analyzed regions. However, in this case, remarkable errors can be found in the impregnated regions suggesting spectral shifts due to chemical bonding and interactions in treated samples in comparison to reference spectra. **Figure 3-1F** shows a water distribution image which was extracted by integrating the hydroxyl stretching band (from 3135 to 3735 cm^{-1}). The darker region in the image is the modified region which coincides with the modified regions in **Figure 3-1C**. The image displays intensity difference in hydroxyl stretching band between modified and unmodified regions in the same cell wall. Comparison of average spectra proved that the intensity of the water band decreases in modified regions (see **Figure 3-S1** in the Supporting Information).

Improved Wood Performance

To quantify changes in the wood property profile due to the insertion of flavonoids, we conducted a variety of tests on the bulk material (**Figure 3-2**). The equilibrium moisture content (EMC) at 20 °C/80% relative humidity of flavonoid impregnated samples was around 11.7 ± 0.6% and of activated (tosylated) samples around 14.0 ± 0.2%, whereas the unmodified (reference) samples had an EMC of 16.9 ± 0.4%. Hence, the equilibrium moisture content of the modified spruce wood was only about 70% of the unmodified wood, whereas for simple activation (tosylation) it was about 83% of the reference (**Figure 3-2C**). The anisotropic shrinkage of wood cell walls is the result of the cell wall contraction with the removal of

water from the cell wall cavities. In our study we measured the tangential cell walls of the cross sections of wood fibers in unmodified, activated and modified cell walls before (wet) and after drying (dry) (see **Figure 3-S2** in the Supporting Information). In all cases, cell walls shrank by drying (**Figure 3-2D**). However, although shrinkage of the unmodified and activated cell walls was about 28 and 25% respectively, the shrinkage of the modified cell walls was found to be around 15%, which represents a significant improvement in dimensional stability (shrinkage values decreased of about 45% between untreated wood and modified wood).
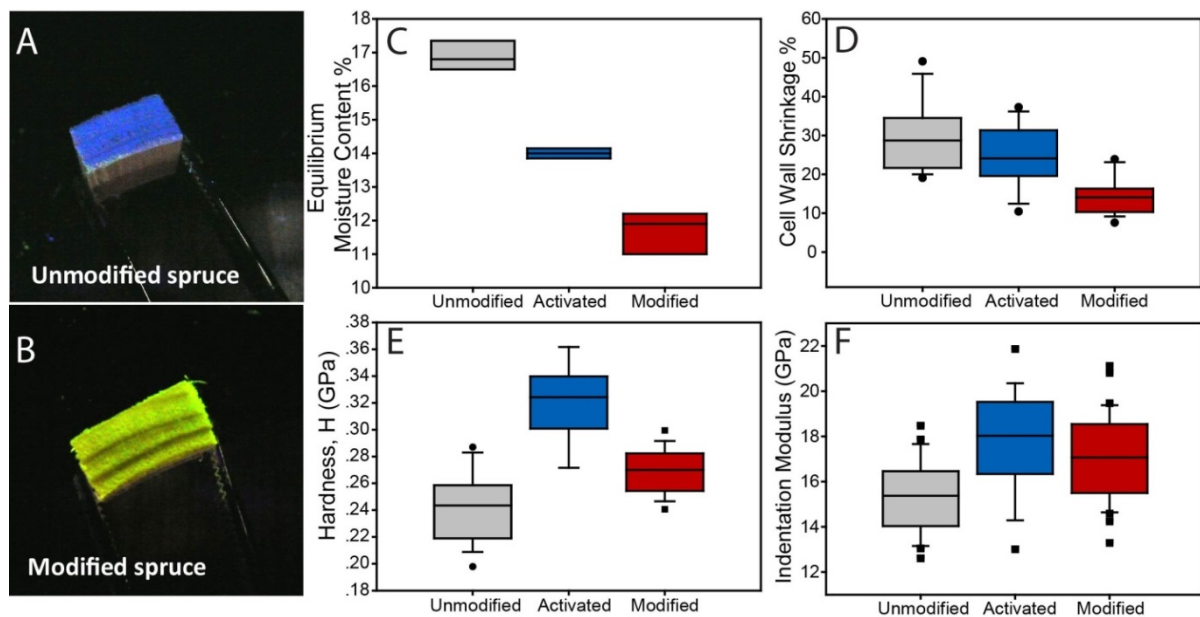
Figure 3-2. Physical properties of cell walls. (A, B) Unmodified and modified spruce blocks under 254 nm UV light. (C) EMC of unmodified, activated (tosylated), and modified samples. (D) Cell wall shrinkage of unmodified, activated (tosylated), and modified samples. (E , F) Hardness and indentation modulus of unmodified, activated (tosylated), and modified cell walls.

Hardness and indentation modulus of reference, activated and modified cell walls were determined by nanoindentation (**Figure 3-2E, F**). Both, hardness and indentation modulus showed a significant (P < 0.001, U-test) increase of about 10% from unmodified cell walls to flavonoid loaded cell walls, which indicates an improvement of mechanical properties due to flavonoid insertion. Interestingly, the tosylated (activated) samples show the highest hardness and indentation modulus.

The weight percentage gain (calculation based on the weight difference between untreated and modified wood samples) is a good indicator of an efficient impregnation (i.e., chemical bonding or interaction between the introduced chemical and wood cell wall polymers).[1] Activation by reaction of tosyl chloride with cell wall components increased weight of the

samples by 19%. Subsequent flavonol impregnation increased the total weight percentage gain (WPG) to 23%. The flavonoids alone are therefore accountable for a 4% weight increase (data not shown). This nonleachable weight gain was interpreted as the result of a stable interaction between cell wall polymers and flavonoids..

Polymer Interactions in the Cell Wall

Raman spectroscopy demonstrated the ability of 3-HF to interact both with aromatic groups from lignin and tosyl groups inserted into the cell wall. The necessity of the activation reaction with tosyl chloride becomes obvious when comparing the results obtained on activated cell wall, with the impregnation of 3-HF without activation (**Figure 3-3A−D**). Interestingly, although 3-HF enters the cell wall of nonactivated samples (i.e., reference wood) using scrupulously identical conditions, the flavonoids content loaded in the cell wall is lower, and the molecules are more easily washed away (with most solvents, including water, **Figure 3-3C, D**), failing to establish any durable interaction with the cell walls.
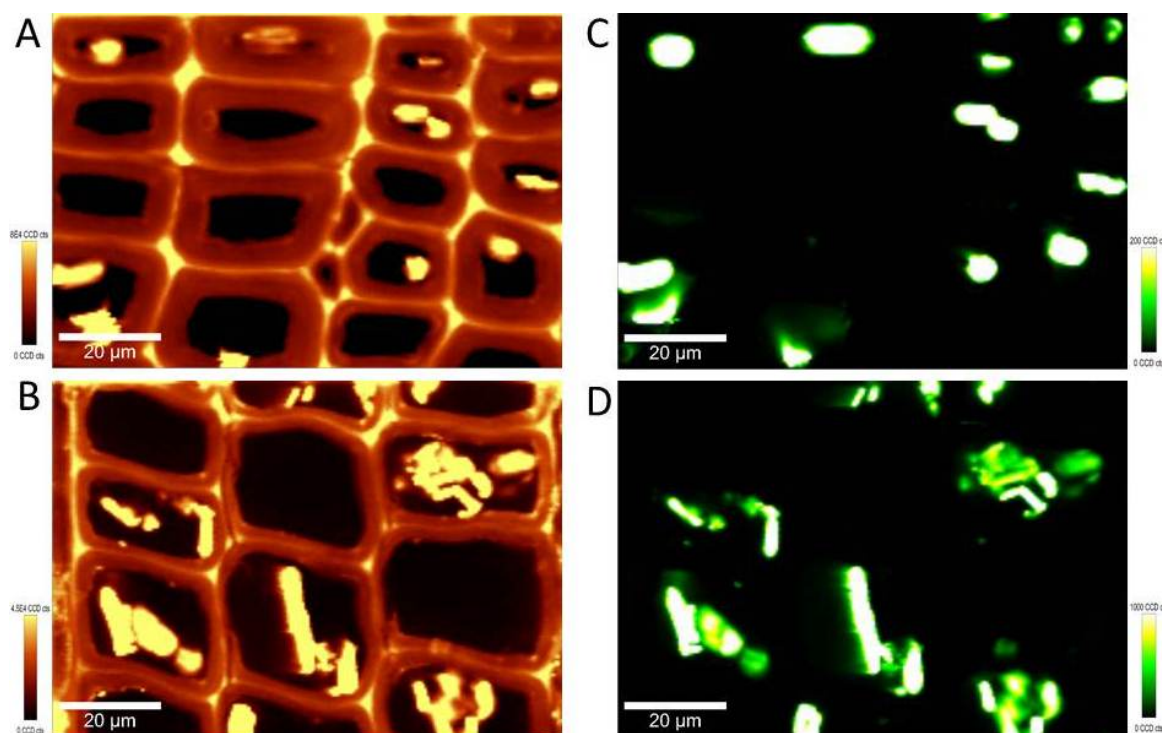
Figure 3-3. Confocal Raman microscopic images of impregnation of 3-hydroxy flavone in the cavities of nonactivated cell walls. (A, B) Raman images (100 × 70 μm^2) of latewood and earlywood cell wall regions that were calculated by integrating from 200 to 3600 cm^{-1}. (C, D) Raman images (100 × 70 μm^2) of flavonoid distribution after water leaching of cell walls that were calculated by integrating of flavonoid band between 665 and 685 cm^{-1} from the multispectral data set.

To derive the basic principle of the modification process it was essential to understand how flavonoids interact with wood cell wall polymers and affect wood properties. As shown by Raman imaging (**Figure 3-1C, F**), there is a clear colocalization of tosyl groups and 3-HF in the secondary cell wall (S2). Although these results may immediately suggest a covalent bonding of 3-HF to cell wall polymers via a nucleophilic substitution reaction with the tosyl group, the evidence of an ether linkage formation is not trivial.
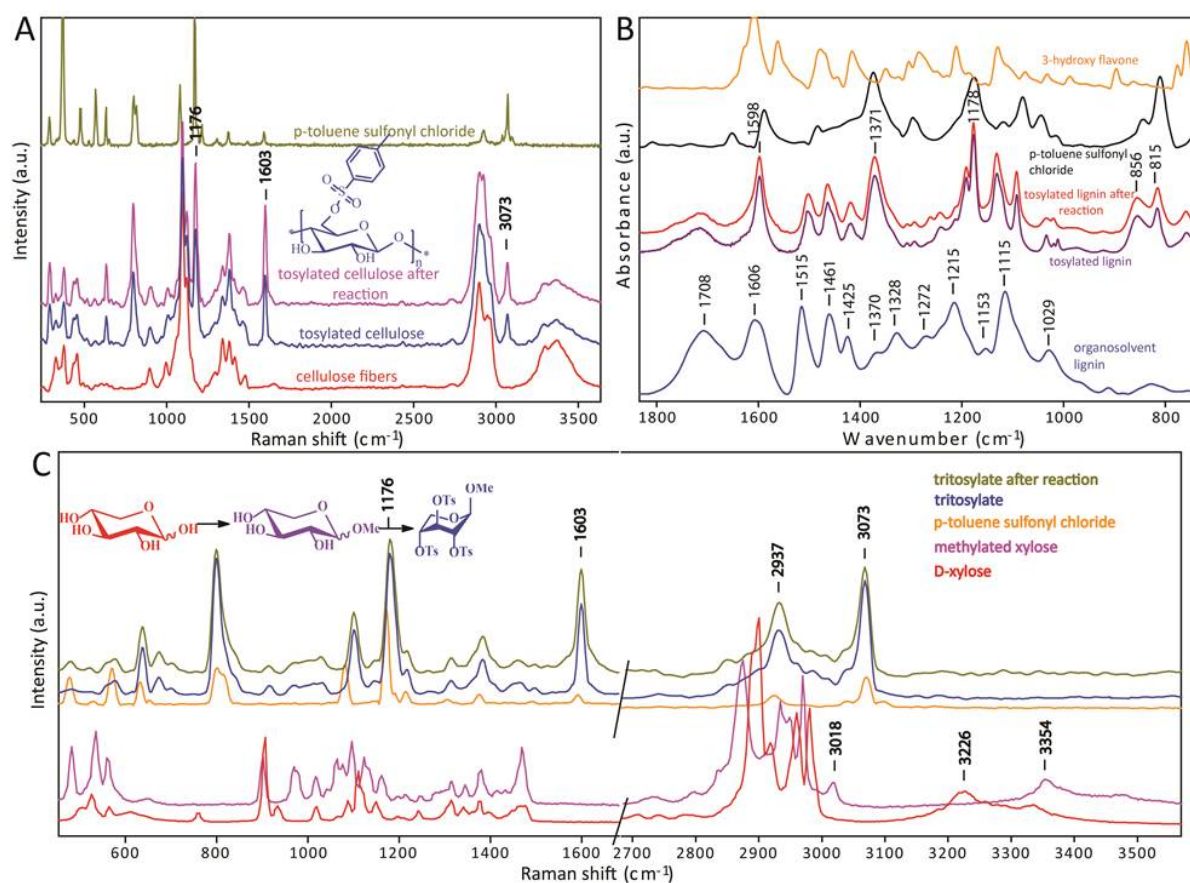
Figure 3-4. (A) Raman spectrum of cellulose fibers, tosylated cellulose fibers, tosylated cellulose fibers after 3-HF reaction and tosyl chloride. (B) ATR-FTIR spectrum of 3-hydroxy flavone, tosyl chloride, tosylated lignin after reaction, tosylated lignin, organosolv. lignin. (C) Raman spectrum of D-xylose, methylated xylose, tosyl chloride, tosylated methyl xylose, and tosylated methyl xylose after reaction.

Indeed, vibrational spectroscopy of lignocellulosic materials yields spectra characterized by many overlapping signals from the main cell wall constituents (lignin, cellulose, and hemicellulose). [24] Therefore, we checked whether 3-HF can form ether bonds with individual cell wall polymers activated by tosylation. After reactions, Raman and IR spectra of modified polymers (cellulose, organosolv. lignin, and xylose (hemicelluloses)) clearly show the absence of characteristic 3-HF peaks (**Figure 3-4**).

The Raman spectrum of tosylated cellulose shows asymmetric stretching of sulfonyl group (vas SO^2) at 1372 cm^{-1}, and symmetric stretching of sulfonyl group (vs SO_2) at 1176 cm^{-1} (**Figure 3-4A**).[25] The C−H stretching band of aromatic ring at 3073 cm^{-1} also belongs to tosyl group covalently bonded to the cellulose. Same bands can be observed in the Raman spectrum of tritosylated xylose with the fingerprints of xylose at 800−1500 cm^{-1} region (**Figure 3-4C**). Tosylated lignin which has additional IR bands from tosyl group can clearly identified at (v$_{as}$ SO_2) 1372 cm^{-1}, (v$_s$ SO^2) 1178 cm^{-1}, 856−815 cm^{-1} C−H$_{arom}$ symmetric and asymmetric bending (**Figure 3-4B**).[26]
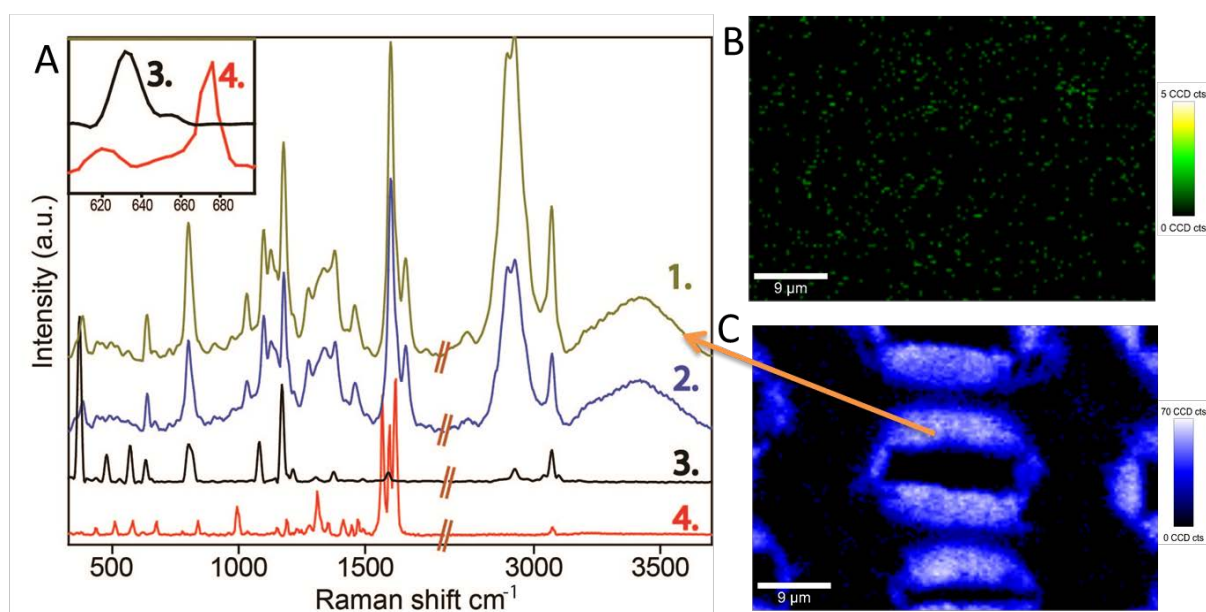
Figure 3-5. Raman spectroscopy and imaging measurements after acetone leaching. (A) Spectral band from 300 to 3600 cm^{-1} of acetone leached flavonoid inserted (modified) cell walls (1); tosylated cell walls (2); tosyl chloride (3); and 3-hydroxy flavone (4). (B) Raman image (50 × 35 μm^2) of 3-HF distribution in secondary cell walls after acetone leaching (calculated by integration of flavonoid band, 665−685 cm^{-1}). (C) Raman image (50 × 35 μm2) of tosyl group distribution in secondary cell walls after acetone leaching (calculated by integration of tosyl band, 795−810 cm^{-1}).

Further, leaching tests performed on modified cell walls showed that 3-HF is easily washed out of the cell wall region (See **Figure 3-5**) using aprotic solvents (which are good solvents for 3-HF, such as acetone or acetonitrile), whereas it is hardly removed when using highly polar protic solvents such as methanol or water as shown in **Figure 3-1C**. This can be seen in **Figure 3-5A** where spectrum 1 belongs to acetone leached cell walls, whereas spectrum 2 represents the tosylated cell walls. In spectrum 1 Raman bands of tosyl groups can be found without any intensity decrease (compare to tosyl chloride (spectrum 3)), but no Raman band being characteristic for 3-HF can be found in the spectrum (compare to 3-hydroxy flavone (spectrum 4)). Raman spectra shown in this figure confirm that leached wood has a similar

Raman signature when compared to activated wood. These results confirm that tosylation is unaffected by leaching, and that 3-HF is not covalently attached to wood (it is easily washed out of wood using acetone as solvent). This finding is also supported by Raman images B and C in **Figure 3-5**.

These results indicate the absence of covalent bonds between the cell wall polymers and 3-HF which could be a consequence of the mild reaction conditions which were chosen to avoid cell wall polymer destruction and cell wall deformation. This suggests that flavonoids most likely interact with aromatic groups present in the cell wall, i.e. lignin or tosyl groups linked to cell wall polymers. Hence the concomitant presence of flavonoid molecules and tosyl groups in the S2 region (**Figure 3-1C, D**) has to be based on other types of interactions. Previous studies on the crystal structure of 3-HF demonstrated the presence of intramolecular H-bonding between the hydroxyl group and the ketone, and intermolecular interactions including stacking of conjugated aromatic rings, and H-bonding in between neighboring stacks.[27,28] Given the ability of 3-HF to enter the cell wall, and to form intra- and intermolecular associations via weak hydrogen bonding and π-stacking, the occurrence of such interactions with lignin polymers and tosylated cell wall polymers in the treated spruce samples is highly probable.
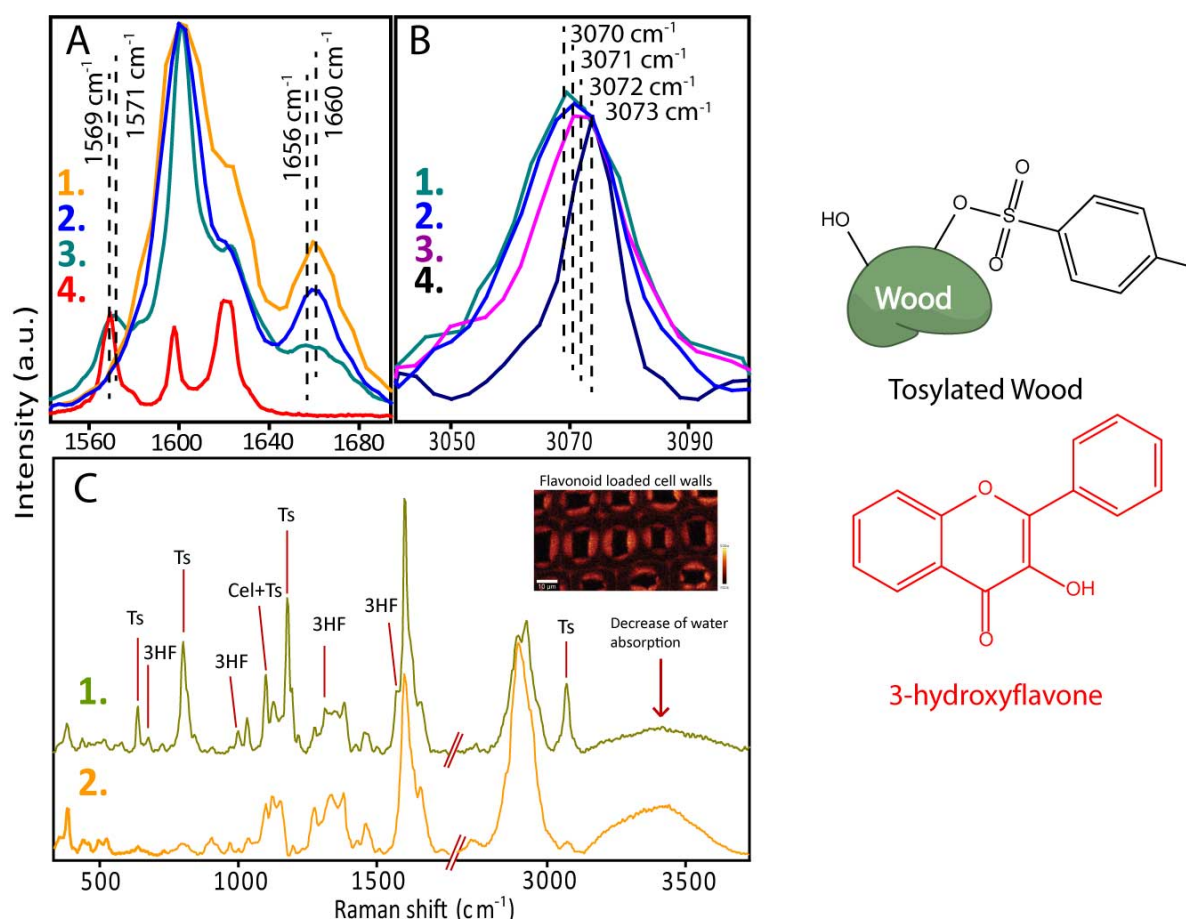
Figure 3-6. Chemical characterization of cell walls with Raman spectroscopy. (A) Spectral band from 1500 to 1730 cm^{-1} (aromatic region) of (1) untreated cell walls, (2) activated (tosylated) cell walls, (3) modified cell walls, (4) 3-hydroxy flavone. (B) Spectral band from 3000 to 3100 cm^{-1} (aromatic C−H stretching of tosyl group[26]) of (1) modified region of cell walls, (2) tosylated cell walls, (3) tosylated cellulose fibers, (4) tosyl chloride. (C) Raman spectrum of (1) modified region, (2) untreated cell walls. Schematic drawings on the right sight of the spectra show binding of the tosyl chloride to the cell wall hydroxyl groups and structural drawing of 3-hydroxyflavone.

Evidence of π-stacking can be found in Raman spectra frequency shifts of the aromatic systems which were observed in the modified cell wall (**Figure 3-6A**). The Raman spectra provide information on aromatic vibration bands of 3-HF, and lignin (spectral region from 1500 to 1700 cm^{-1}, **Figure 3-6A**). Indeed, the most intense and not-overlapped Raman band of 3-HF, which belongs to C2=C3 and C=O conjugated stretching vibrations,[29] can be observed at 1569 cm^{-1}. Upon impregnation of 3-HF in the activated cell wall, we observed a slight blue shift of the flavonol band (**Figure 3-6A**, Spectra 3 and 4, 1569 to 1571 cm^{-1}), whereas the lignin aromatic bands red-shifted from 1660 to 1656 cm^{-1} (**Figure 3-6A**, spectra 1 and 3).

Considering a possible interaction between lignin and 3-HF conjugated systems, such an opposite frequency shift is characteristic of a donor−acceptor interaction[30] and is therefore supporting the existence of weak bonding via π−π stacking. It is interesting to note that the

lignin band is solely affected by the flavonol addition (with weak interactions), and not by the reaction with tosyl chloride. The effects of tosylation can be observed in the higher frequency spectral region where the band assigned to the aromatic C−H stretching of tosyl groups can be found (**Figure 3-6A**).[26] There is a clear red shift after reaction with the cell wall and addition of 3-HF (**Figure 3-6B**, spectra 1, 2, and 3). In the case of tosyl groups, characterized by the presence of both donor and acceptor substituents on the aromatic ring, the type of intermolecular interactions is more difficult to discern. The Raman shift observed may be caused by a CH or OH...π interaction or π−π interactions with 3-HF.
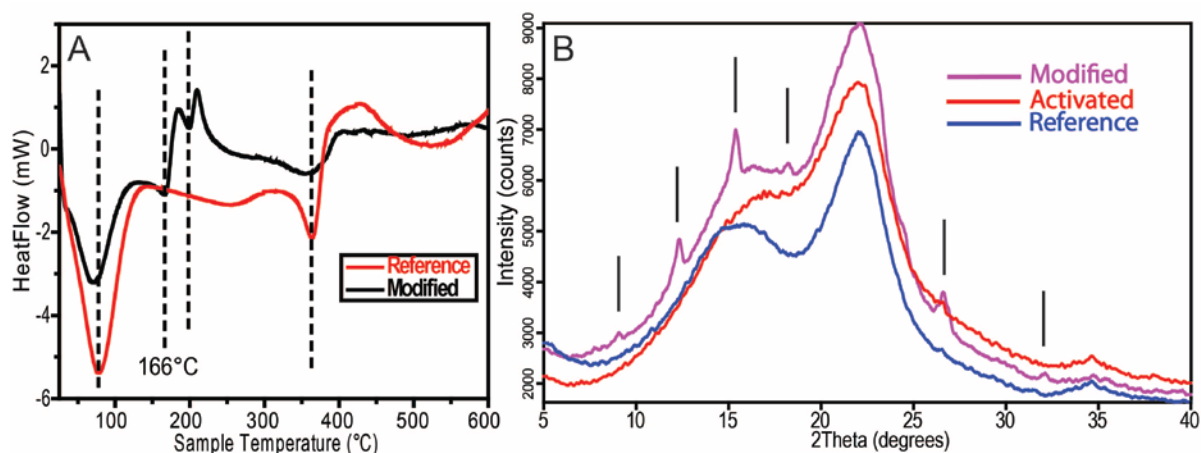
Figure 3-7. (A) Differential scanning calorimetry analysis data of modified and reference spruce samples. (B) X-ray powder diffraction profiles: modified, activated, and reference samples.

Another important aspect of the assembly and interaction of cell wall constituents in the modified wood is whether 3-HF can built crystalline domains in the cell walls. This issue was addressed by differential scanning calorimetry and X-ray powder diffraction (**Figure 3-7**). In case of modified cell wall, DSC revealed an endotherm at 166 °C (**Figure 3-7A**), corresponding to the melting of 3-HF. Therefore, it appears that the flavonol crystallized within small domains in the cell wall. This is confirmed by X-ray powder diffraction analysis as diffraction peaks of relevant crystalline 3-HF[31] can be observed in the modified sample (**Figure 3-7B**). Although 3-HF is known to form intermolecular interactions quite easily, to the point of forming polymer like structures,[24] it is surprising to observe crystallization in such confined domains.

In line with our results, we propose that the aromatic groups provided by activation with tosyl chloride acts as a nucleation center for the growth of 3-HF crystals within the cell wall. In the case of nonactivated wood, the possibilities of weak interactions of such nature are present

(with lignin), but considerably reduced, and explain the inability of 3-HF to stay in the cell wall in a durable manner.

In contrast to prior studies,[16,17] we used a rather hydrophobic flavonol in our study. In the cited studies, flavonoid molecules comprise up to five hydroxyl groups, explaining the easier impregnation of the cell wall. As shown here, loading of 3-HF in nonactivated cell wall was low, but tosylation (i.e., modification of OH groups) renders the cell wall slightly more hydrophobic, hence favoring the initial insertion of 3-HF into activated cell walls. Hence, inserting hydrophobic molecules into wood cell walls following a tosylation pretreatment provides an alternative and well-suited way to significantly reduce the water uptake of cell walls and improve the dimensional stability of wood.

Conclusions

We established a new method to facilitate cell wall insertion of hydrophobic polycyclic compounds via a pretreatment with tosyl chloride. The lesson to be learnt from nature is that it could be beneficial to impregnate wood cell walls with hydrophobic substances rather using treatments with hydrophilic flavonol compounds. The combined effects of hydrophobicity increase, and improved accessibility of aromatic moieties provided by the tosylation, contribute to a significant enhancement of the insertion and stability of flavonoids in the cell wall. Hence by overcoming the challenge of establishing the hydrophobic substances in an essentially hydrophilic environment of the cell wall, we were able to improve the dimensional stability of wood considerably at the expenses of a relatively small amount of the modifying flavonoid.

Acknowledgements

References

1. Hill, C. A. S., *Wood Modification: Chemical, Thermal and Other Processes*; Wiley: New York, 2006.

2. Rowell, R. M., *Handbook of Wood Chemistry and Wood Composites*; CRC Press: Florida, 2000.

3. Fengel, D., Wegener, G., *Wood - Chemistry, Ultrastructure, Reactions*; Walter de Gruyter: Berlin, New York, 1984.

4. Salmen, L.; Burgert, I. *Holzforschung* **2009**, *63* (2), 121-129.

5. Skaar, C., *Wood-Water Relations*; Springer-Verlag: Berlin, 1988.

6. Mai, C. and Militz H. *Wood Sci. Technol.* **2004**, *37* (5), 339-348.

7. Mai, C. and Militz H. *Wood Sci. Technol.* **2004**, *37* (6), 453-461.

8. Magel, E.A., Hillinger, C., Wagner, T., Höll, W. *Phytochemistry* **2001**, *57* (7), 1061-1068.

9. Pallardy,S.G., Kozlowski, T.T., *Physiology of Woody Plants*; Elsevier: Amsterdam, 2008.

10. Taylor, A.M.; Gartner, B.L.; Morrell, J.J. *Wood Fiber Sci*. **2002**, *34* (4), 587–611.

11. Magel, E.A. Biochemistry and physiology of heartwood formation. In *Cell and Molecular Biology of Wood Formation*; Savidge, R., Barnett, J., Napier, R., Eds. BIOS: Oxford, UK, 2000; pp 363–376.

12. Magel, E. and Hübner, B. *Bot. Acta* **1997**, *110*, 314–322.

13. Magel, E.; Drouet A.; Claudot, A.; Ziegler, H. *Trees* **1991**, *5* (4), 203–207.

14. Magel, E.; Jay-Allemand C.; Ziegler, H. *Trees* **1994***, 8* (4), 165–171.

15. Smith, A.L.; Campbell, C. L.; Diwakar, M.P.; Hanover, J.W.; Miller, R.O. *Holzforshung* **1989**, *43* (5), 293-296.

16. Sakai, K.; Matsunaga, M.; Minato, K.; Nakatsubo, F. *J. Wood Sci*. **1999**, *45* (3), 227-232.

17. Matsunaga, M.; Obataya, E.; Minato, K.; Nakatsubo, F. *J. Wood Sci*. **2000**, *46* (2), 122-129.

18. Obataya E.; Ono T.; Norimoto M. *J. Mater. Sci*. **2000**, *35* (12), 2993–3001.

19. Bariska, M.; Pizzi, A. *Holzforschung* **1986**, *40* (5), 299-302.

20. McGeary R. P.; Amini S. R.; Tang V. W. S.; Toth, I. Nucleophilic substitution reactions on pyranose polytosylates. *J. Org. Chem*. **2004**, *69* (8), 2727-2730.

21. Gindl, W.; Gupta, H.S.; Schöberl, T.; Lichtenegger H.C.; Fratzl, P. *Appl. Phys. A* **2004**, *79* (8), 2069–2073.

22. Gierlinger, N.; Schwanninger M. *Spectroscopy* **2007**, *21* (2), 69-89.

23. Gierlinger, N.; Schwanninger M. **2006**, *140* (4), 1246-1254.

24. Agarwal, U.P.; Ralph, S.A. *Appl. Spectrosc.* **1997**, *51* (11), 1648–1655.

25. Ham, N. S.; Hambley, A.N. *Aust. J. Chem.* **1952**, *6* (2), 135 - 142.

26. Parimala, K.; Balachandran, V. *Spectrochim. Acta A* **2011**, *81* (1), 711-723.

27. Binbuga, N.; Schultz, T.P.; Henry, W.P. *Tetrahedron Lett.* **2008**, *49* (40), 5762–5765.

28. Etter, M. C.; Urbańczyk-Lipkowska, Z.; Baer, S.; Barbara, P. F. *J. Mol. Struct.* **1986**, 144, 155–167.

29. Wang, M.; Teslova, T.; Xu, F.; Spataru, T.; Lombardi, J. R.; Birke, R. L. *J. Phys. Chem. C* **2007**, *111* (7), 3038-3043.

30. Hunter, C. A.; Sanders, J. K. M. *J. Am. Chem. Soc.* **1990**, *112* (14)*, 5525-5534.

31. Calabrò, M. L.; Tommasini, S.; Donato, P.; Raneri, D.; Stancanelli, R.; Ficarra, P.; Ficarra, R.; Costa, C.; Catania, S.; Rustichelli, C.; Gamberini, G. *J. Pharm. Biomed. Anal.* **2004**, *35*, 365-377.

Supporting information

Flavonoid Insertion into Cell Walls Improves Wood Properties

Mahmut A. Ermeydan[1], Etienne Cabane[2,3], Admir Masic[1], Joachim Koetz[4] and Ingo Burgert[1,2,3]

[1]Max Planck Institute of Colloids and Interfaces, Department of Biomaterials, Potsdam, Germany

[2]ETH Zürich, Institute for Building Materials, Zürich, Switzerland

[3]Empa - Swiss Federal Laboratories for Material Testing and Research, Applied Wood Research Laboratory, Dübendorf, Switzerland

[4]University of Potsdam, Institute of Chemistry, Potsdam, Germany

Table 3-S1: Summary of Raman bands for 3-HF, wood components, and tosyl group, used for analysis: tosyl group (Tosyl), lignin (Lig) and/or carbohydrate components (cellulose [Cel], glucomannan [GlcMan], and xylan [Xyl]).[1-9]

Wavenumber (cm^{-1})		Component	Assignment
Reference Cell Wall	Modified Region		
	3071	Tosyl	Aromatic C-H str.
2945	2946	Lig, GlcMan, and Cel	CH str. in O-CH$_3$ asym.
	2925	Tosyl	Asym. CH$_3$ str.
2892	2895	Cel	CH and CH$_2$ stretching.
1660	1655	Lig	Ring conjugated C=C stretching of coniferyl alcohol; C=O str. of coniferaldehyde
1621	1621 / 1629	Lig / 3-HF	Ring conjugated C=C stretching of coniferaldehyde / C$_2$=C$_3$ stretching; C=O stretching
1600	1600	Lig	Aryl sym. ring stretching.
1570	1573	3-HF	C$_2$=C$_3$ stretching; C=O stretching; OH bending
1512	1501	Lig	Aryl ring asym. stretching.
1460	1458	Lig and Cel	HCH and HOC bending
1426	1422	Lig	O-CH$_3$ deformation; CH$_2$ scissoring; guaiacyl ring vibration
1381	1381	Cel	HCC, HCO, and HOC bending
1338	1341	Cel	HCC, HCO, and HOC bending
1326	1330	Cel	HCC and HCO bending
	1313	3-HF	rings A&B, C-H (ip) bending; O-H bending
1275	1275	Lig / 3-HF	Aryl-O of aryl OH and aryl O-CH3; guaiacyl ring (with C=O group) mode / rings A&B, C-H (ip) bending; O-H bending
	1216	Tosyl / 3-HF	CC str. and CH3 (ip) bending. / C-OH stretching ; ring B C-H (ip) bending
	1193	3-HF	C-OH stretching; ring B C-H (ip) bending
	1177	Tosyl	Sym. SO$_2$ stretching.
1150	1153	Cel	Heavy atom (CC and CO) stretching. / HCC and HCO bending
1122	1126	C, Xyl, and GlcMan	Heavy atom (CC and CO) stretching.
1098	1098	C, Xyl, and GlcMan and Tosyl	Heavy atom (CC and CO) stretching. / C-H (ip) bend.
1035	1031	Cel / 3-HF	Heavy atom (CC and CO) stretching. / ? ring B C-H (ip) bending.
999	998	Cel / 3-HF	Heavy atom (CC and CO) stretching./ rings A, B, C, C-C deformation.
903	907	Cel	HCC and HCO bending at C6.
	842	3-HF	rings A, B, C, CC deformation.
	800	Tosyl	C-H (op) stretching.
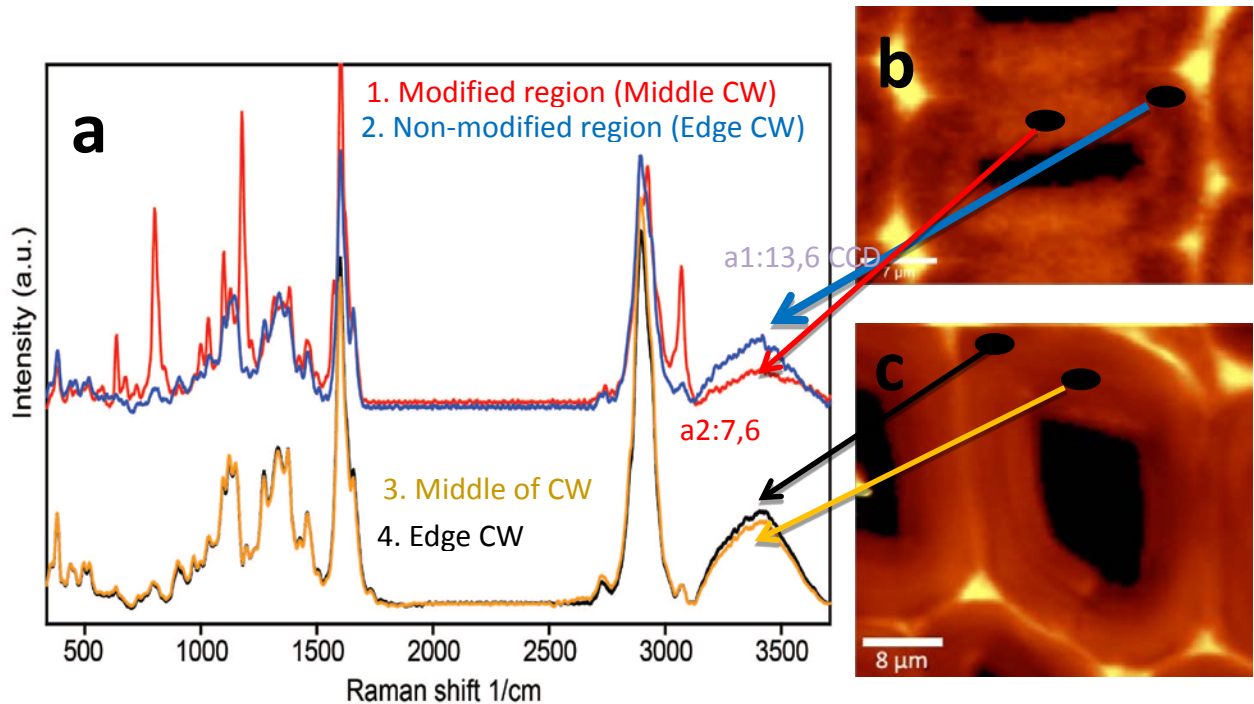
Figure 3-S1. Comparison of water band intensity on the same cell wall of modified (a1-2 ,b) and un-treated cell walls (a3-4, c). a. (spectral range: 350-3650cm^{-1}) Raman spectra of 1. Modified region selected on the modified cell walls (middle of the cell wall). 2. Non-modified region selected on the modified cell walls (edge of the cell wall). 3. Middle of selected un-treated cell wall. 4. Edge of selected un-treated cell wall b. Raman image of modified cell walls by integration between 300-3650 cm^{-1}. c. Raman image of un-treated cell walls by integration between 300-3650 cm^{-1}

Comparison of water band intensity and the water distribution in the cell walls (Figure 3-1F) indicate a reduced water uptake of the cell walls. Two points on the same cell wall (middle cell wall and cell wall edge) were analyzed by using Witec Software. Cross sections of cell walls are filled with water during Raman measurements in all cases and water band intensity ratios show an intensity decrease in the same cell walls. Raman bands of un-treated cell walls are not changed at various points on the cell walls (See Figure 3-S1A. Spectrum 3-4, Figure 3-S1C) whereas an intensity decrease can be observed for the modified sample (Figure S1A. Spectrum 1-2, Figure 3-S1B).
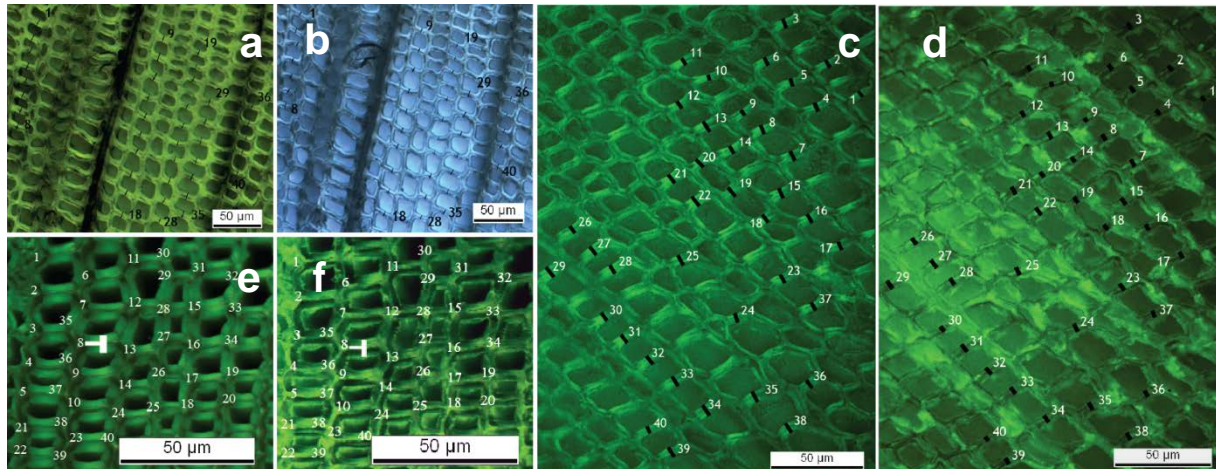
Figure 3-S2. Light microscope images of cross sections of wet (**2a, 2c, 2e**) and dry (**2b, 2d, 2f**) fibres: **2a & 2b** are reference cell walls, **2c & 2d** are activated (tosylated) cell walls and **2e & 2f** are modified cell walls.

Cell wall swelling/shrinkage behavior was calculated on the same cell walls from micrographs taken in dry and wet conditions shown above.
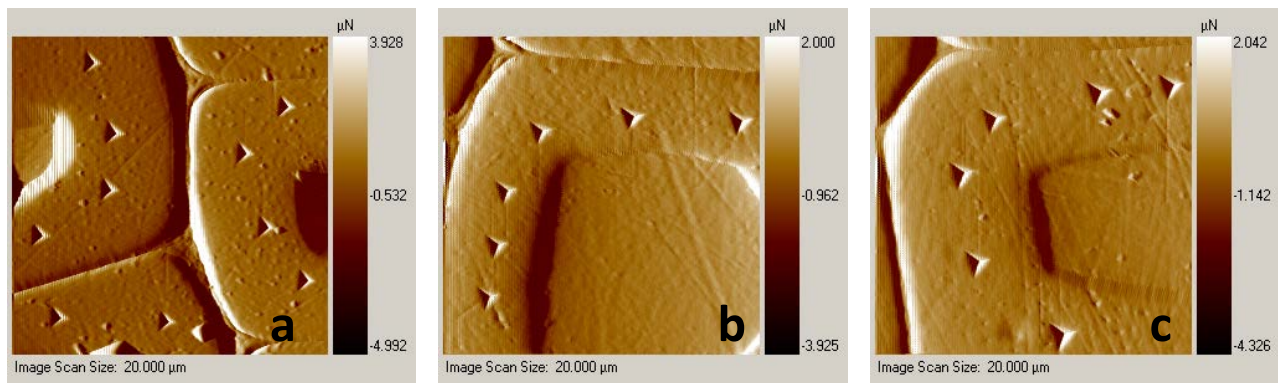
Figure 3-S3. AFM gradient images of nano-indented cell walls of un-treated(a), activated (b), modified (c) cell walls.

References

1. Ham, N. S; Hambley, A.N. *Aust. J. Chem.* **1952**, *6*, 135 - 142.

2. Wiley J.H.; Atalla R.H. *Carbohydr. Res.* **1987**, *160*, 113–129.

3. Agarwal, U.P.; Ralph, S.A. *Appl. Spectrosc.* **1997**, *51*, 1648–1655.

4. Edwards, H.G.M.; Farwell, D.W.; Webster, D. *Spectrochimica Acta Part A* **1997**, *53*, 2383–2392.

5. Agarwal U.P. An overview of Raman spectroscopy as applied to lignocellulosic materials. In: Advances in lignocellulosics characterization; Argyropoulos, E., Ed. TAPPI Press, Atlanta 1999; pp 201–225.

6. Saariaho, A.M.; Jääskeläinen, A.S.; Nuopponen, M.; Vuorinen, T. *Appl. Spectrosc.* **2003**, *57*, 58–66.

7. Gierlinger, N.; Schwanninger M. *Plant Physiol.* **2006**, *140*, 1246-1254.

8. Wang, M.; Teslova, T.; Xu, F.; Spataru, T.; Lombardi, J. R.; Birke, R. L. *J. Phys. Chem. C* **2007**, *111*, 3038-3043.

9. Parimala, K.; Balachandran, V. *Spectrochimica Acta Part A* **2011**, *81*, 711-723.

Chapter 4. Improvement of Wood Material Properties via *in-situ* Polymerization of Styrene into Tosylated Cell Walls

Mahmut A. Ermeydan,[a] Etienne Cabane,[bc] Notburga Gierlinger,[bc] Joachim Koetz[d] and Ingo Burgert[bc]*

[a] *Max Planck Institute of Colloids and Interfaces, Department of Biomaterials, Potsdam, Germany.*

[b] *ETH Zurich, Institute for Building Materials, Zurich, Switzerland.*

[c] *Empa - Swiss Federal Laboratories for Material Testing and Research, Applied Wood Research Laboratory, Dübendorf, Switzerland.*

[d] *University of Potsdam, Institute of Chemistry, Potsdam, Germany.*

Abstract

As an engineering material derived from renewable resources, wood possesses excellent mechanical properties in view of its light weight but also has some disadvantages such as low dimensional stability upon moisture changes and low durability against biological attack. Polymerization of hydrophobic monomers in the cell wall is one of the potential approaches to improve the dimensional stability of wood. A major challenge is to insert hydrophobic monomers into the hydrophilic environment of the cell walls, without increasing the bulk density of the material due to lumen filling. Here, we report on an innovative and simple method to insert styrene monomers into tosylated cell walls (i.e. –OH groups from natural wood polymers are reacted with tosyl chloride) and carry out free radical polymerization under relatively mild conditions, generating low wood weight gains. In-depth SEM and confocal Raman microscopy analysis are applied to reveal the distribution of the polystyrene in the cell walls and the lumen. The embedding of polystyrene in wood results in reduced water uptake by the wood cell walls, a significant increase in dimensional stability, as well as slightly improved mechanical properties measured by nanoindentation.

Introduction

Wood has been an essential engineering material for humankind since ancient times due to its global abundance, light weight, excellent mechanical properties, and processability. In modern societies, wood still has a significant impact because of its sustainability, with increasing utilization as an indoor and outdoor construction material. However, due to its hygroscopic nature, wood swells and shrinks by absorbing and desorbing water upon humidity changes, which makes it dimensionally instable.[1–3]

The quest for solutions against this major disadvantage has led to a number of studies with the aim to modify wood and further improve its quality. Increasing demand for high quality products, environmental awareness of societies, increasing prices and concerns about use of tropical hardwoods accelerated research activities in the field.[2,3]

Various esterifications and etherifications,[2–4] silylations,[5–7] and polymerization reactions have been tried so far. However, none of these approaches entirely fulfilled the required product properties (e.g. long-term dimensional stability, increased or retained mechanical properties, moderate increases in density, absence of by-products, reasonable commercialization prizes, minimized or no environmental/health risk, etc.). To date, only a few modification methods have been introduced to the market, such as acetylation,[8,9] or furfurylation,[4] mainly because of limitations in up-scaling and product costs.

The wood treatments can be classified according to the targeted wood components and the type of interactions created within the wood structure. Hydrophilic reactants are known to penetrate the hygroscopic wood cell walls easily and can be used to establish covalent bonds addressing functional hydroxyl groups of the natural polymers (lignin, cellulose, and hemicellulose). Another approach consists in bulking the micro- and nano-voids in the cell walls with reagents that can be locked in wood and provide permanent dimensional stability and water repellence.[2–4,10]

One possibility to lock new material in wood is to introduce monomers with low molecular weight and convert them into polymer chains in situ. Several publications report on the modification of wood by polymerizing monomers impregnated in wood blocks.[11–19] Among the hydrophobic monomers studied, styrene has several advantages related to up-scale possibilities and easy polymerization at mild temperatures. Styrene itself is highly hydrophobic and has very limited penetration into the cell wall. In some studies, minor amounts of hydrophilic solvents

(methanol or ethanol) were used with styrene, which resulted in an improvement of dimensional stability with very high weight gains only,[3] most probably due to the absence of polymer within the cell walls.

Indeed, it is well known that the addition of new material inside the lumen of the wood cells only has little effect on the hygroscopic nature of wood.[2,3,12,17] In order to improve the treatment efficiency, it is of high importance to load cell walls rather than lumen. By doing this, a limited weight gain upon modification is possible and wood's light weight advantages can be retained.

Polymerization of hydrophobic molecules does not take place in the cell wall without pre-treatment.[18] In a previous study, our group has introduced "activation" of cell walls by a pre-treatment which allows for further impregnation by hydrophobic molecules (flavonoids) and resulted in a reduction of moisture uptake up to 31%.[20] In short, the "activation" of the cell walls consists in reacting some of the –OH groups from the wood polymer network with tosyl chloride moieties. This chemical pre-treatment was shown to hydrophobize wood cell walls, hence improving the penetration of hydrophobic molecules in a second stage.[20] The mild conditions used for this two-step modification treatment are suitable for wood, and avoid significant losses in natural properties, as opposed to other techniques. Following this preceding work with flavonoids, here we aim at successfully inserting hydrophobic polymers within spruce cell walls for a further modification development. Polystyrene chains entangled within the cell wall structure would yield a more durable treatment and enhanced bulking in the wood micro- and nano-voids with affordable starting materials.

Hence, we postulate that the tosylation technique could be advantageously used with hydrophobic monomers to prepare wood–polymer materials. Here we demonstrate that polystyrene chains are present in the cell walls, which means that they contribute to the improvement of the dimensional stability of spruce wood (Picea abies) without dominant densification.

Experimental

Materials

para-Toluene sulfonyl chloride (TsCl), dry pyridine (Py), dimethyl formamide (DMF), styrene (St), azobisisobutyronitrile (AIBN), and acetone were bought from Sigma-Aldrich and used as received.

Chemical modification of wood cubes

Wood sampling. Norway spruce (Picea abies) wood cubes (1 cm x 1 cm x 0.5 cm; radial x tangential x longitudinal) were cut along the grain, and dried in oven (see ESI **Figure 4-S1**†). For each of the different treatments, fifteen cubes were used and assigned as follows: reference wood (Ref – unmodified), tosylated wood (Ts1 – low weight gain tosylation, Ts2 – high weight gain tosylation), modified wood (St – in situ styrene polymerization without pre-treatment, St1 – pre-treated with low WPG tosylation followed by in situ styrene polymerization, St2 and St3 – pre-treated with high WPG tosylation followed by in situ styrene polymerization). After the treatments, ten cubes from each group were used for physical characterization (i.e. swelling, water uptake, anti-swelling efficiency, and equilibrium moisture content tests). Five cubes from each set were used for structural and chemical analysis. A detailed description of the experimental workflow is given in ESI (**Figure 4-S1**†), and the sample nomenclature is clarified in **Figure 4-1**.

Step 1: tosylation of wood cubes. The tosylation conditions used in this work are reported elsewhere.[20] The wood cubes were dried at 60°C for one day, and their weight was measured (oven dry weight). Cubes were placed in 40 ml of dry pyridine. After one day of swelling, the reaction flask was cooled down in an ice bath before adding para-toluene sulfonyl chloride (TsCl). We immersed wood blocks in pyridine for 24 h before starting tosylation reaction as mentioned (St1 sample set was directly put into pyridine–tosyl chloride solution). The amount of TsCl added was calculated as one equivalent of TsCl per OH functionality in wood (n(OH), calculated as anhydrous glucopyranose equivalent, AGU, MW = 162 g mol^{-1}). Tosylated wood was produced with a low weight gain (Ts1) and a high weight gain (Ts2). The wood and TsCl were allowed to react at 5°C for one day. After reaction completion, the control cubes were washed with acetone and the other samples were cleaned with pyridine before step two.

Step 2: styrene impregnation and polymerization. After washing of the tosylated wood cubes to get rid of unreacted tosyl groups, a styrene solution in DMF or pyridine (St : Py – 50 : 50 v/v for St1 and St2, St : DMF – 60/40 v/v for St3), containing 1% of AIBN as initiator was added to the wood blocks. The cubes were stored in this solution for one day, in order to maximize monomer impregnation in wood cell walls before starting the polymerization. Prior to reaction, the solution was degassed by bubbling argon for 30 minutes to get rid of oxygen. The reaction flasks were heated at 75 °C overnight to polymerize styrene. After reaction completion, the cubes were washed with several volumes of acetone, then with water, and finally dried in the oven at 65 °C for 24 h.

Characterization

Swelling coefficient (S), anti-swelling efficiency (ASE), and water uptake (WU). Initial weights and dimensions of all three sets of cubes (5 x unmodified, 5 x control, 5 x modified) were measured. Then the cubes were placed into deionized water in separate flasks and stirred for 5 days with moderate shaking. Weights and dimensions were measured after 5 days and then the cubes were stored in an oven at 103 °C for drying (first cycle). Weights and dimensions of the dry cubes were measured and samples were placed again in deionized water for the second water-soaking and drying cycle (second cycle). The degree of dimensional stability was obtained by calculating swelling coefficient (S) and anti-shrinking/anti-swelling efficiency (ASE) as reported.[21] The water repellence efficiency was given by the water uptake calculations. The equations for S, ASE, and water uptake calculations are given in ESI (**Figure 4-S2**†).
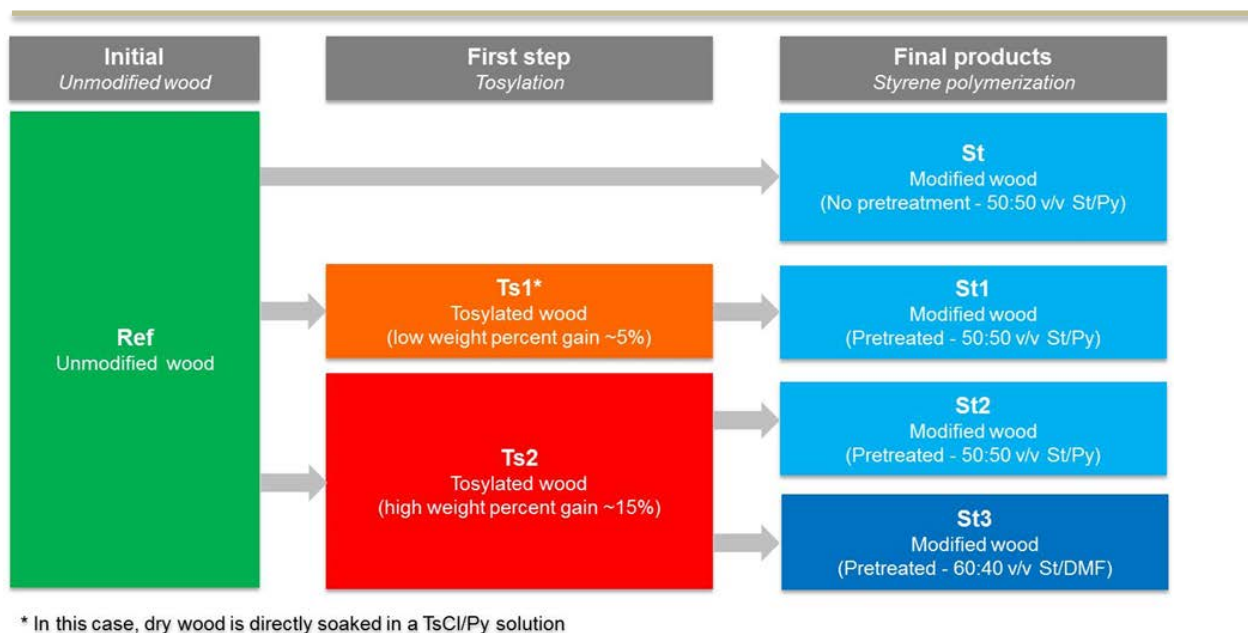
Figure 4-1 Nomenclature for the reaction of spruce wood cubes with different steps and conditions.

Equilibrium moisture content (EMC). Reference, tosylated, and modified samples were equilibrated in a sealed container at a relative humidity of 75% obtained with a saturated solution of NaCl at room temperature. Weight equilibrium of the samples was recorded by weighing samples until constant weight. Afterwards, samples were oven-dried at 103 ± 2 °C and weighed again to determine final moisture content. For each treatment 5 samples were measured. Equation for the EMC calculation is given in the ESI (**Figure 4-S3**†).

Volume change and weight percentage gain (WPG). Dimensions and weights of the wood cubes were measured before and after treatments in order to determine volume and weight changes caused by chemicals introduced.

Raman imaging and spectroscopy. 40 mm thick cross-section slices were cut on a rotary microtome (LEICA RM2255, Germany) and kept between glass slides with a drop of water to retain cell walls in wet condition. The cross-section of modified spruce wood was analysed using confocal Raman microscopy. Spectra were acquired with a confocal Raman microscope (alpha300, WITec GmbH, Ulm, Germany) equipped with an objective (60x, NA = 0.8, 0.17 mm coverslip correction, from Nikon Instruments, Amstelveen, The Netherlands). A 532 nm laser with λ = 532 nm (Crysta Laser, Reno, NV, USA) is focused with a diffraction limited spot size of 0.61λ/NA and the Raman signal detected with an air cooled, back illuminated CCD camera (DV401-BV, Andor, Belfast, North Ireland) behind a spectrograph (UHTS 300, WITec) with a spectral resolution of 3 cm^{-1}. For mapping, an integration time of 0.4 s was chosen, every pixel corresponding to one spectrum acquired every 0.5 mm. Two-dimensional chemical images of cellulose, lignin, and tosylated tissues were compiled by Witec Project software using the integration filter. A classical integration method could not be used to generate polystyrene image, due to the weak intensity of the polystyrene band at 1005 cm^{-1}. The Raman images of polystyrene distribution were obtained using the "advance fitting" option of the Witec Plus software. The polystyrene band at 1005 cm^{-1} was fitted to multispectral data set by a Gaussian function yielding an image showing the distribution of this specific band from the data set (for detailed information please see **Figure 4-S4** in the ESI†). The intensity profiles of polystyrene, cellulose, and lignin were obtained along the marked line on the Raman image by plotting the intensity of selected bands assigned to the different components (lignin, cellulose, polystyrene).

Scanning electron microscopy (SEM). The morphologies of the modified and reference wood samples were documented via imaging cross-sections using an (E)SEM device (FEI FEG-ESEM Quanta 600, FEI Company, Hillsboro, OR, USA) with a backscattered electron (BSE) detector operated at 7.5–10 kV with a 10 mm sample-detector distance, 4.0/5.0 nm spot size, and 0.75 torr pressure.

Nanoindentation. The mechanical characterization of tracheid cell walls was carried out on a Dimension DI-3100 atomic force microscope (Digital Instruments, Veeco Metrology Group, Santa Barbara, CA) equipped with a Hysitron add-on force transducer for nanoindentation (Surface, Hueckelhoven, Germany). For this purpose, samples were dried overnight in an oven at

60 °C and subsequently embedded in AGAR resin (AGAR low viscosity resin kit, AGAR Scientific Ltd., Stansted, UK). Specimens were impregnated with the embedding resin and cured overnight in an oven at 60 °C. 2 mm thick slices were cut from the resin block. The embedded specimens were glued onto metal discs (15 mm AFM specimen discs), and the surface was smoothed with a Leica Ultracut-R ultramicrotome equipped with a Diatome Histo diamond knife. Quasi-static indentation tests were performed in a force-controlled mode; the indenter tip (Berkovich-type triangular pyramid) was loaded to a peak force of 250 mN at a loading rate of 100 mN s^{-1}, held at constant load for 15 s, and unloaded at a rate of 100 mN s^{-1}.

Results and discussion

Loading of spruce wood with polystyrene

Wood modification process. In the first step, our aim was to address the –OH groups of the cell wall components (lignin, cellulose, and hemicellulose), via a covalent reaction with tosyl chloride. In a previous study, it was shown that such a treatment is effective in reducing the hydrophilicity of wood, and facilitates the penetration of hydrophobic chemicals in the second treatment step.[20] In the second step, wood was impregnated with a solution of styrene containing an azoinitiator (AIBN). Since styrene is a hydrophobic molecule, it was dissolved in a good solvent for wood such as DMF or pyridine to maximize cell wall penetration.[22] The free radical polymerization of styrene was then conducted for 18 hours at 75 °C (**Figure 4-2**).
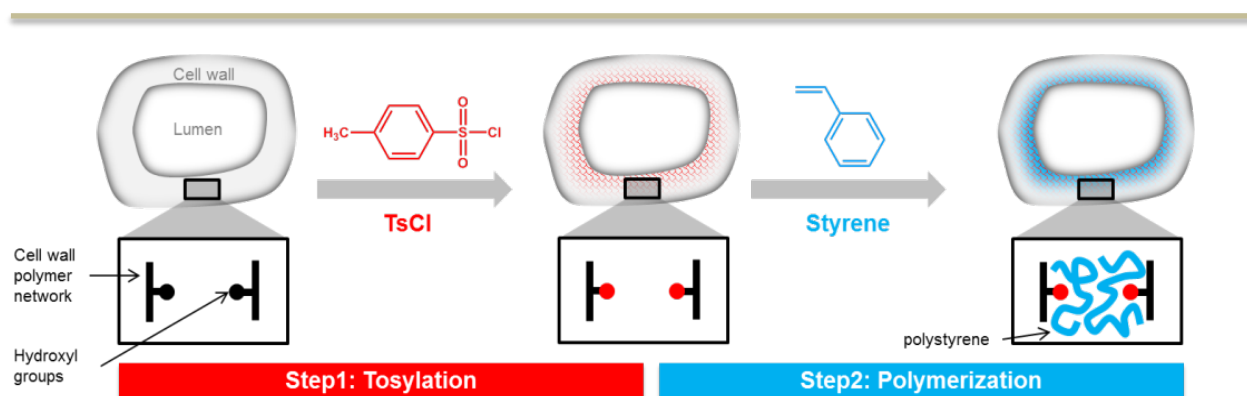
Figure 4-2 Schematic representation of the modification route: functionalization of cell wall –OH groups with tosyl groups, followed by in situ polymerization of styrene monomer.

Prior to in depth characterization of cell walls, we can already collect important information on the success of the wood modification by the weight gains and the dimensional changes

immediately after reaction. The weight gains determined after tosylation (step 1), polymerization (step 2), and after full treatment (cumulative) are respectively named WPG1, WPG2, and WPG, and are given in **Table 4-1**. For the tosylation pre-treatment, WPG1 directly relates to the number of hydroxyl groups reacted with tosyl chloride. As we reported before, the amount of tosyl in wood after the first step has a critical influence on the insertion of hydrophobic compounds in wood. By reacting the –OH groups with TsCl, the hydrophilic nature of the cell wall is changed to a more hydrophobic environment, hence improving penetration of non-polar molecules such as styrene. The total weight gains after full treatment, i.e. after washing with a good solvent for polystyrene, show that in all experiments a significant amount of polymer was retained in the wood structure.

Table 4-1. Summary of weight percent gains and volume changes of spruce wood blocks after tosylation and polymerization reactions with various TsCl/St compositions.

	Tosylation		Polymerization	Total	
Exp. ID	WPG1 (%)	Vol. change (%)	WPG2 (%)	WPG (%)	Vol. change (%)
St	N/A	N/A	38.8	38.8	-1.2
St1	3.1 – Ts1	-0.6 – Ts1	35.7	40.0	-1.7
St2	14.2 – Ts2	0.9 – Ts2	19.7	36.3	1.6
St3	16.7 – Ts2	1.7 – Ts2	30.2	52.0	4.0

Table 4-1 also provides information on the dimensional changes of the wood cubes upon treatment. A positive change in volume (i.e. the wood cubes are slightly swollen after treatment) rejects the presence of material in the cell wall, via a bulking effect (experiment St2 and St3). Theoretically, filling up only the wood lumen with materials should result in a constant volume. The shrinkage (negative volume change observed for St and St1 sample series) is most likely due the release of internal stresses due to rearrangements of cell wall polymers during the solvent treatment.

The results given in **Table 4-1** suggest that in the case of modification treatments without tosylation (St experiment) or with very little tosyl groups in cell wall (St1), the polymer added in step 2 does not enter cell wall. On the contrary, it seems that when a significant amount of tosyl group functionalizes wood, the polymer is present in the cell wall to some extent (St2 and St3). Understanding the polymer distribution in wood is of high importance. It has already been shown that the location of a polymer or any other added material in wood has a strong influence on the overall properties of the modified wood.[23,24] If the added material sits in the lumina area, then

properties such as dimensional stability (which is directly related to cell wall deformation) or biodegradability will hardly be changed.

In order to affect such properties, the added material (a polymer in our case) should be located within the wood cell wall. In the next part, we carefully studied the chemical composition, morphology and structure of the wood after full treatment using Scanning Electron Microscopy (SEM) as well as confocal Raman imaging and spectroscopy. Results of a semiquantitative method which was developed to estimate polymer content in the cell walls will also be discussed.

Polymer location using Raman spectroscopy. Confocal Raman microscopy is a powerful technique for the detailed analysis of plant cell walls in general.[25–27] With this technique, the chemical signatures of the different cell wall constituents of wood as well as the polystyrene can be singled out within the complex spectra obtained. Typical spectra of reference, tosylated, and modified cell walls, as well as pure polystyrene are presented in **Figure 4-3**. For polystyrene the band at 1005 cm^{-1}, which belongs to ring breathing of benzenes, was used for integration.[28] The Raman bands of tosyl groups on tosylated and modified cell walls can be assigned to asymmetric stretching of sulfonyl group (v_{as} SO$_2$) at 1372 cm^{-1}, and symmetric stretching of sulfonyl group (v_s SO2) at 1176 cm^{-1} (**Figure 4-3d**).[29] The C–H stretching band of aromatic ring at 3073 cm^{-1} also belongs to tosyl groups covalently bonded to the cell wall polymers. The Raman images shown in **Figure 4-3** were obtained via scanning of a latewood cross-section from fully treated wood (St3), followed by integration of relevant peaks for wood constituents, tosyl groups, and polystyrene
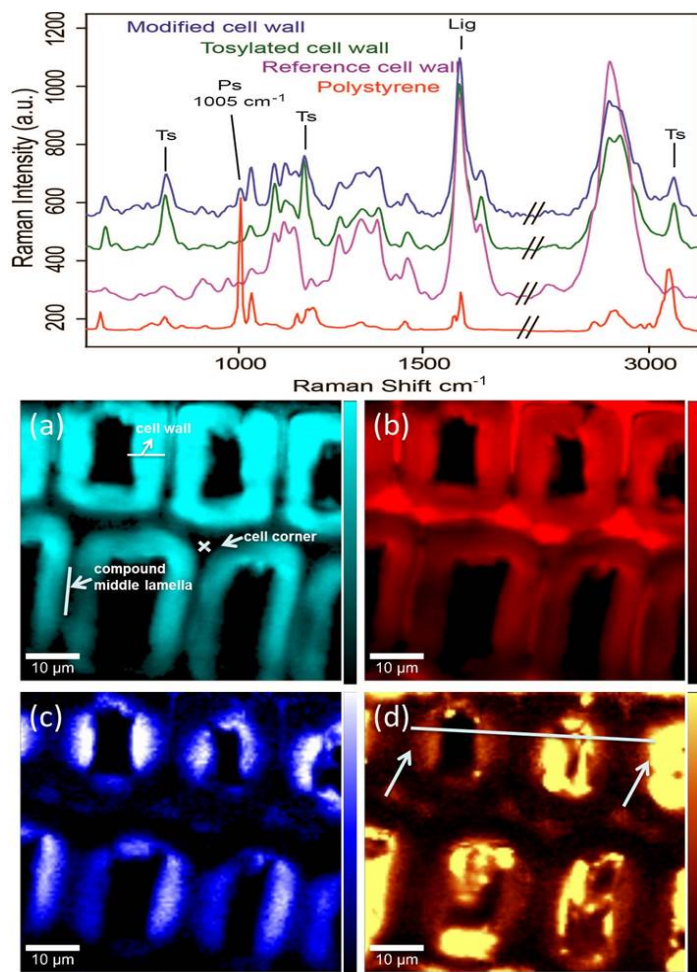
Figure 4-3 Top: comparison of full Raman spectra of polystyrene, reference cell wall, tosylated cell wall, and fully modified cell wall with polystyrene. Bottom: Raman images (55-60 mm²) of latewood cell wall tissue. Images were plotted by integration of Raman bands from spectral data set: (a) CH-groups (2860–3020 cm⁻¹), (b) lignin (1555–1645 cm⁻¹), (c) tosyl groups (780–825 cm⁻¹), and (d) polystyrene distribution in the cell wall and in the lumen which was plotted by the advance Gaussian fitting of the single band at 1005 cm⁻¹.

(see methods part). **Figure 4-3a** and **b** represent the CH-groups and lignin distributions and help to visualize the cell wall structure. Integration of the CH-groups clearly depicts the secondary cell wall regions (bright turquoise zones), while the lignin intensity is higher in the cell interstitial space, cell corners (CC) and compound middle lamella (CML) (bright red zones). The tosyl groups distribution indicates that functionalization took place deep within the secondary cell wall (**Figure 4-3c**), and the high intensity regions suggest that the chemicals diffused from the lumen interface towards inner cell wall regions. **Figure 4-3d** represents the polystyrene distribution, which was generated by using a Gaussian fitting as explained in methods part (see also ESI **Figure 4-S4**†). This image clearly shows that styrene polymerized in the lumen area of some cells. Regions with weak intensity (orange zones in **Figure 4-3d**) also reveal the presence of polymer in the secondary cell wall. However, the strong contrast between pure polymer in the lumen, and polystyrene enriched regions of the cell wall makes it difficult to interpret these images.
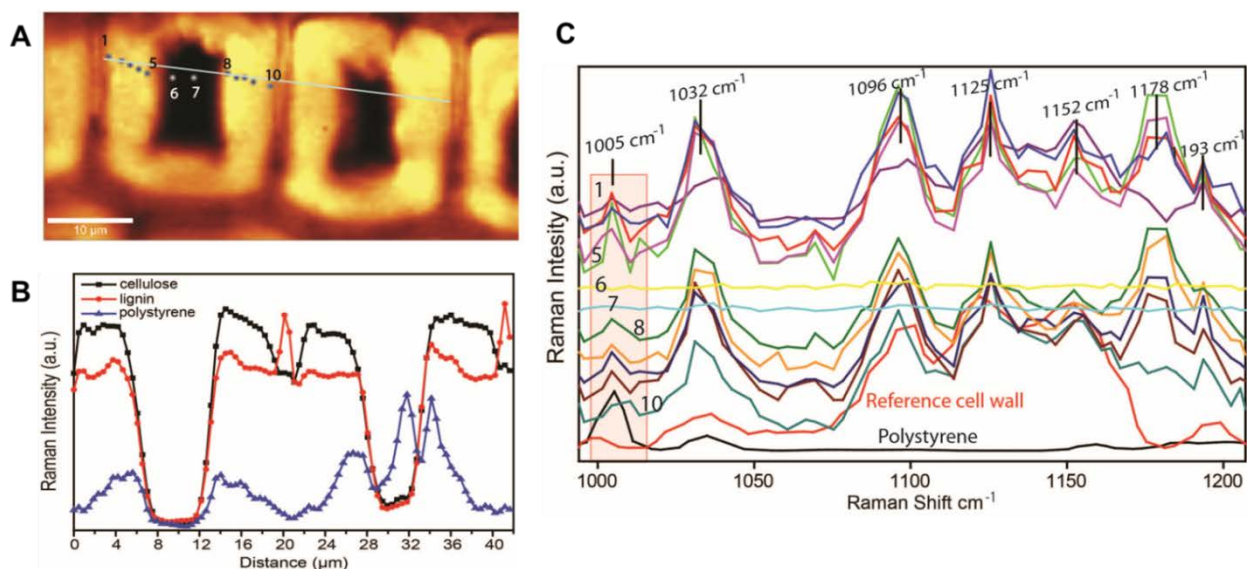
Figure 4-4 (A) Raman image from C–H stretching integration and visualization of the profile line and measurement points. (B) Intensity profiles of cellulose, lignin, and polystyrene in cell walls and lumen along the line shown in (A). (C) Raman spectra of the 10 points shown in (A), compared to polystyrene and reference cell wall spectra.

In order to get a better understanding of the distribution of polystyrene in cell walls, Raman intensity profiles of a specific band from polystyrene (1005 cm^{-1}) were recorded along a line drawn across two latewood cells, as shown in **Figure 4-4A**. The intensity profiles of cellulose and lignin recorded along the line and superimposed with the polystyrene profile were used to assess the presence of polymer in the cell wall (**Figure 4-4B**). The null intensity regions correspond to the empty lumen area, and are immediately framed by high intensity regions representing the cell walls. Besides the characteristic distribution patterns of cellulose and lignin, the plot clearly shows an overlap with polystyrene in the cell wall regions. These profiles indicate that polystyrene chains can be found in cell wall, up to 2–3 mm below the lumen interfacial area (reflected in the schematic illustration in **Figure 4-2**). Along the polystyrene profile, the peak around 31 mm corresponds to polymer present in the lumen, which was observed in **Figure 4-3d**. The Raman spectra associated to the points shown on **Figure 4-4A** are given in **Figure 4-4C**. These spectra can be compared with the reference wood spectrum and the pure polystyrene spectrum, and show that the peak at 1005 cm^{-1} can be used as a clear marker for the presence or absence of polystyrene in wood.
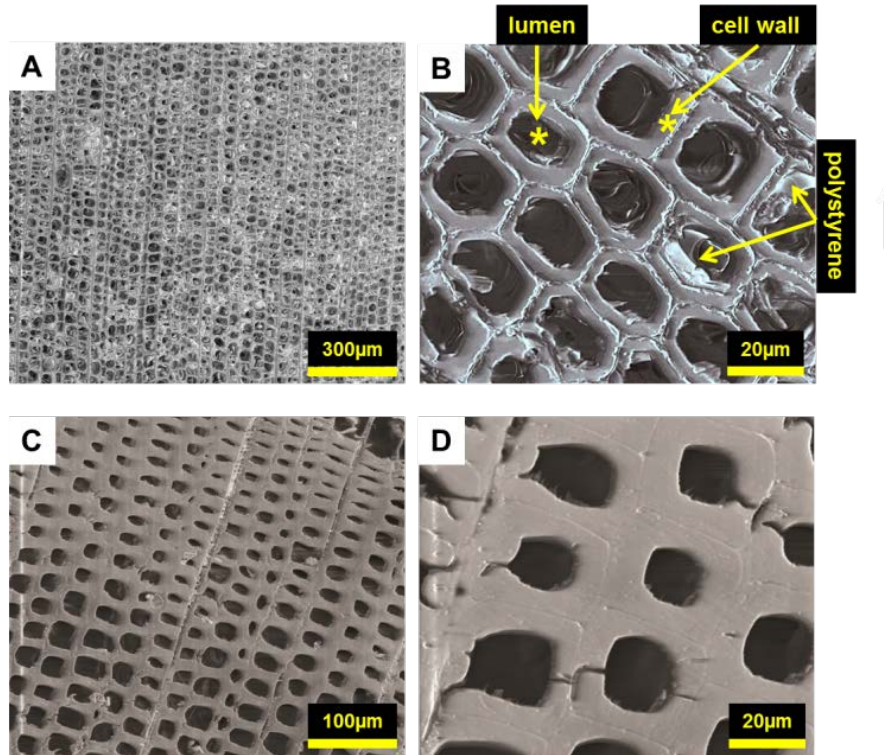
Figure 4-5 SEM images of microtomed cross-sections. (A) and (B): fully modified wood (St3). (C) and (D): unmodified, reference spruce wood.

Polymer location and content studied with SEM. To support findings from Raman spectroscopy, and propose an estimation of polymer content in the different wood regions, a series of SEM pictures of cube cross sections was performed (**Figure 4-5**). In order to have an idea of the polymer distribution within the cubes, the images were taken from cross sections 0.5 to 1 mm below the initial cube surfaces. SEM images of unmodified cell walls are provided as reference (**Figure 4-5C** and **D**). During the reaction process, wood cubes are soaked in the reaction solution; therefore polymerization in the cell lumen cannot be avoided. Although a large amount of unbound polymer chains is extracted upon washes with acetone, SEM images show that some cells are still partially or fully filled with polymer residues (**Figure 4-5A** and **B**).

The repartition of polystyrene between cell wall and lumen area could be estimated through a semi-quantitative method based on SEM image analysis and measured polymer weight gain. Details about the calculation are given in the ESI (**Figure 4-S5**†). Based on the assumption that polymerization does not take place in the cell walls of the polystyrene samples without pretreatment (St), we calculated the following cell wall loading for the other experiments: St1 1.3%, St2 17.6%, and St3 22.7%.

These results correlate well with the initial tosyl content in wood (WPG1), and support our hypothesis that tosylation enhances penetration of styrene in the second step of the modification, and consequently allows for higher polymer loading. Besides the presence of polymer within cell lumina, SEM pictures reveal that the modification process does not damage the overall wood structure, leaving well defined cells, without noticeable destruction.

Improved wood properties

Water uptake and swelling upon water sorption were measured using the water-soaking method developed by Rowell et al.[21] This method is based on subsequent cycles of drying and wetting, and is particularly efficient to assess the stability of the treatment, to estimate the water repellence (or water uptake), and to measure the dimensional change of wood in response to water sorption.

Water repellence. The results (after the first and second cycles) in **Figure 4-6** show that for all modification treatments (i.e. Ts1, Ts2, St, St1, St2, and St3) the water uptake was reduced to some extent when compared to reference wood. As expected, the tosylation step already makes wood more hydrophobic, and the water repellence efficiency correlates with the degree of hydroxyl functionalization (a trend illustrated by the water uptakes for Ts1 and Ts2 experiments). According to the graph, all treatments with polystyrene have enhanced hydrophobic properties when compared to both unmodified and tosylated wood: after five days in water, unmodified wood gained about 160% water, while all wood–polystyrene composites only gain about 70%. Wood samples with polystyrene in lumen only (St experiment) also show a clear reduction in water uptake similar to St3 in the first water-soaking cycle. It is well known that lumen
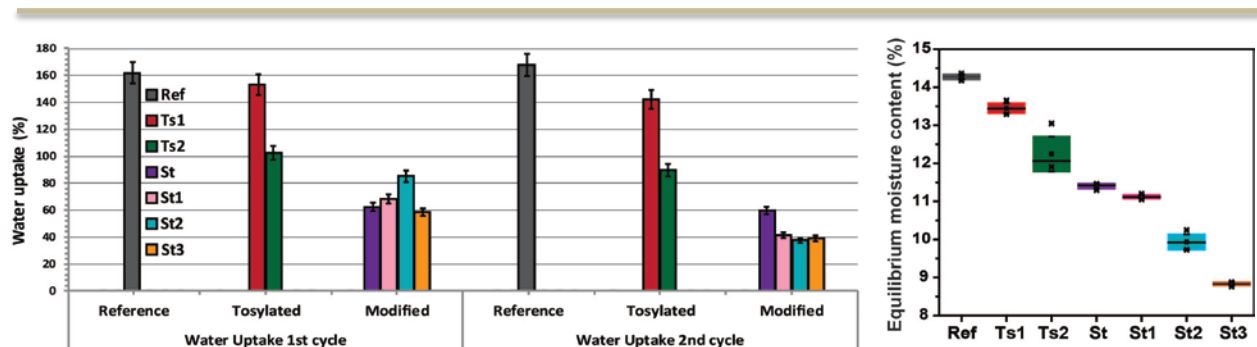
Figure 4-6 Left: water uptake values for unmodified wood (Ref), tosylated wood (Ts1, Ts2), and modified wood (St, St1, St2, and St3). Right: equilibrium moisture content (EMC) values of reference, tosylated, and modified samples.

filling by polymers decreases the space available for water, blocks cell cavities and consequently retards or avoids water entrance into the cell walls.[30–32] Interestingly, after the first drying cycle better results are achieved with wood samples combining activation with tosyl and subsequent polymerization (namely St1, St2, and St3 experiments): those samples have higher polymer contents in the cell walls, which further reduces the space available for water molecules. The significant differences of water uptake between cycle 1 and cycle 2 for pre-treated and polymerized samples (St1, St2, and St3) may be explained by a re-organization of the polystyrene chains inside the cell walls during the first drying in a way that polymers further occupy the nanovoids (**Figure 4-6**). As stated in the experimental part, wood cubes were dried at 65 °C after the chemical treatment, but at 103 °C during the water uptake experiments. The glass transition temperature (Tg) of pure polystyrene is around 100 °C (depending on the molecular weight).[33] Therefore, during the drying step for the water uptake measurements, polystyrene chains may flow freely within the wood cell wall and re-organization and additional filling of nanovoids can take place.

Equilibrium moisture content (EMC) measurements of tosylated and modified samples at room temperature and at a relative humidity of 75% also reject the improved hydrophobic character of treated samples (**Figure 4-6**). In such conditions, reference wood had an EMC of 14.3%. All modified samples adsorb less moisture with a minimum of 9.9% and 8.8% for St2 and St3 experiments respectively, which means that humidity adsorption of St3 is almost 40% reduced (and 31% for St2).

Dimensional stability. We looked at the swelling and shrinkage behaviour of the wood cubes upon soaking–drying cycles, from which we can calculate volumetric swelling coefficient (S) and anti-swelling efficiency (ASE) according to the equations given in ESI (**Figure 4-S2**†). Swelling and antiswelling efficiency are basic quantities that reject improvements in terms of dimensional stability of wood based materials. The average volumetric swelling values of the different treatments after the water-soaking cycles, and the anti-swelling efficiency values can be seen in **Figure 4-7**. The swelling coefficient is directly related to volume changes during water uptake–drying cycles: a low swelling value corresponds to high dimensional stability.
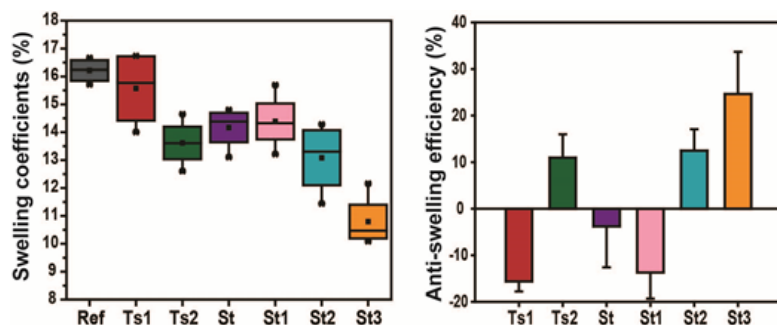
Figure 4-7 Left: average swelling values from the first immersion cycle. Right: anti-swelling efficiency values for tosylated wood (Ts1, Ts2), and treated wood (St, St1, St2, and St3) from the first immersion cycle.

ASE compares the swelling of untreated wood to the swelling of modified samples: a high ASE value means high dimensional stability (see ESI† for equations). In accordance with the water uptake results, the tosylation step (Ts2) already provides some anti-swelling efficiency (**Figure 4-7**). The samples of experiment Ts2 (high WPG1) show ASE values around 15%, whereas Ts1 (low WPG1) samples present negative values (-15%). This negative value may be explained by the rearrangements of the cell wall polymer during the solvent impregnation, which make the cell wall more accessible to water, and which is not compensated by the reduction of the –OH functionalities. The shrinkage of the Ts1 samples directly after reaction reported in Table 1 also supports this hypothesis.

The best ASE was observed with St3 samples (which have the highest WPG, and presented the most significant bulking effect after treatment) with values around 25% after first water immersion cycle, which represents a significant improvement. Cell wall modifications that exclusively lead to cell lumen filling and fail in modifying the cell wall itself have limited efficiency. This is clearly shown by the negative ASE value observed for the St sample set, where the polymer is found in lumen only. The difference between the ASE values of St2 and St3 suggests that the total polymer content in the cell wall plays an important role on the final properties.

Nanomechanical properties of cell walls. Mechanical properties of reference, tosylated (Ts2) and modified (St3) cell walls were investigated by nanoindentation. Both hardness and indentation modulus showed a significant ($P < 0.001$, U-test) increase of about 17% and 12% respectively from the unmodified cell walls to modified cell walls (**Figure 4-8**). Further, the tosylated cell walls show the highest increase in hardness and indentation modulus, with values of about 30% and 13%, respectively. However, we assume that this could be a result of embedding material diffusion inside the cell walls.
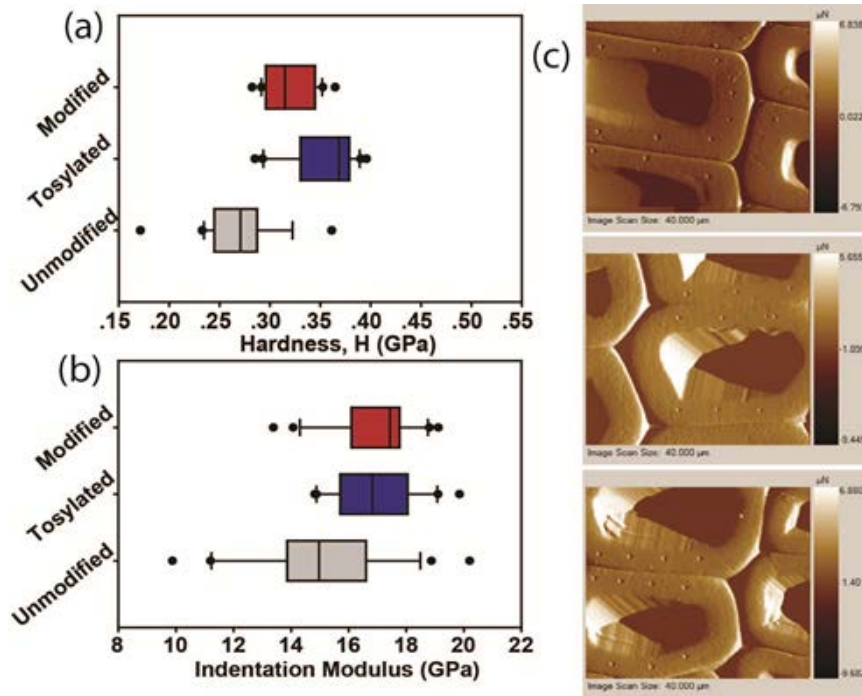
Figure 4-8 (a) Hardness and (b) indentation modulus of unmodified, tosylated (Ts2), and modified cell walls (St3). (c) AFM images of indented cell walls (from top bottom: reference, tosylated, and modified cell walls).

Conclusions

In this work, a series of composites of spruce bulk wood and polystyrene were produced with different pre-treatments (no tosylation, low weight gain tosylation and high weight gain tosylation). We demonstrated that the diffusion of hydrophobic monomers into the cell walls and their polymerization was significantly enhanced with the pre-functionalization of hydroxyl groups, resulting in an efficient cell wall bulking. The method uses mild conditions (i.e. the wood retains its mechanical properties) and yields new wood materials with limited weight gain and improved properties: both dimensional stability and hydrophobicity are increased. Such improvements are highly desirable and will help promoting the use of wood as a material from renewable resources with more reliable properties.

Acknowledgements

Notes and references

1. D. Feldman, Journal of Polymer Science: Polymer Letters Edition, 1985, 23, 601-602.

2. C. A. S. Hill, Wood Modification: Chemical, Thermal and Other Processes, John Wiley & Sons Ltd., Chichester, 2006.

3. R. M. Rowell, Handbook of Wood Chemistry and Wood Composites, 2nd edn., CRC Press, Boca Raton, 2012.

4. S. Lande, M. Eikenes, M. Westin and H. Schneider Marc, in Development of Commercial Wood Preservatives, American Chemical Society, 2008, vol. 982, pp. 337-355.

5. C. Mai and H. Militz, Wood Science and Technology, 2004, 37, 339-348.

6. C. Mai and H. Militz, Wood Science and Technology, 2004, 37, 453-461.

7. C. Zollfrank, Wood Science and Technology, 2001, 35, 183-189.

8. R. M. Rowell, A.-M. Tillman and R. Simonson, J Wood Chem Technol, 1986, 6, 427-448.

9. R. M. Rowell, Forest Products Journal, 2006, 56, 4-12.

10. J. Stamm Alfred, in Wood Technology: Chemical Aspects, AMERICAN CHEMICAL SOCIETY, 1977, vol. 43, pp. 115-140.

11. E. L. Ellwood, R. C. Gilmore and A. J. Stamm, Wood Science and Technology, 1972, 4, 137-141.

12. A. J. Stamm, Wood and cellulose science, Ronald Press Co., New York,, 1964.

13. S. Bach, M. N. Belgacem and A. Gandini, Holzforschung, 2005, 59, 389.

14. R. Devi and T. Maji, Wood Science and Technology, 2012, 46, 299-315.

15. W. Gindl, F. Zargar-Yaghubi and R. Wimmer, Bioresource Technology, 2003, 87, 325-330.

16. R. E. Ibach and R. M. Rowell, Holzforschung, 2001, 55, 358.

17. W. L. E. Magalhães and R. R. da Silva, Journal of Applied Polymer Science, 2004, 91, 1763-1769.

18. Y. Zhang, S. Y. Zhang, D. Q. Yang and H. Wan, Journal of Applied Polymer Science, 2006, 102, 5085-5094.

19. M. G. S. Yap, L. H. L. Chia and S. H. Teoh, J Wood Chem Technol, 1990, 10, 1-19.

20. M. A. Ermeydan, E. Cabane, A. Masic, J. Koetz and I. Burgert, ACS Applied Materials & Interfaces, 2012, 4, 5782-5789.

21. R. Rowell and W. Ellis, Wood and Fiber Science, 1978, 10, 104-111.

22. G. I. Mantanis, R. A. Young and R. M. Rowell, Wood Science and Technology, 1994, 28, 119-134.

23. Furuno T., Imamura Y. and K. H., Wood Science and Technology, 2003, 37, 349-361.

24. M. Morita and I. Sakata, Wood Science and Technology, 1991, 25, 215-224.

25. N. Gierlinger, C. Hansmann, T. Röder, H. Sixta, W. Gindl and R. Wimmer, Holzforschung, 2005, 59, 210-213.

26. N. Gierlinger, T. Keplinger and M. Harrington, Nat. Protocols, 2012, 7, 1694-1708.

27. N. Gierlinger and M. Schwanninger, Spectroscopy, 2007, 21, 69-89.

28. W. H. Tsai, F. J. Boerio, S. J. Clarson, E. E. Parsonage and M. Tirrell, Macromolecules, 1991, 24, 2538-2545.

29. N. S. Ham and A. N. Hambly, Australian Journal of Chemistry, 1953, 6, 135-142.

30. E. Baysal, A. Sonmez, M. Colak and H. Toker, Bioresource Technology, 2006, 97, 2271-2279.

31. R. R. Devi, I. Ali and T. K. Maji, Bioresource Technology, 2003, 88, 185-188.

32. M. H. Schneider, K. I. Brebner and I. D. Hartley, Wood Fiber Sci, 1991, 23, 165-172.

33. J. Rieger, J Therm Anal, 1996, 46, 965-972.

Supporting information

Improvement of wood material properties via in-situ polymerization of styrene into tosylated cell walls

Mahmut A. Ermeydan,[a] Etienne Cabane,[bc] Notburga Gierlinger,[bc] Joachim Koetz[d] and Ingo Burgert[bc]*

[a]Max Planck Institute of Colloids and Interfaces, Department of Biomaterials, Potsdam, Germany

[b]ETH Zürich, Institute for Building Materials, Zürich, Switzerland

[c]Empa - Swiss Federal Laboratories for Material Testing and Research, Applied Wood Research Laboratory, Dübendorf, Switzerland

[d]University of Potsdam, Institute of Chemistry, Potsdam, Germany
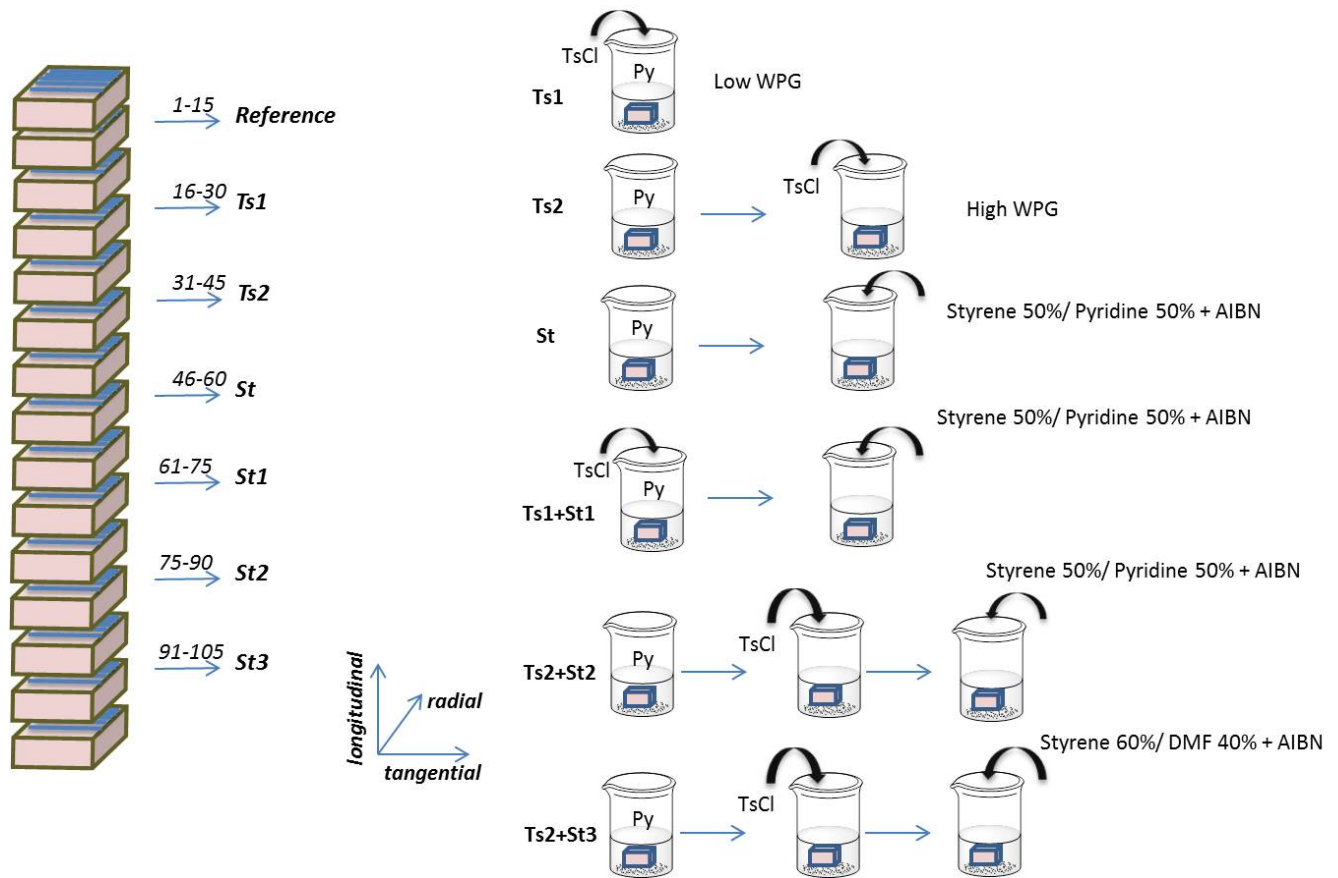
Figure 4-S1. Left: wood sampling: fifteen (1x1x0.5 cm^3) wood cubes for each set cut from spruce, in the longitudinal direction. Right: schematic representation of experimental flow. Ts1 (tosylation – low WPG), Ts2 (tosylation – high WPG), St (Styrene polymerization without tosylation pre-treatment), St1 (low WPG tosylation + styrene polymerization), St2 (high WPG tosylation + styrene polymerization), St3 (high WPG tosylation + styrene polymerization).

$$S(\%) = \frac{(V_i - V_{ii})}{V_{ii}} \times 100$$

where S(%): volumetric swelling; V_i: wood volume after wetting with liquid water; V_{ii}: wood volume of oven-dried samples before wetting

$$ASE(\%) = \frac{S_{um} - S_m}{S_{um}} \times 100$$

where ASE(%): antishrinking/antiswelling efficiency resultin from the modification; S_m: modified volumetric swelling coefficient; S_{um}: unmodified volumetric swelling coefficient.

$$WU(\%) = \frac{(w_{ii} - w_i)}{w_i} \times 100$$

where WU(%): percentage of water uptake of the samples; w_i: initial weight of the sample; w_{ii}: wet weight of the sample after water-soaking

Figure 4-S2. Equations for Swelling (S), Anti-swelling efficiency (ASE), and Water Uptake (WU)

$$EMC(\%) = \frac{(m - m_{od})}{m_{od}} \times 100$$

where EMC: is the moisture content;
m is the mass of the wood (with moisture) and
m_{od} is the oven-dry mass of the wood (i.e. no moisture)

Figure 4-S3. Equation for Equilibrium Moisture Content (EMC).

Raman imaging and spectroscopy - Advanced Fitting tool:

The tool for advanced fitting (WitecPlus software) allows spectra to be fitted with Gaussian curve function. First dataset was background subtracted, and used to fit polystyrene curve at 1005 cm^{-1} to the data set by keeping the width of the curve constant.

(a)
$$y = y_0 + \sum_{i=0}^{n-1} Amp_i\, e^{-0.5\left(\frac{x-x_i}{s_i}\right)^2}$$

$$w_i = s_i\sqrt{8\ln(2)}$$
$$A_i = Amp_i s_i \sqrt{2\pi}$$

n	$=$	*Number of Gauss Functions*
y_0	$=$	*Offset*
x_i	$=$	*Center*
s_i	$=$	*Width (Standard Deviation)*
Amp_i	$=$	*Amplitude*
w_i	$=$	*Width (FWHM)*
A_i	$=$	*Area*

(b)

Name	Auto	Start Value	Value	Vary
y0	☐	10	10	☐
x0	☐	1005.0214	1005.0214	☐
s	☐	4.5	4.5	☐
Amp	☑	31.222355	31.222355	☑

(c)
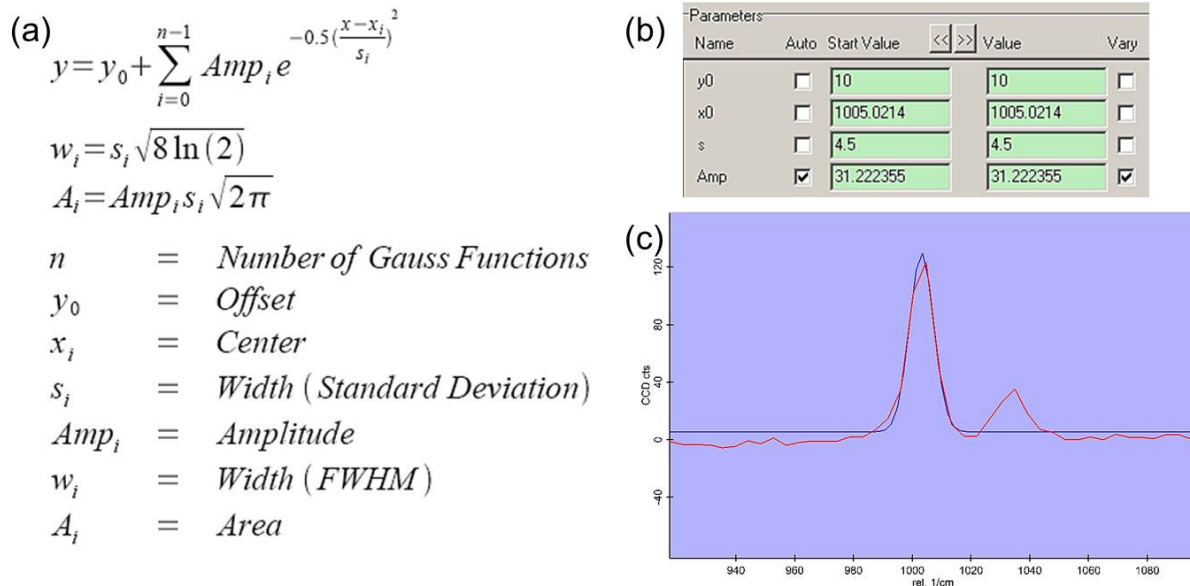
Figure 4-S4: (a) Gaussian function and nomenclature of parameters used in the function. (b) parameter values to obtain related polystyrene image. (c) Gaussian fit of polystyrene curve at 1005 cm^{-1} in the data set.

WPG% / Area Fraction Analysis:

	Image area (mm²)	Filled area (mm²)	Cell wall area (%)	Cell wall area (mm²)	Polymer area (mm²)	WPG (%)	M (untreated wood) (g)	M (PSt added) (g)	M (PSt) in lumen (g)	M (PSt in the cell wall) (g)	the % of PSt in the cell wall (%)
St	1,712	1,368	37,13	0,636	0,732	38,8	10,00	3,88	3,88	0,00	0,0
St1	1,712	1,27	35,33	0,605	0,665	35,7	10,00	3,57	3,52	0,05	1,3
St2	1,712	0,959	38,11	0,652	0,307	19,7	10,00	1,97	1,62	0,35	17,6
St3	1,712	1,093	38,1	0,652	0,441	30,2	10,00	3,02	2,34	0,68	22,7

Figure 4-S5: SEM images of (a) St, (b) St1, (c) St2, and (d) St3 samples used for semi-quantitative polymer WPG%
determination in the cell walls. (e) WPG% and area values to calculate polymer content in cell walls.

From the SEM pictures, we can determine the area occupied by the cell wall material (Cell wall area), and
the area occupied by the polymer in the lumen (Polymer area).
(Polymer area) = (Filled area)-(Cell wall area)
From the total weight percent gain determined after full modification, we know exactly how much
polymer (in grams) was added to the wood. Assuming that for experiment St (no pretreatment), the
polymer added is only located in the lumen part (which is consistent with literature), we can calculate
the amount of polymer located in the lumen of other experiments (M (PSt) in lumen) as a function of the
area occupied by the polymer on the SEM picture.
(M (PSt) in lumen) = (Polymer area of St1)/ (Polymer area of St) x (M (PSt) in lumen for St)
Once we have the weight of polymer in the lumen, we can get to the weight of polymer in the cell wall
since we know the total amount of polymer:
M(PSt in the cell wall) = M (PSt added) – M(PSt in the lumen)
% of Pst in the cell wall = M (Pst in the cell wall)/ M (Pst added) x 100

Chapter 5. Fully biodegradable modification of wood for improvement of dimensional stability and water absorption properties by poly(ε-caprolactone) grafting into the cell walls

Mahmut A. Ermeydan,[abc] Etienne Cabane,[ab] Philipp Hass, [ab] Joachim Koetz[d] and Ingo Burgert[ab*]

[a] *Max Planck Institute of Colloids and Interfaces, Department of Biomaterials, Potsdam, Germany.*

[b] *ETH Zurich, Institute for Building Materials, Zurich, Switzerland.*

[c] *Empa - Swiss Federal Laboratories for Material Testing and Research, Applied Wood Research Laboratory, Dübendorf, Switzerland.*

[d] *University of Potsdam, Institute of Chemistry, Potsdam, Germany.*

Abstract

Materials derived from renewable resources are highly desirable in view of more sustainable manufacturing. Among the available natural materials, wood is one of the key candidates, because of its excellent mechanical properties. However, wood and wood-based materials in engineering applications suffer from various restraints, such as dimensional instability upon humidity changes. Several wood modification treatments increase water repellence, but the insertion of hydrophobic polymers can result in a composite material which cannot be considered as renewable anymore. In this study, we report on the grafting of the fully biodegradable poly(ε-caprolactone) (PCL) inside the wood cell walls by Sn(Oct)2 catalysed ring-opening polymerization (ROP). The presence of polyester chains within the wood cell wall structure is monitored by confocal Raman imaging and spectroscopy as well as scanning electron microscopy. Physical tests reveal that the modified wood is more hydrophobic due to the bulking of the cell wall structure with the polyester chains, which results in a novel fully biodegradable wood material with improved dimensional stability.

Introduction

Wood has been known and used as a renewable raw and engineering material for thousands of years and is still nowadays an essential building material due to desirable features such as light weight, processability, good mechanical properties, sustainability, and aesthetic appearance.[1–3] A further strong argument in view of the development towards more sustainable societies is that wood is suitable for energetic recovery at the end of its service time, after an ideally long-lasting carbon storage in a high value application.

However, wood has some drawbacks, related to the cell wall hydrophilic nature, which limit its long term usage as an engineering material. Wood cell walls are composed of longitudinally oriented cellulose fibrils embedded within an amorphous hemicellulose and lignin matrix,[4] and as such, they can absorb large amounts of water from the environment. Water absorption and desorption cycles due to humidity changes cause swelling and shrinking of the cell walls, leading to dimensional instability that can result in severe deformation or crack initiation and failure of the wood material.[1–3] In addition, the presence of water in the cell wall provides an appropriate environment for fungal attack resulting in the biodegradation of wood.[1,3,5]

Research in the field of wood modification focuses mainly on decreasing the water uptake of cell walls, in order to increase wood dimensional stability. It is well known that chemicals have to penetrate into the cell wall structure and have to be locked inside in order to have a strong impact on wood properties.[1,3,6] As an example, the formation of covalent bonds between –OH groups of cell wall polymers and small reactive molecules is a well-documented approach.[7–9] Another option is in situ grafting polymerization of monomers.[1,3,10] Various challenges have to be considered when modifying wood cell walls, for example, the use of mild conditions to avoid degradation of the cell wall structure during modification reactions, or the elimination of harmful by-products. In addition, the hygroscopic nature of the cell walls is a severe barrier to the introduction of hydrophobic materials, and impedes the insertion of small molecules solubilized in polar solvents. There are several studies on in situ polymerization of hydrophobic monomers inside wood, but very few of them report on the successful insertion of polymers inside the cell wall structure, and as a result, on an efficient improvement of dimensional stability.[11–15] Recently, our group reported on a wood pre-treatment enhancing the introduction of hydrophobic molecules within the cell wall.[16] We successfully inserted hydrophobic flavonoid molecules

inside the cell walls, yielding a wood material with reduced water uptake as well as increased dimensional stability.

In addition to the research on improving wood properties, the development of novel wood based engineering materials is also driven by ecological concerns (sustainability, ecoefficiency, and recyclability of the products). In the field of wood modification with synthetic polymers, the commonly used chemicals yield wood-polymer composite materials that have to be considered as plastics when it comes to recycling.[17] To overcome this drawback, it is preferable to utilize biodegradable polymers for modification and develop waste-free materials.[18] The main strategies to eliminate the disposal problem of materials are the utilization of polymeric materials derived from renewable resources (e.g. wood flour, starch, cellulose, and chitin) and the production of composites with biodegradable synthetic materials (such as polyesters including poly(ε-caprolactone), poly(lactic acid), poly(3-hydroxybutyrate), and poly(glycolic acid)).[18–22] Poly(ε-caprolactone) (PCL) is one of the most widely evaluated and systematically studied biodegradable synthetic polymers.[18,19] It is a semi-crystalline hydrophobic polyester that can be polymerized by ring opening polymerization initiated by alcohols. The combination of PCL with wood derived products has been investigated previously, mainly for the development of biodegradable materials based on wood particles or components (such as wood flour and PCL blends, or grafting of caprolactone from cellulose).[23–25]

In view of the abovementioned advantages of PCL, we regarded caprolactone as an interesting candidate for in situ polymerization of wood and we report here on the first attempt to graft solid wood with poly(caprolactone) chains. For that purpose, we prepared a fully biodegradable material obtained by the ROP of caprolactone monomer initiated by –OH groups from cell wall components. Dimensional stability and water repellence of the modified wood are significantly improved, while the natural attributes of wood are retained, which shows that the new material can potentially be used as a fully green material.

Experimental

Materials

ε-Caprolactone (CL), tin(II) 2-ethylhexanoate (Sn(oct)2), dry dimethyl formamide (DMF), dry toluene, and acetone were bought from Sigma-Aldrich and used as received.

Chemical modification of wood cubes

Wood sampling. Sixty Norway spruce (Picea abies) sapwood cubes (1 cm × 1 cm × 0.5 cm; radial × tangential × longitudinal, respectively) were cut along the grain, and dried in an oven at 63 °C overnight. The cubes were divided into four sets of fifteen cubes: one set as reference wood (i.e. untreated), one set as controls (i.e. placed under the reaction conditions without the reactive compounds), and two sets for full modification. After treatment, ten cubes from each set were used for physical characterization (i.e. leaching, swelling (S), water uptake (WU), anti-swelling efficiency (ASE) tests, equilibrium moisture content (EMC), and contact angle measurement). The rest of the cubes were used for structural, chemical, and mechanical analysis. A detailed description of the experimental workflow is given in ESI (**Figure 5-S1†**), and the reaction scheme and sample nomenclature are summarized in **Figure 5-1**.
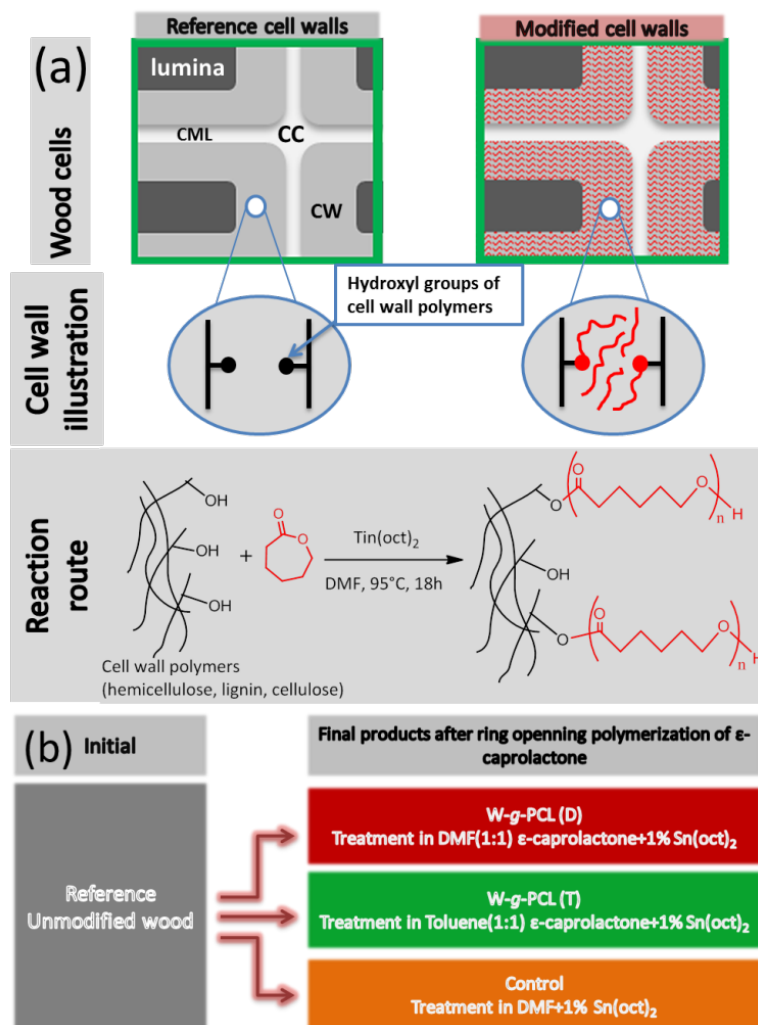
Figure 5-1 (a) Schematic illustration and reaction route of polycaprolactone grafting on the cell wall polymers (CML: compound middle lamella, CC: cell corner, CW: cell wall). (b) Nomenclature for the treatment of spruce wood blocks under different conditions.

Impregnation and in situ ring opening polymerization of PCL. The wood cubes were dried at 63 °C for one day to reach a nearly dry wood cube with estimated moisture content around 1%. Cubes were placed in 50 ml of anhydrous DMF or toluene. After one day of swelling, the cubes were placed in flasks containing a solution of ε-caprolactone (20 g) with 2% (w/w) of $Sn(Oct)_2$ as the initiator. The cubes were stored in this solution for one day in order to maximize monomer impregnation in wood cell walls before polymerization. Prior to the reaction, 20 ml of dry DMF or toluene were added to the flask and the solution was degassed by bubbling argon for 30 minutes. The reaction flasks were heated to 95 °C for 18 hours to polymerize ε-caprolactone. After reaction completion, the wood cubes were washed with several volumes of acetone (approx. 4 hours), then with water (24 hours), and finally dried in the oven at 63 °C for 24 hours. Additional acetone washing was carried out by Soxhlet extraction for 96 hours to estimate how much polycaprolactone is chemically grafted on cell wall polymers. All solvents used for polymerization reactions and washing steps (DMF, toluene, acetone) are good solvents for both the ε-caprolactone monomer and the poly(caprolactone) polymer.

Characterization

Raman spectroscopy and imaging. 30 μm thick cross sections were cut on a rotary microtome (LEICA RM2255, Germany) in a region 0.5–1 mm below the surface of the wood cubes and placed between the glass microscope slide and the coverslip with a drop of water to maintain cell walls under wet conditions. Spectra were acquired with a confocal Raman microscope (alpha300, WITec GmbH, Ulm, Germany) equipped with an objective (60×, NA = 0.8, 0.17 mm coverslip correction from Nikon Instruments, Amstelveen, The Netherlands). A 532 nm laser (Crysta Laser, Reno, NV, USA) was focused with a diffraction limited spot size of 0.61 λ/NA and the Raman signal was detected with an air cooled back illuminated CCD camera (DV401-BV, Andor, Belfast, North Ireland) behind the spectrograph (UHTS 300, WITec) with a spectral resolution of 3 cm^{-1}. For mapping, an integration time of 0.4 s was chosen, and every pixel corresponds to one spectrum acquired every 0.5 μm. Two-dimensional chemical images of the wood components and added polyester were compiled using WitecProject software with the integration filter.

Scanning electron microscopy (SEM) and energy dispersive X-ray (EDX) analysis. Structural details of the treated and untreated wood samples were analysed using an (E)SEM device (FEI FEG-ESEM Quanta 600, FEI Company, Hillsboro, OR, USA) with a backscattered

electron (BSE) detector operated at 7.5 kV with a 10 mm sample–detector distance, 4.0 nm spot size, and 0.75 Torr pressure. EDX analysis was performed using the INCA Energy 300 system (Oxford Instruments, UK) with an X-Max 80-Detector. Samples were coated with platinum before analysis.

Volume change and weight percentage gain (WPG). Dimensions and weights of the wood cubes were measured before and after all treatments (polymerization, water immersion, and drying) in order to determine the volume and weight changes caused by the chemical treatment.

Swelling coefficient (S), anti-swelling efficiency (ASE), and water uptake (WU). The reference, control and treated cubes were immersed in deionized water for five days with moderate shaking (soak cycle 1). Then cubes were placed in an oven at 103 °C overnight for drying (drying cycle 1). Samples were immersed again in deionized water for the second water soaking and subsequent drying cycles. The degree of dimensional stability of the modified wood cubes was obtained by calculating the S and the ASE as reported.[26] The equations for swelling, anti-swelling efficiency, and WU calculations are given in ESI (**Figure 5-S2†**). The water repellence is given by the WU calculations. Equilibrium moisture content (EMC). Wood exposed to a constant relative humidity with a constant temperature absorbs or releases water and reaches a constant moisture content called the EMC. Reference, control, and PCL-grafted samples were equilibrated in a sealed system with a relative humidity of 75% (obtained with a saturated solution of NaCl) at room temperature. When the samples reached equilibrium (i.e. constant weight), samples were oven-dried at 103 °C and weight differences were calculated to determine the final moisture content. For each set, five samples were used for the measurements. The equation for the EMC calculation is given in the ESI (**Figure 5-S3†**).

Contact angle measurements. Contact angle measurements were performed on a cross-section (RT-plane) of five samples per set (reference, control, W-g-PCL(D), and W-g-PCL(T)). All samples are acclimatized in normal climate (20 °C and 65% relative humidity) until equilibrium. To avoid any surface aging effects on the measurement, the cross-section was smoothened with a sledge microtome GSL 1 (WSL, Birmensdorf, Switzerland) less than 24 h before the measurement. A standard contact angle measuring device (SCA 20, dataphysics) was used to apply 11 µl droplets of distilled water (LiChrosolv ®) on the smoothened cross-section and to record its evolution by taking images with an appropriate frame rate, which lay between 0.5 and 25 frames per second. Besides the comparison of the different treatments with the untreated wood samples, the procedure was repeated on plastic sheets to estimate the amount of water evaporated

during the experiment. The determination of the contact angles was done using the software included in the SCA 20 contact angle measuring device. For the comparison of the different surfaces, the evolution of the contact angle was fitted using a linear function and its first parameter (climax) was used. When possible, the fitting procedure started after the droplet was stabilized on the surface.

Nanoindentation. The mechanical characterization of tracheid cell walls was carried out as reported elsewhere,[16] on a Hysitron Triboscan UBI-1 nanoindentation system (Minneapolis, MN). For this purpose, samples were dried overnight at 63 °C and subsequently embedded in AGAR resin (AGAR low viscosity resin kit, AGAR Scientific Ltd, Stansted, UK). Specimens were immersed into the embedding resin and cured overnight at 60 °C. 2 mm thick slices were cut from the resin blocks. The embedded specimens were glued onto metal discs (15 mm AFM specimen discs). Surfaces were smoothed by polishing. Quasi-static indentation tests were performed in a force-controlled mode, the indenter tip (Berkovich-type triangular pyramid) was loaded to a peak force of 250 μN at a loading rate of 100 μN s^{-1}, held at constant load for 15 s, and unloaded at a rate of 100 μN s^{-1}.

Results and discussion

Poly(caprolactone) grafting inside the cell walls

Poly(caprolactone) can be prepared by catalyzed ring-opening polymerization of ε-caprolactone, mainly using metal based catalysts (poor metals such as aluminum and tin based catalysts, alkaline earth metals, transition metals, and rare earth metals),[27–30] but also enzymatic or organic catalytic systems.[31] The hydroxyl groups present in the reaction media act as coinitiators, and the polymerization proceeds through the activated stannous alkoxide species formed in situ.[32,33] The –OH groups of carbohydrates (such as cellulose) were already used as initiators for the ROP of caprolactone, yielding cellulose grafted with PCL chains.[34–38] Within wood, our aim was to use the abundant –OH groups present on the cell wall polymers (cellulose, lignin, and hemicellulose) to initiate the polymerization of ε-caprolactone and obtain wood grafted with polyester chains. The penetration of caprolactone in the cell wall structure is a critical step in the modification. As reported in the literature, a preferred solvent for the ε-caprolactone ROP is toluene.[30,39,40] However, it is known that the wood swelling potential of toluene is limited in comparison to DMF, which swells wood to a greater extent.[41] Since ROP of caprolactone was reported to take

place in different solvents, including DMF,[42] we ran the experiments with both solvents (W-g-PCL(D) for DMF and W-g-PCL(T) for toluene). One set of wood cubes was placed in the same reaction conditions as the experiment W-g-PCL(D), but without the monomer. These samples (control(DMF)) were used for comparison with the fully treated samples. The WPG and dimensional changes resulting from the different treatments are summarized in **Table 5-1**.

The weight percent gain (WPG %) and volume change which were determined after ring opening polymerization provide a first indication of the success of the modification. W-g-PCL(D) showed the highest WPG and permanent volume change after polymer modification. The positive dimensional changes of W-g-PCL(D) and W-g-PCL(T) samples can be related to the presence of polymers within the wood cell wall: it has been shown already that a permanent volume change after a successful modification is mainly due to cell wall bulking with new material.[43,44] The values in **Table 5-1** reported for control samples indicate a slight weight loss and a permanent volume reduction of about 7%. These observations may be explained by the leaching of some cell wall components, mainly extractives, and the DMF treatment resulted in a re-organization of the cell wall polymers (especially in the amorphous lignin/hemicellulose matrix). The WPG reduction after additional acetone washing by Soxhlet extraction reveals that homopolymers that were not attached to the cell wall polymers were removed which also resulted in a reduction of the cell wall bulking effect.

Residual tin was determined after the first washing step and was found in small amounts with a homogeneous distribution across the cell wall by EDX analysis (estimation based on EDX calculation: ~1% (w/w)) (**Figure 5-S4†**).

Table 5-1 Summary of weight percent gains and volume changes of spruce wood cubes after ring opening polymerization reactions with DMF and toluene, and control conditions: after initial washing and Soxhlet extraction.

| Exp. ID	Initial washing		Soxhlet extraction	
	WPG (%)	Vol. change (%)	WPG (%)	Vol. change (%)
W-g-PCL(DMF)	17,9	5,5	11,2	3,6
W-g-PCL(Toluene)	11,2	2,4	5,2	1,8
Control (DMF)	-1,1	-7,3	N/A	N/A

Distribution of polymer in wood

To determine the spatial distribution of poly(caprolactone) after polymer modification at the cell and tissue levels, a series of SEM pictures of cube cross sections was performed. SEM images of unmodified reference cell walls are shown in **Figure 5-2a** and **b**. **Figure 5-2c** and d show that no noticeable cell wall deformations were observed for the control, which indicates that the modification process in DMF did not affect the wood tissue microstructure.

During the reaction process, wood cubes were completely immersed in the reaction solution, and it is highly expected that polymerization takes place also in the cell lumina due to trace amounts of water molecules in the solution, which can compete with cell wall –OH groups for the initiation of caprolactone ROP. However, the PCL free chains in solution were washed away with acetone after modification, and as a result, **Figure 5-2e** and **f** reveal that the cell wall lumina are essentially empty for the W-g-PCL(D) samples. This result indicates that the weight gain of W-g-PCL(D) samples is mostly due to polymer bulking in the cell walls.
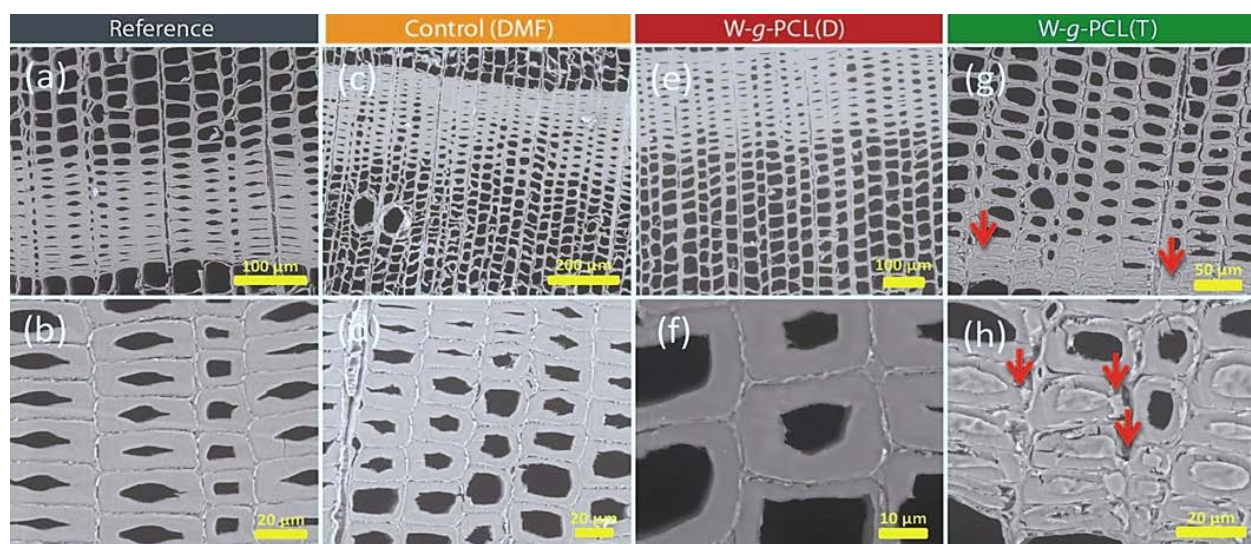
Figure 5-2 SEM images of microtomed cross-sections: (a–b) untreated cell walls; (c–d) control cell walls (i.e. treated with DMF + Sn(oct)2 at 95 °C); (e–f) in situ polycaprolactone grafted cell walls in DMF, and (g–h) in situ polycaprolactone grafted cell walls in toluene.

Although the samples modified in toluene (W-g-PCL(T)) were submitted to the same washing steps, some unbound polymer chains remain in the cell lumina and completely fill the micropores in the latewood regions (**Figure 5-2g** and **h**). This might be due to differences in the solvent system which affect the degree of polymerization. Toluene is one of the most favourable solvents for

efficient ε-caprolactone polymerizations under homogeneous conditions, which results in a high degree of polymerization.[45] However, toluene has limited wood swelling capabilities, which hinders the penetration of monomer into the cell wall, and therefore, one observes only little polymer in the cell wall, and some lumen filling with high molecular weight chains, when toluene is used as a solvent. In contrast, it is reported that ε-caprolactone polymerization with metal initiators in DMF can hinder the polymerization,[46] which may lead to shorter polymer chains that can in turn be more easily washed away and thus explain the absence of polyester in the cell lumina. Additionally, the excellent swelling properties of DMF allow for a more widespread polymerization inside the cell wall.

In addition to SEM analysis, we investigated chemical changes in the modified spruce cell wall structure to determine whether poly(caprolactone) was polymerized within the cell walls. In this regard, confocal Raman microscopy is a powerful technique for the detailed analysis of plant cell walls which provides spectroscopic analysis of cell wall constituents and can be used to construct chemical imaging of the desired components.[47–49]

Typical Raman spectra of W-g-PCL(D), W-g-PCL(T), reference, and poly(caprolactone) polymer are shown in **Figure 5-3**. The spectra recorded for polymer grafted cell walls display the specific wood bands.[48,50]
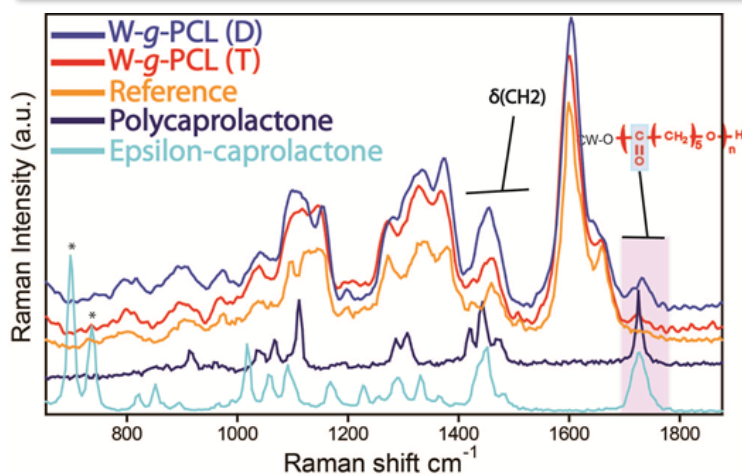
Figure 5-3 Raman spectrum of poly(caprolactone) grafted cell walls [W-g-PCL(D), W-g-PCL(T)] compared with the reference, poly(caprolactone) and epsilon-caprolactone spectra in the 600–1900 cm^{-1} spectral range.

In addition to the wood Raman bands, important changes were observed in the 1400–1500 cm^{-1} and 1700–1750 cm^{-1} regions. As shown in **Figure 5-3**, poly(caprolactone) has strong bands between 1400 and 1500 cm^{-1} which belong to δ(CH2) vibrations and a strong band at 1725 cm^{-1} which belongs to ν(C=O) vibration.[51] In the Raman spectra of polymer grafted cell walls, we observed a clear signal related to the presence of –CH2– groups from PCL. In addition, the C=O

bond of the polyester can be easily visualized after modification. From the intensity distribution of the new peaks, it is clear that the modification in DMF resulted in higher PCL cell wall contents. These polyester peaks were clearly absent in the reference wood samples. In the Raman spectrum shown in **Figure 5-3**, the Raman bands of ε-caprolactone monomer at 695 and 735 cm^{-1} (assigned to breathing motion vibrations in the seven member ring structure) cannot be found, which indicates that the modified cell walls contain only polymerized caprolactone.

The Raman images shown in **Figure 5-4** were obtained via scanning of a latewood cross-section from poly(caprolactone) grafted cell walls, and integration of the relevant peaks for wood constituents and poly(caprolactone) found in the spectra (see characterization).
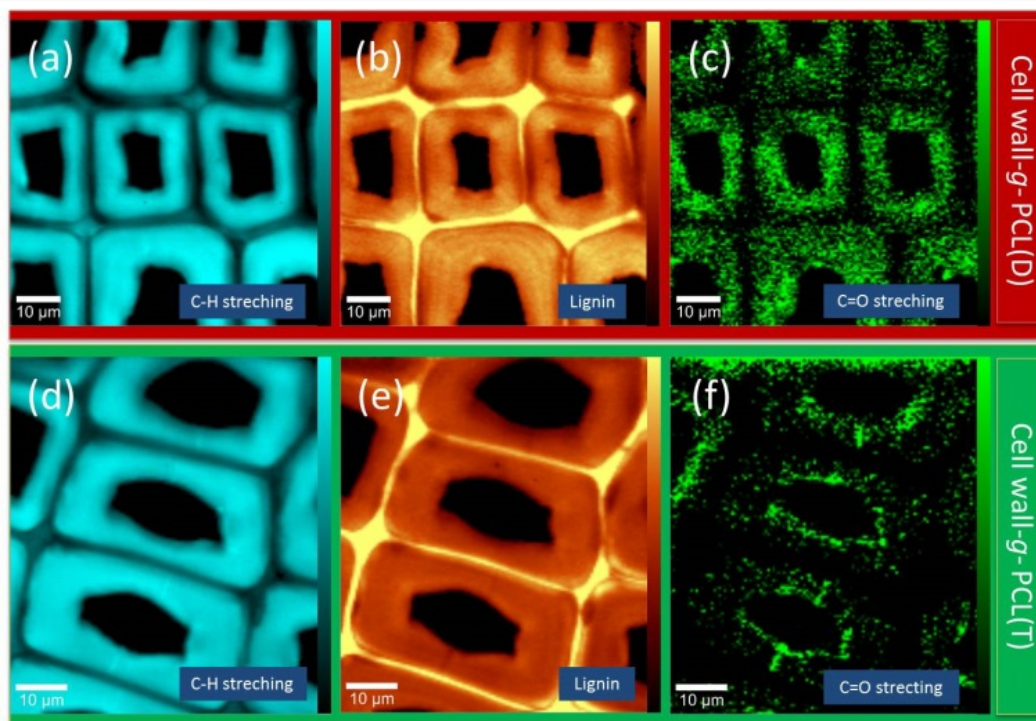
Figure 5-4 Raman images (a–c: 70 × 70 μm² and d–f: 60 × 70 μm²) of the latewood cell wall tissue. Images were plotted by integration of Raman bands from the spectral data set: (a, d) C–H stretching groups (mainly cellulose) (2850–3010 cm⁻¹), (b, e) lignin (1555–1660 cm⁻¹), and (c, f) polycaprolactone carbonyl group (1715–1735 cm⁻¹).

In **Figure 5-4**, images **a** and **d** represent the CH groups (from cellulose) and the lignin distributions are shown in images **b** and **e**, depicting the overall cell wall structure. The distribution of cellulose highlights the secondary cell wall regions (bright turquoise zones), whereas the lignin has higher intensity in the cell corners and compound middle lamella (bright yellow zones). The poly(caprolactone) distribution of polymer grafted cell walls (W-g-PCL(D) in

Figure 5-4c, W-g-PCL(T) in **Figure 5-4f**) indicates that polymerization took place in the cell walls for both experiments (green zones). In the W-g-PCL(D) cell walls, the poly(caprolactone) polymers are rather homogeneously distributed across almost the whole secondary cell wall, in contrast to the toluene experiment W-g-PCL(T), where poly(caprolactone) is predominantly located in a cell wall region close to the lumen. In both cases, brighter regions represent higher intensity of the related components, and the images clearly show that the penetration of the monomer (consequently the polymer) inside the cell wall is more efficient when a good solvent for wood such as DMF is used.

Improved wood properties

To evaluate improvements in dimensional stability and WU (water uptake) behaviour of the polyester grafted wood, we used the water-soaking method developed by Rowell et al.[26] This method based on subsequent cycles of drying and wetting is a common measurement protocol to assess the efficiency of wood modification treatments by the determination of changes in WU and dimensional stability as a response to water sorption/desorption.

Stability of polymers in wood and water repellence

Wood eventually loses weight during repeated soaking–drying cycles due to the removal of extractives and non-bound modifying compounds. The mass losses recorded for the different samples are given in **Figure 5-5a**. The significant difference between the mass loss of reference wood and treated samples may be explained as follows: the untreated wood loses extractives during the soaking–drying cycles, but for the other samples, those substances were most likely removed during the various modification steps. Samples containing poly(caprolactone) (W-g-PCL(D) and W-g-PCL(T)) show only little weight loss, indicating that the added material in the modified wood is locked within the wood structure. The increase in weight loss of W-g-PCL(D)
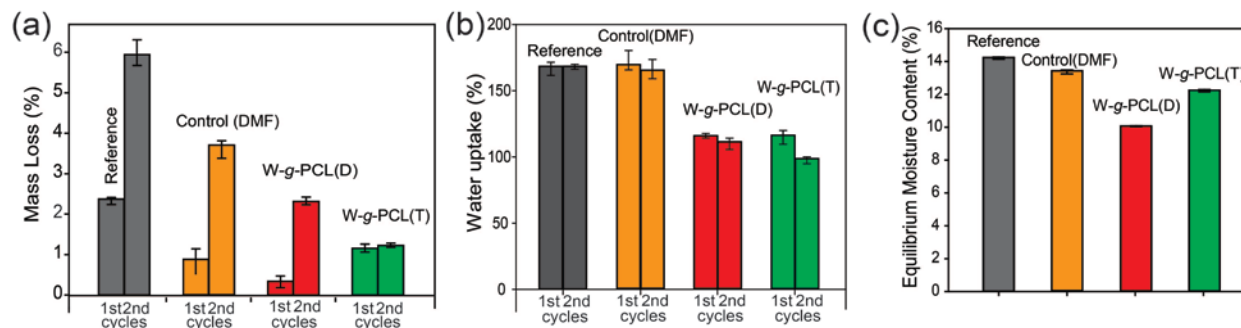
Figure 5-5 (a) Determination of cumulative mass loss due to leaching of unbound material after the cubes were immersed for five days in water (1st cycle) and after another five days of immersion in water (2nd cycle). (b) WU values for reference wood, polymerized wood (W-g-PCL(D), W-g-PCL(T)), and control(DMF). (c) EMC results at 75% relative humidity for reference wood, polymerized wood (W-g-PCL(D), W-g-PCL(T)), and control (DMF).

during the second cycle may be explained by removal of the shorter polymer chains from the cell lumen. The WU ability of the samples (after the first and second water immersion cycles) is shown in **Figure 5-5b**. After five days in water (1st cycle), the unmodified (reference) wood sample gains about 160% water, while wood-PCL composites gain about 100%. The trend is similar after the second immersion period. As expected, the grafted hydrophobic poly(caprolactone) chains provide some degree of protection against water uptake: the treated samples in DMF show at least 30% reduction in WU when compared to unmodified wood.

Another way to evaluate the affinity of the wood samples for water is to calculate the EMC. In this case, the samples were placed in a climate chamber with standard temperature (20 °C) and a relative humidity of 75%, to examine the WU exclusively at the cell wall level. Under these conditions, reference (unmodified) wood has an EMC of about 14%, as shown in **Figure 5-5c**. This value is slightly lower than literature values reported for Norway spruce (14.4%), and can be explained by the natural variability of wood.[52] The polymer grafted samples show less moisture adsorption. The highest hydrophobization is shown for the W-g-PCL(D) samples with an EMC of about 10%, which represents a 30% reduction of moisture content when compared to reference samples, and correlates well with the WU experiment.

Dimensional stability of polymer grafted wood

In order to evaluate the improvement of dimensional stability of modified wood, we observed the swelling and shrinkage behavior of the wood cubes upon water soaking–drying cycles. Calculations of volumetric S and ASE were made according to the equations given in ESI (**Figure 5-S2†**). The volumetric S values of the polymer grafted samples (W-g-PCL(D) and W-g-

PCL(T)) were compared with the reference (unmodified) and control (DMF) samples after each water-soaking and drying cycle (**Figure 5-6**).
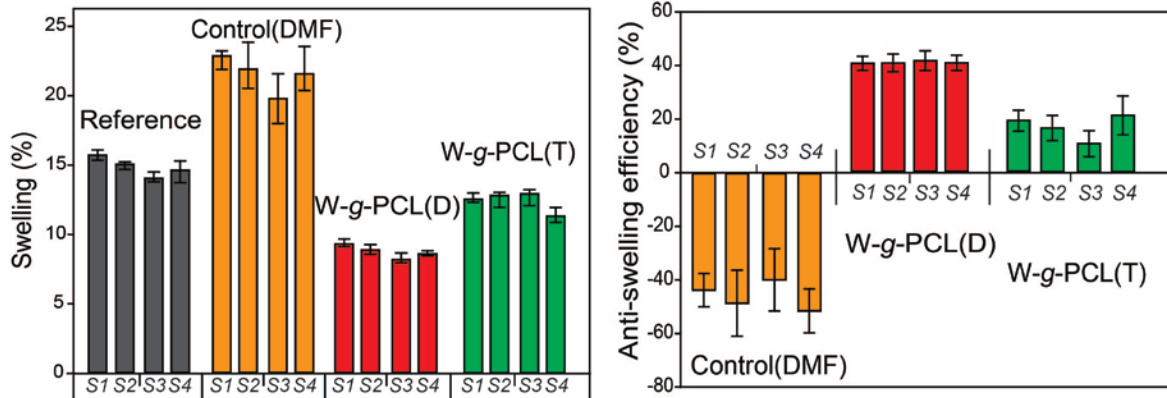
Figure 5-6 Left: average volume swelling values from the immersion and drying cycles. Right: ASE values for treated wood cubes (W-g-PCL(D), W-g-PCL(T), control(DMF)).

The wood volume changes upon water soaking and drying cycles are a result of swelling and shrinking of the wood cell walls. The volume of native wood typically swells 15 to 20%, depending on species, tissue type and environmental conditions. When hydrophobic material bulks the cell wall, the water affinity for wood is decreased, and less space is available for the water molecules to enter the cell wall, resulting in decreased swelling. A lower swelling value corresponds to a higher dimensional stability. As shown in **Figure 5-6**, the swelling of the W-g-PCL(D) samples is reduced to about 8%, while the reference wood samples swell to about 16%.

The ASE compares the swelling of unmodified wood with the swelling of treated wood. A high ASE value corresponds to high dimensional stability (see **Figure 5-S2†** for equations). The negative ASE of control samples may be explained by the removal of extractives and the re-arrangement of cell wall polymers (lignin/hemicelluloses), both phenomena contributing to a better water penetration in wood, and hence enhanced swelling. In contrast, the ASE values observed for W-g-PCL(D) samples, with values above 40% after each water immersion and drying cycle, indicate that the treatment strongly increases the dimensional stability of wood. The lower ASE values observed for the W-g-PCL(T) samples can be directly correlated with the amount of PCL located in the cell wall shown in **Figure 5-4c–f**, and confirm that the choice of solvent for the modification largely influences the final polymer content in the cell wall.

Contact angle measurements

The bulk wood modification also results in new surface properties. In **Figure 5-7**, we show representative curves for the evolution of the contact angle on different surfaces. The evolution of the contact angle on a plastic sheet (for comparison), the W-g-PCL(T), and W-g-PCL(D) treated surfaces fit to the applied linear function. The untreated and DMF treated surfaces absorbed the water droplet in less than 2 s and less than 0.5 s, respectively. Due to the lack of droplet stabilization, the fitting was performed using all available data points. The fast water absorption in the control samples is also reflected in the mean values for the contact angle changes which was about six times faster after the pure DMF treatment (mean climax reference: $-62.45°$ s^{-1}; control: $-374.7°$ s^{-1}). The comparison of the curves shows that both modification methods increase the hydrophobicity of the wood surface. After the W-g-PCL(D) treatment the contact angle decreased about 200 times more slowly than without the treatment (W-g-PCL(D): $-0.335°$ $s{-1}$). Although the total weight percent gain was higher for the modification with DMF and the spatial distribution showed a higher concentration in the cell wall for this method, the modification with toluene (W-g-PCL(T)) even led to a contact angle decrease that was again 10 times slower than that for W-g-PCL(D) (climax W-g-PCL(T): $-0.034°$ s^{-1}). Since the measurements were performed on cross sections with cut open cells, this behavior is probably due to the partially filled cell lumina, as was seen in Figure 2, which was not visible for W-g-PCL(D). However, the comparison with the plastic sheet ($-0.0097°$ s^{-1}) shows that there is still a considerable amount of water that is absorbed into the wood substrate.
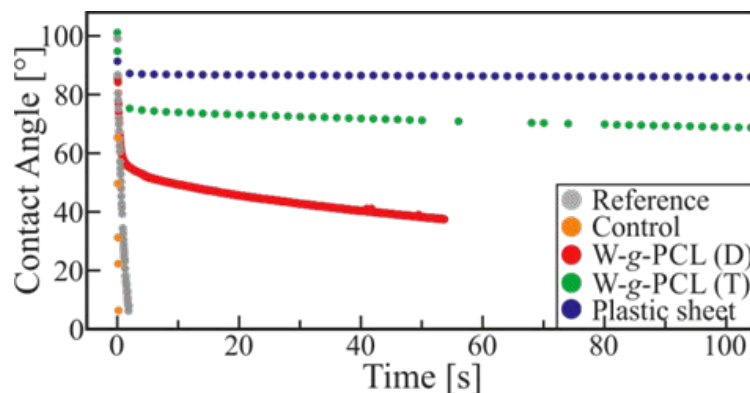
Figure 5-7 Contact angle measurements of reference, control(DMF), W-g- PCL(D), W-g-PCL(T), and plastic sheet.
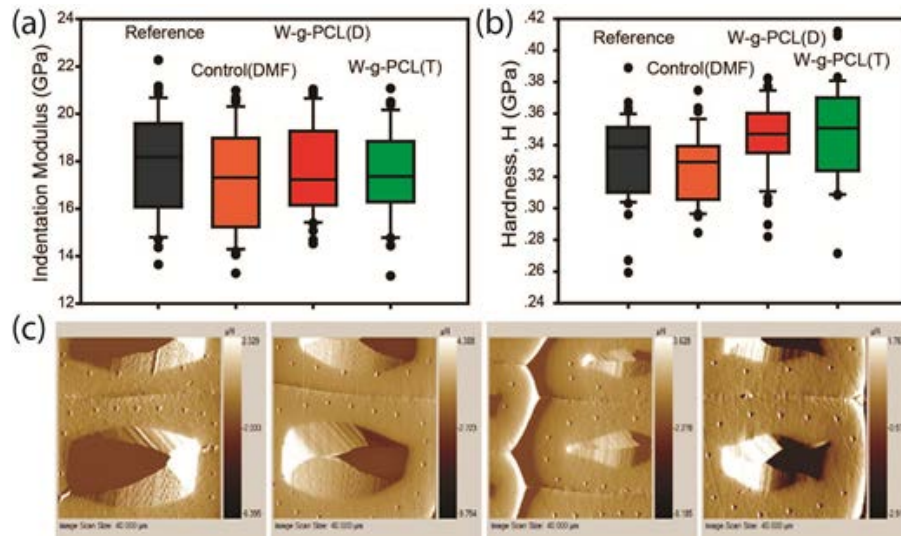
Figure 5-8 (a) Indentation modulus and (b) hardness of reference, polycaprolactone grafted, and DMF treated cell walls. (c) SPM (Scanning Probe Microscopy) images of nano-indented cell walls. Left-to-right: reference, control(DMF), W-g-PCL(D), W-g-PCL(T).

Nanomechanical properties of cell walls

The mechanical properties of reference, control(DMF) and poly(caprolactone) grafted cell walls were investigated by nanoindentation (**Figure 5-8**). The indentation modulus of modified cell walls and references were not significantly different ($P \geq 0.05$, U-test). PCL grafted cell walls show a slight ($P < 0.05$, U-test) increase in hardness when compared to the unmodified cell walls. The nanoindentation analysis essentially shows that the modification did not alter the mechanical properties of the cell walls.

Conclusions

We reported here a first attempt at grafting of polyesters within wood cell walls. The hydroxyl functionalities present in cell wall polymers were used to initiate the ring opening polymerization of caprolactone. Based on the solvent utilized in the process, different amounts of polymer could be introduced in the cell wall, yielding materials with different properties. The wood samples modified in DMF show the most significant improvements, both in terms of hydrophobic properties and dimensional stability, and this without altering the mechanical properties of the wood. Using a fully biodegradable synthetic polymer like poly(caprolactone), we were able to produce a novel wood product with improved performance, while preserving the advantage of an environmentally friendly material, which can be easily disposed or is eligible for energetic recovery. Since a wider utilization of wood-based materials is often hindered by intrinsic

drawbacks and/or recycling issues, we believe that this new approach will help in enhancing the implementation of wood in given and novel applications.

Acknowledgements

Notes and references

1. R. M. Rowell, Handbook of wood chemistry and wood composites, CRC Press, Boca Raton, FL, 2005.
2. D. Fengel and G. Wegener, Wood: chemistry, ultrastructure, reactions, ed. W. de Gruyter, Berlin, New York, 1984.
3. C. A. S. Hill, Wood modification: chemical, thermal and other processes, John Wiley & Sons, Chichester, England, Hoboken, NJ, 2006.
4. L. J. Gibson, J. R. Soc. Interface, 2012, 9, 2749–2766.
5. A. Schirp and M. P. Wolcott, Wood Fiber Sci., 2005, 37, 643–652.
6. T. Furuno, Y. Imamura and H. Kajita, Wood Sci. Technol., 2004, 37, 349–361.
7. S. Donath, H. Militz and C. Mai, Wood Sci. Technol., 2004, 38, 555–566.
8. C. Mai and H. Militz, Wood Sci. Technol., 2004, 37, 339–348.
9. R. M. Rowell, Adv. Chem. Ser., 1984, 175–210.
10. L. Nordstierna, S. Lande, M. Westin, O. Karlsson and I. Furo, Holzforschung, 2008, 62, 709–713.
11. T. Nakagami and T. Yokota, Mokuzai Gakkaishi, 1983, 29, 240–247.
12. T. Furuno and T. Goto, Mokuzai Gakkaishi, 1979, 25, 488–495.
13. T. K. Timmons, J. A. Meyer and W. A. Cote, Wood Sci., 1971, 4, 13–24.
14. M. A. Ermeydan, E. Cabane, N. Gierlinger, J. Koetz and I. Burgert, RSC Adv., 2014, 4, 12981–12988.
15. E. Cabane, T. Keplinger, V. Merk, P. Hass and I. Burgert, ChemSusChem, 2014, 7, 1020–1023.

16. M. A. Ermeydan, E. Cabane, A. Masic, J. Koetz and I. Burgert, ACS Appl. Mater. Interfaces, 2012, 4, 5782–5789.

17. J. E. Winandy, N. M. Stark and C. M. Clemons, 5th Global Wood and Natural Fibre Composites Symposium, in Kassel, Germany, April 27–28, 2004.

18. R. W. Lenz, Adv. Polym. Sci., 1993, 107, 1–40.

19. T. Nakamura, Y. Shimizu, Y. Takimoto, T. Tsuda, Y. H. Li, T. Kiyotani, M. Teramachi, S. H. Hyon, Y. Ikada and K. Nishiya, J. Biomed. Mater. Res., 1998, 42, 475–484.

20. M. S. Reeve, S. P. Mccarthy, M. J. Downey and R. A. Gross, Macromolecules, 1994, 27, 825–831.

21. R. W. Lenz and R. H. Marchessault, Biomacromolecules, 2004, 6, 1–8.

22. A. M. Reed and D. K. Gilding, Polymer, 1981, 22, 494–498.

23. S. Akahori and Z. Osawa, Polym. Degrad. Stab., 1994, 45, 261–265.

24. U. Raberg and J. Hafren, Int. Biodeter. Biodegr., 2008, 62, 210–213.

25. R. Sabo, L. W. Jin, N. Stark and R. E. Ibach, Bioresources, 2013, 8, 3322–3335.

26. R. M. Rowell and W. D. Ellis, Wood Fiber, 1978, 10, 104–111.

27. R. F. Storey and J. W. Sherman, Macromolecules, 2002, 35, 1504–1512.

28. J. Libiszowski, A. Kowalski, A. Duda and S. Penczek, Macromol. Chem. Phys., 2002, 203, 1694–1701.

29. A. Duda, S. Penczek, A. Kowalski and J. Libiszowski, Macromol. Symp., 2000, 153, 41–53.

30. J. T. Wiltshire and G. G. Qiao, Macromolecules, 2006, 39, 4282–4285.

31. M. Labet and W. Thielemans, Chem. Soc. Rev., 2009, 38, 3484–3504.

32. H. R. Kricheldorf, I. Kreiser-Saunders and A. Stricker, Macromolecules, 2000, 33, 702–709.

33. R. F. Storey and J. W. Sherman, Macromolecules, 2002, 35, 1504–1512.

34. P. V. Persson, J. Schroder, K. Wickholm, E. Hedenstrom and T. Iversen, Macromolecules, 2004, 37, 5889–5893.

35. L. Liu, Y. Wang, X. Shen and Y. E. Fang, Biopolymers, 2005, 78, 163–170.

36. H. Lonnberg, Q. Zhou, H. Brumer, T. T. Teeri, E. Malmstrom and A. Hult, Biomacromolecules, 2006, 7, 2178–2185.

37. H. Lonnberg, K. Larsson, T. Lindstrom, A. Hult and E. Malmstrom, ACS Appl. Mater. Interfaces, 2011, 3, 1426–1433.

38. R. Kusumi, Y. Teramoto and Y. Nishio, Polymer, 2011, 52, 5912–5921.

39. K. Makiguchi, T. Satoh and T. Kakuchi, Macromolecules, 2011, 44, 1999–2005.

40. B. Kiskan and Y. Yagci, Polymer, 2005, 46, 11690–11697.

41. G. I. Mantanis, R. A. Young and R. M. Rowell, Holzforschung, 1994, 48, 480–490.

42. X. H. He, L. Zhong, K. Wang, S. F. Luo and M. R. Xie, J. Appl. Polym. Sci., 2010, 117, 302–308.

43. C. A. S. Hill and G. A. Ormondroyd, Holzforschung, 2004, 58, 544–547.

44. M. H. Schneider and K. I. Brebner, Wood Sci. Technol., 1985, 19, 67–73.

45. S. A. Mirmohammadi, M. Imani, H. Uyama, M. Atai, M. B. Teimouri and N. Bahri-Lale, Polym. Int., 2013, 63, 479–485.

46. A. Kavros, Y. L. Robinson and S. Rimmer, J. Chem. Res., Synop., 1999, 452–453.

47. N. Gierlinger, T. Keplinger and M. Harrington, Nat. Protoc., 2012, 7, 1694–1708.

48. N. Gierlinger and M. Schwanninger, Plant Physiol., 2006, 140, 1246–1254.

49. N. Gierlinger and M. Schwanninger, Spectrosc. – Int. J., 2007, 21, 69–89.

50. H. G. M. Edwards, D. W. Farwell and D. Webster, Spectrochim. Acta, Part A, 1997, 53, 2383–2392.

51. G. Kister, G. Cassanas, M. Bergounhon, D. Hoarau and M. Vert, Polymer, 2000, 41, 925–932.

52. Forest Products Laboratory (U.S.), Wood handbook: wood as an engineering material, The Laboratory, Madison, Wis., Centennial edn, 2010.

Supporting information

Fully biodegradable modification of wood for improvement of dimensional stability and water absorption properties by poly(ε-caprolactone) grafting into the cell walls

Mahmut A. Ermeydan,[abc] Etienne Cabane,[ab] Philipp Hass,[ab] Joachim Koetz[d] and Ingo Burgert[ab]*

[a] ETH Zurich, Institute for Building Materials, Zurich, Switzerland.

[b] Empa - Swiss Federal Laboratories for Material Testing and Research, Applied Wood Research Laboratory, Dübendorf, Switzerland.

[c] Max Planck Institute of Colloids and Interfaces, Department of Biomaterials, Potsdam, Germany.

[d] University of Potsdam, Institute of Chemistry, Potsdam, Germany.
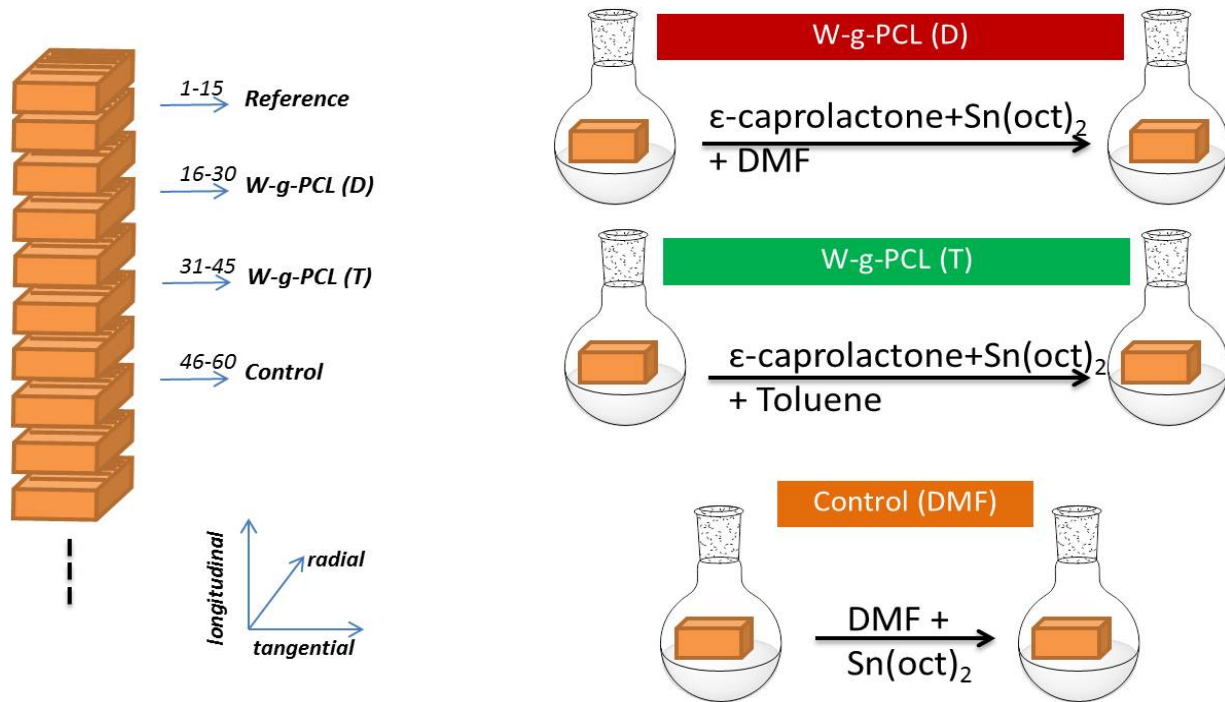
Supporting information Figure 5-S1. On the left side: Fifteen (10x10x5 mm) wood cubes for each set which were cut perpendicular to the same longitudinal axis and categorized as shown. **On the right side**: Schematic representation of reaction flow. W-g-PCL(D) (ring opening polymerization of ε-caprolactone in DMF), W-g-PCL(T) (ring opening polymerization of ε-caprolactone in Toluene), Control (DMF) (Control reaction of wood with DMF and initiator).

Equations for swelling coefficient (S), anti-swelling efficiency (ASE), and water uptake (WU):

$$S(\%) = \frac{(V_i - V_{ii})}{V_{ii}} \times 100$$

where S(%): volumetric swelling; V_i: wood volume after wetting with liquid water; V_{ii}: wood volume of oven-dried samples before wetting

$$ASE(\%) = \frac{S_{um} - S_m}{S_{um}} \times 100$$

where ASE(%): antishrinking/antiswelling efficiency resultin from the modification; S_m: modified volumetric swelling coefficient; S_{um}: unmodified volumetric swelling coefficient.

$$WU(\%) = \frac{(w_{ii} - w_i)}{w_i} \times 100$$

where WU(%): percentage of water uptake of the samples; w_i: initial weight of the sample; w_{ii}: wet weight of the sample after water-soaking

Supporting information Figure 5-S2.

Equation for equilibrium moisture content (EMC):

$$EMC(\%) = \frac{(m - m_{od})}{m_{od}} \times 100$$

where EMC: is the moisture content;
m is the mass of the wood (with moisture) and
m_{od} is the oven-dry mass of the wood (i.e. no moisture)

Supporting information Figure 5-S3.
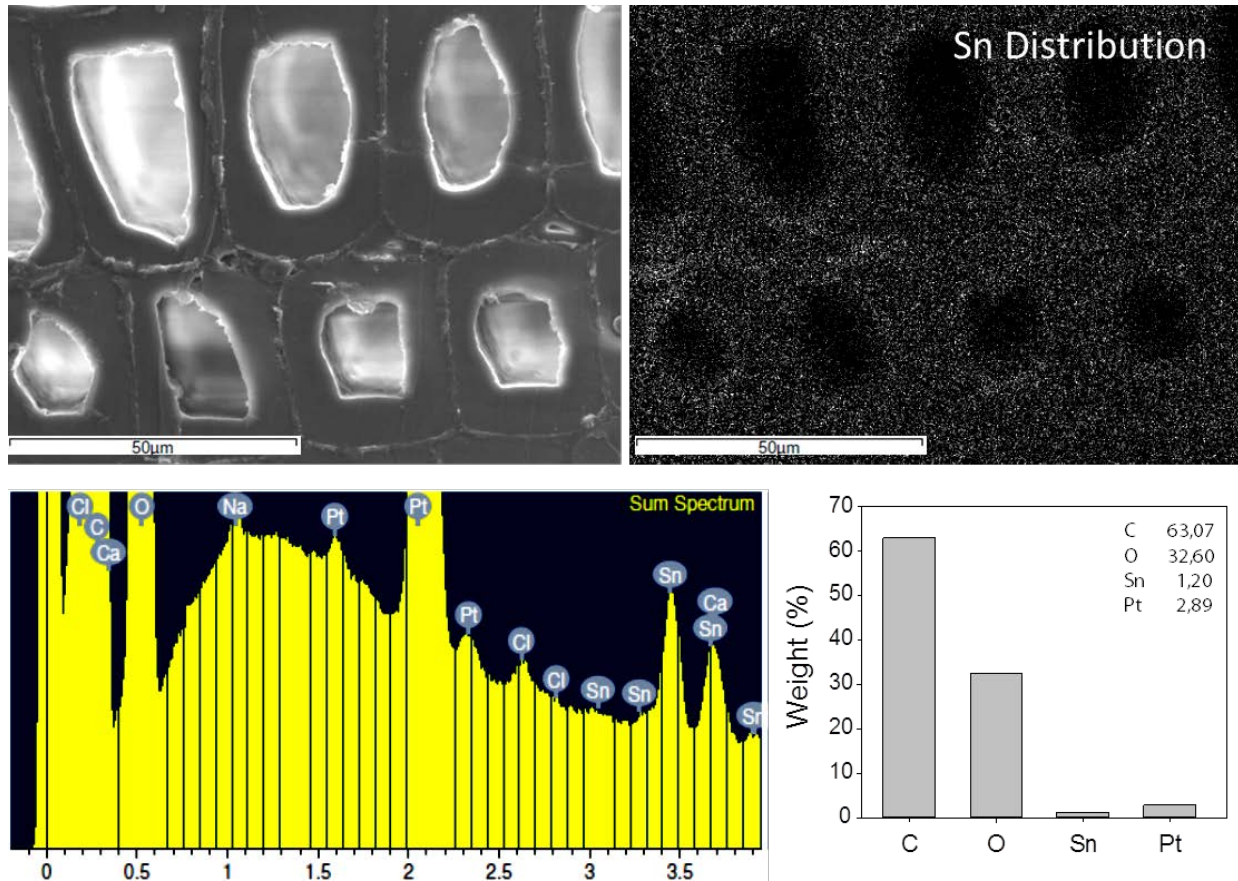
Supporting information Figure 5-S4. EDX analysis of the W-g-PCL(D) demonstrates the existence of Tin(Sn) inside the wood cell walls.

Chapter 6. General Discussion and Conclusions

The main goal of the thesis was to prepare and characterize novel chemically modified wood materials to create more efficient alternatives to current methods. The previous chapters have presented the results from the last three years in the form of three manuscripts (Chapters 3 to 5). As the papers presented in this cumulative thesis already discussed the results individually, this general discussion section rather focuses on i) a general understanding and correlation of the three manuscripts ii) conclusions, new directions for research inspired by the outcome of the thesis and, iii) application potential of the work (outlook).

Chemistry of Modifications.
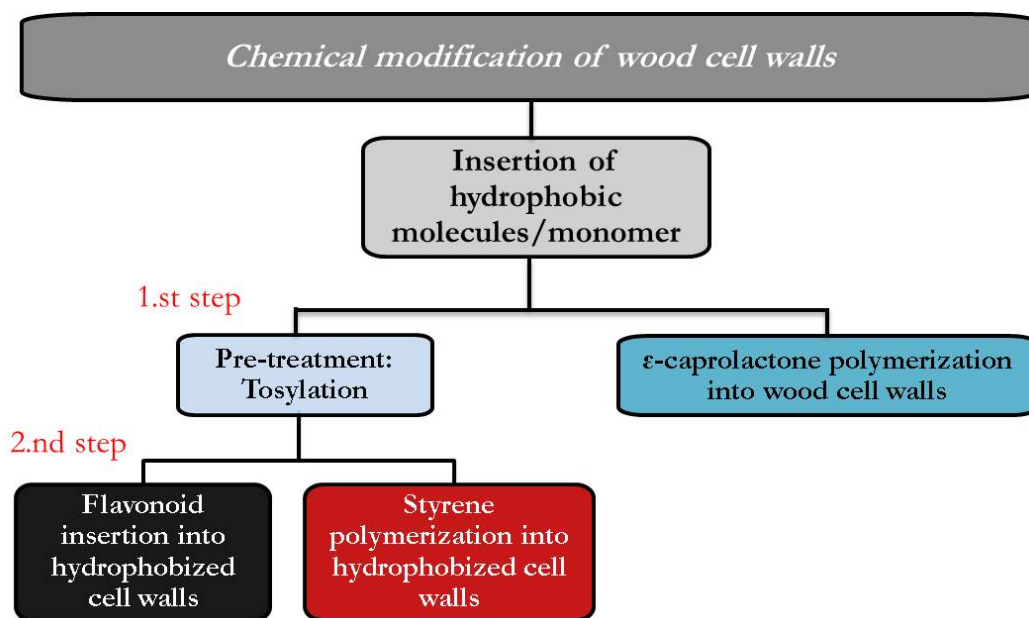
Figure 6-1. Schematic illustration of pathways of three projects:: flavonoid, polystyrene and epsilon-caprolactone modifications.

The idea of the first manuscript (Chapter 3) emerged by inspiration of heartwood formation in the black locust tree (*Robinia pseudoacacia*). Heartwood is a natural occurrence in tree stem which is formed at the end of a variety of metabolic processes at the sapwood−heartwood transition zone. During heartwood formation, some phenolic substances (extractives) are inserted into the cell walls.[22] Heartwood phenolics are responsible for several wood features such as an increased durability of wood. There are a few reports on biomimetic wood modifications that mainly focus on inserting rather hydrophilic flavonoids or phenolics into wood.[65, 66, 89] The basic problem of

inserting hydrophilic flavonoids into wood is the water solubility of inserted molecules which can limit their exterior and long term usage. In addition, flavonoid existence in the cell walls after modification wasn't proved using spectroscopic tools but only by physical analysis such as vibrational properties, equilibrium moisture content(EMC) or anti-swelling efficieny(ASE),[65, 66, 89]. It was reported that heartwood extractives impregnated into the cell wall are more effective than those in the cell lumen in terms of durability,[90, 91] thus the final location of impregnated material is critical for the modification processes. One of the reported works on biomimetic modification showed that the moisture uptake is only slightly reduced (up to 8%) with high weight percentage gains[89] with insertion of some phenolics extracted from Brazilwood (*Caesalpinia echinata*) which indicates that the impregnated substances were mainly inserted in the lumen part instead of cell walls. Another study by the same research group showed that improvement of ASE was only observed for water soluble simple phenolics, but samples which were impregnated with natural polycyclic molecules (flavonoids) dissolved in methanol didn't show an improved ASE.[65] Learning from reported biomimetic modifications and in contrast to the previous studies, it was decided to insert hydrophobic flavonoids into the cell walls instead of hydrophilic ones to be able to increase efficiency of moisture repellency and to avoid removal of the inserted material by water washing. However, after some unsuccessful experimental work based on pH or solvent exchange (data not shown), soon it became clear that the insertion of hydrophobic molecules into the cell wall required a pre-treatment of the cell wall and the idea of cell wall tosylation (activation) emerged at that point. Tosylation is generally used in organic and polymer chemistry to further make S_N2 reactions[92] because tosyl groups attached to the hydroxyl groups become better leaving groups for further displacement reactions.[93] Tosyl chloride is a very active reagent against hydroxyl groups and can react under mild conditions.[83] One of the criteria for efficient wood modification is that chemical reactions should not alter the cell wall structure. It was found that nano-mechanical properties of tosylated cell walls were even better than the untreated samples (Chapter 3) which shows tosylation has no damaging effect on cell walls. Finally, insertion of hydrophobic 3-hydroxy flavone into the already swollen wood cell walls (by pyridine) was achieved by diffusion with a solution of flavonoid dissolved in acetone. It was proven by Raman investigations that the success of insertion depends on pre-treatment. Consequently, the targeted improvements (i.e. better water repellency, better dimensional stability) were obtained with this treatment.

As mentioned in the flavonoid manuscript (Chapter 3), the flavonoids should remain in the cell wall for long periods; nevertheless it was intended to develop even more stable cell wall modification. Based on the successful results of the first project, hydrophobic styrene monomers were polymerized inside the cell walls. This allowed us to verify the tosylation process by introducing the styrene monomers and the possibility of polymerization reaction that took place in wood cell walls was proved. Also due to the low cost of the styrene monomer, it would be a good candidate for an industrial perspective instead of using rather expensive commercial flavonoids. In the past, several studies were performed using polystyrene for wood modification. So far polystyrene could only be found in the lumina after polymerization [14, 15], because styrene itself is hydrophobic and does not have the ability to swell the wood cell wall and penetrate it.[15]

Even though lumen modifications can increase water repellency because polymers formed in the lumen repel water, block entry of voids and retard water access in the cell walls[14], there are many reported studies on such modifications which fail to increase dimensional stability of the wood because hydrophobic monomers cannot penetrate cell walls.[14, 15] A few of the early reported studies mention achievement of cell wall penetration to some extent but they suffer from the methods used which cause cell wall alteration or largely densified wood material.[14, 15, 94-97] However, in this study it could be shown that pre-treated and further *in-situ* styrene polymerized wood samples in a monomer(1:1)solvent solution have much better dimensional stability and water repellency properties than untreated reference samples.

In the final part of the thesis wood was modified in a way that the final product is fully biodegradable. In contrast to the first two projects no pre-treatment (tosylation) was used. Again a hydrophobic monomer was diffused into the cell walls and polymerized *in-situ*, in a one-step reaction (**Figure 6-1**). By establishing covalent bonds with hydroxyl groups of the cell wall polymers, polycaprolactone provided a stable and successful modification (Chapter 5).

The mechanisms of cell wall modification are quite challenging and need further investigations due to the complex structure and content of the cell walls. However, some interpretations and guesses can be made by comparing the experimental facts. As it is known, styrene type vinyl monomers cannot enter the hygroscopic cell wall due to their hydrophobic and non-polar character, but there is no literature discussing diffusion or polymerization of ε-caprolactone inside the cell walls. Apart from styrene modification, the ability of making graft polymerization of ε-caprolactone initiated by hydroxyl groups of cell wall polymers may lead to simultaneous

hydrophobization of the cell wall during the reaction and further *in-situ* polymerization becomes possible.

All three modification methods were solution based, that means wood was impregnated in solutions of chemicals/monomers for insertion and further polymerization reactions. Utilization of solvents was quite important for our purpose because swelling of cell walls can increase with appropriate solvents.[98] It was reported that swelling differences by organic solvents are related to basicity of the swelling reagent that's why solvents which are electron donors such as amines are generally excellent wood swelling agents.[98] Swelled cell walls have increased volume which essentially influences the amount of impregnated chemicals. We proofed this fact especially in the polycaprolactone project. Contrary to toluene, utilization of DMF doubled the amount of polycaprolactone grafted in the cell walls.

Table 6-1. Weight gain and volume change of modified samples after chemical treatments in Chapter 1, 2, and 3. Abbreviations used in the table are same abbreviations used in Chapter 3, 4, and 5 and will be further used in discussion part. Mod.Ch3: Chapter 3, modified samples with flavonoid insertion. St(1-3).Ch4: Chapter 4, styrene inserted and in-situ polymerized samples. W-g-PCL(D,T).Ch5 and Control(DMF).Ch5: Chapter 5, caprolactone inserted and in-situ polymerized samples in DMF or toluene and control sample in DMF. There is also a color code for results from each chapter. Chapter 3: black, Chapter 4: red, Chapter 5: blue.

Exp ID	Tosylation		Flavonoid insertion/ Polymerization	Total	
	WPG 1 (%)	Vol. change (%)	WPG 2* (%)	WPG (%)	Vol. change (%)
Flavonoid Project					
Mod.Ch3	19,0	N/A	4,0	23,0	N/A
Polystyrene Project					
St.Ch4	N/A	N/A	38,8	38,8	-1,2
St1.Ch4	3,1	-0,6	35,7	40,0	-1,7
St2.Ch4	14,2	0,9	19,7	36,3	1,6
St3.Ch4	16,7	1,7	30,2	52,0	4,0
Polycaprolactone Project					
W-g-PCL(D).Ch5	N/A	N/A	17,9	17,9	5,5
W-g-PCL(T).Ch5	N/A	N/A	11,2	11,2	2,4
Control(DMF).Ch5	N/A	N/A	-1,1	-1,1	-7,3

After the modification treatments the weight percentage gains (WPG) and permanent volume changes of wood samples were measured (**Table 6-1**). WPG and volume changes are good and quick indicators to show effectiveness of the modification method. From an engineering point of view, low WPG increases are preferred for wood modifications to avoid densification of the material.[14] Permanent volume increases after modifications can be interpreted due to the

impregnation of polymers into the cell walls which consequently may reduce the water uptake and the degree of swelling. Polystyrene inserted samples have the highest WPG values due to partial lumen filling by polystyrene homopolymers (**Figure 4-5**). The most favorable values belong to samples of polycaprolactone project which has large volume changes with small WPG (~17%).

Distribution of inserted materials in the wood cell walls.

To analyze the distribution of modifying agents in the cell walls after modifications, up to now researchers have mainly used energy-dispersive X-ray analysis (EDX)[94, 95, 99], autoradiography[94] and in a few cases Raman microscopy.[100, 101] EDX is not suitable for our purpose since the inserted chemicals consist of C, H, O atoms which are the same as the cell wall components and can therefore be not detected. Such analysis needs so-called labelled chemicals for visualization [halogenated derivatives of the reagents (i.e. bromostyrene,[95, 99] chloroacetic anhydride[95])]. Autoradiography requires tritium-labelled derivatives of modifying agents which limits use of the method. However for confocal Raman imaging analysis there is no need for special reagents or labelling techniques.[102, 103]

In the past, Raman imaging was successfully used on wood to determine distribution of cell wall polymers[81, 104-106] or to get both quantitative and qualitative information about components.[102, 107] Raman microscopy was also used to detect inserted chemicals into cell walls; however in those studies chemical images were not presented.[100, 101] We used Raman microscopy and spectroscopy to make a very detailed investigation of the chemically modified wood cell walls. Chemical images showing spatial distribution and spectroscopic information of inserted materials and cell wall polymers were provided in this thesis. As shown in **Figure 6-2** (Raman micrographs) in all three modification methods diffusion of molecules/monomers takes place from the lumen side of the cells towards inner cell wall. In addition the Raman spectra indicate less or no reaction/impregnation in the cell corners and compound middle lamella regions for all modifications which means modifications only took place in secondary cell walls.
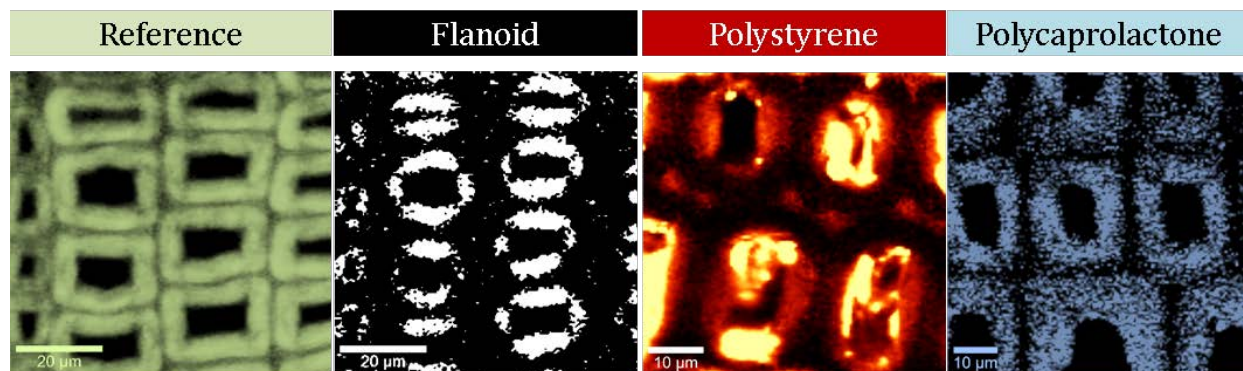
Figure 6-2. Raman images of **(**Left-to-Right): C-H stretching distribution showing chemical image of several cell walls as a reference image for modified cell walls-Flavonoid distribution into the cell walls-Polystyrene distribution into the cell walls and in the lumen-Polycaprolactone distribution into the cell walls.

One of the critical observations in flavonoid and polystyrene modification was the correlation between the distribution of tosyl groups and inserted materials. In both cases impregnated flavonoid molecules and *in-situ* synthesized polystyrene were found exactly in the region of tosyl groups. Additionally, non-covalent interactions of tosyl groups with impregnated flavonoids were also found by Raman spectroscopy. It was concluded that the covalently bonded tosyl groups increased the hydrophobicity of the cell wall and provided a convenient environment for further insertion/impregnation of hydrophobic materials.

A water distribution image of a flavonoid modified sample, which was extracted by integrating the hydroxyl stretching band (from 3135-3735 cm^{-1}), is shown in **Figure 3-1F**. Unfortunately water distribution after modification could not be visualized for the two other modifications because the higher temperatures used for polymerization reactions probably increased fluorescence emission by lignin and thus Raman images for the hydroxyl stretching band could not be generated appropriately (data not shown).

Improvement of Material Properties

Water repellency.

The EMC (Equilibrium moisture content) was measured for water repellency determination in all three projects at a relative humidity around 80% and room temperature. In addition to EMC test, in the polystyrene and polycaprolactone projects, a water uptake test was applied. In all cases the EMC of the modified samples were reduced considerably as shown in **Figure 6-3**. In the flavonoid project (Chapter 3), it was reported that the EMC of flavonoid inserted wood was

reduced about 30% compared to the references. EMC of polystyrene inserted wood (St3) and polycaprolactone grafted wood (W-*g*-PCL(D)) showed a reduction of 40% and 30% respectively (Chapter 4 and 5) against references. Among all three modifications, the best reduction of moisture uptake (the lowest EMC) belongs to effective polystyrene modification (St3 sample) where DMF was used as solvent. However, it also must be highlighted that the tosylation reaction also contributes to the reduction of EMC (~16-17%) which was observed in the flavonoid project. Taking this into consideration the pure effect of polystyrene could be smaller than the effect of polycaprolactone modification which is a one-step process (**Figure 6-1**). EMC of references are different as shown in **Figure 6-3**. This is because of differences in relative humidity in the chamber which differed between 80% (Chapter 3) and 75% (Chapters 4 and 5). Another reason of having different EMCs for reference samples could be the natural variability within the species.
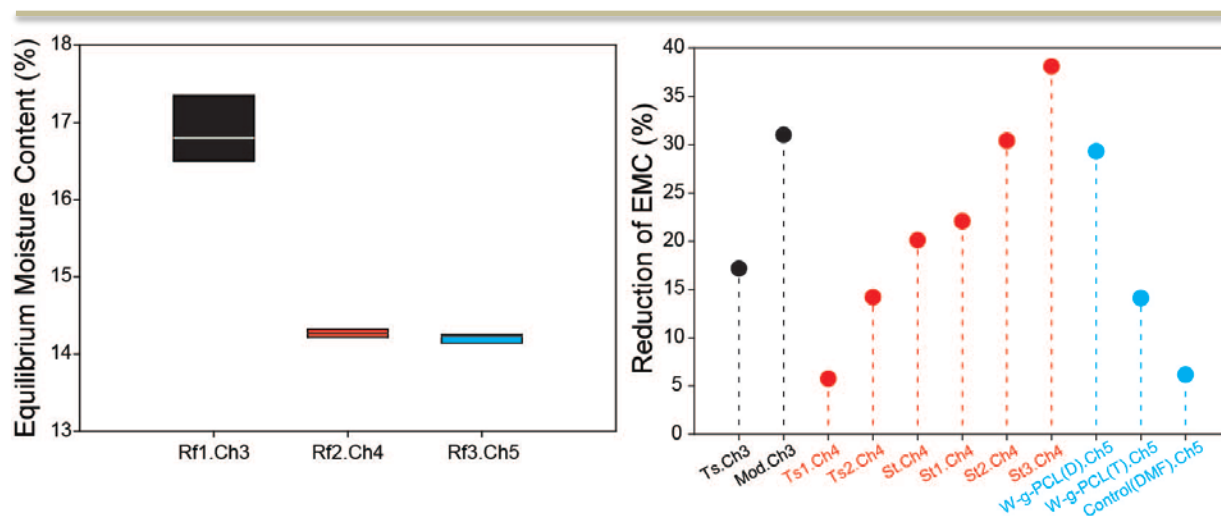
Figure 6-3. Left: Equilibrium moisture content result for reference samples in Chapter 3,4,and 5. Right: Reduction of moisture content (%) after treatments when compared to references in Chapter 3,4, and 5.

Effectiveness of novel modification methods may be understood better when they are compared to current commercial methods (acetylation, furfurylation, DMDHEU treatment). EMC values of acetylated pinewood were reported with a reduction of about 65% on average WPGs (around 20%).[108-111] EMC of furfurylated wood was found with a reduction of about 30-50% with varying WPGs.[111, 112] DMDHEU treated wood showed with a reduced EMC of 33% at about 24% WPG at 80% humidity.[113] In terms of EMC analysis, our modification methods suggest an EMC reduction more than 30% and this value is similar or better than some of those commercial methods (except acetylation). Especially polycaprolactone project promises good performance

having a reduced EMC of above 30% with 17% WPG. The potential of our methods become quite clear since the literature values are based on well-established and optimized processes whereas no optimization steps could yet be performed for our methods.

In the polystyrene and polycaprolactone project, the best reduction values of water uptake against references were reported as being 62,5% for polystyrene inserted wood (St3) and 37,5% for polycaprolactone inserted wood (W-*g*-PCL(D)) as shown in **Figure 6-3**. As expected, the tosylation already reduced water uptake to some extent (Ts2) due to the hydrophobization of the cell walls. Water uptake of references for both studies has similar values of around 160%. In all modifications water uptake was reduced further in the second water immersion cycle as shown in **Figure 6-4**.
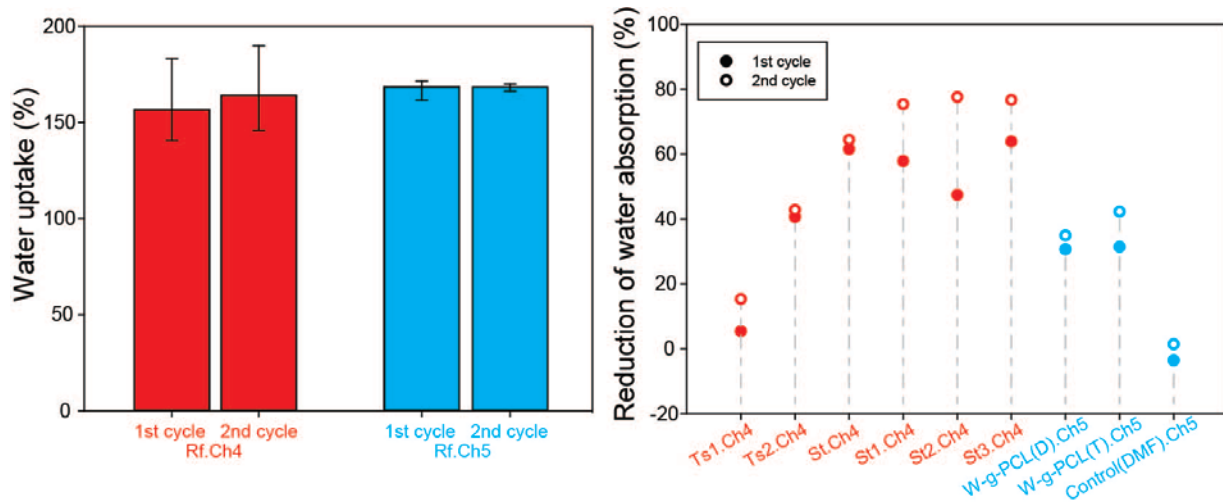
Figure 6-4. Left: Water uptake results of references for Chapter 4 and 5. Right: Reduction of water absorption(%) after treatments when compared to references in Chapter 4 and 5.

Dimensional stability.

Under varying humidity conditions wood shows anisotropic swelling and shrinking which causes internal stresses and eventually may give rise to cracks in the structure.[48, 114] However, when cell walls are filled with small molecules, less swelling and shrinking is observed (i.e. heartwood)[48] which reflects improved dimensional stability. In order to evaluate the improvement of dimensional stability of modified wood, swelling and shrinkage behavior was observed. In Chapter 3, dimensional stability was determined at the cell wall level by calculating mean shrinkage of cell walls. Shrinkage of cell walls was calculated by measuring radial dimensions of

cell walls in wet and dry conditions. In Chapters 4 and 5, to determine dimensional stability, a more established method in wood science was used, which is the anti-swelling efficiency (ASE) calculation. The best ASE value belongs to W-*g*-PCL(D) samples in Chapter 5 as shown in **Figure 6-5**. It was stated in Chapters 4 and 5 that negative ASE values are mainly due to the solvent effect which most probably removes some wood extractives and re-organizes cell wall polymers (lignin and hemicelluloses). But efficient modifications compensate negative effect of solvents and improve ASE.
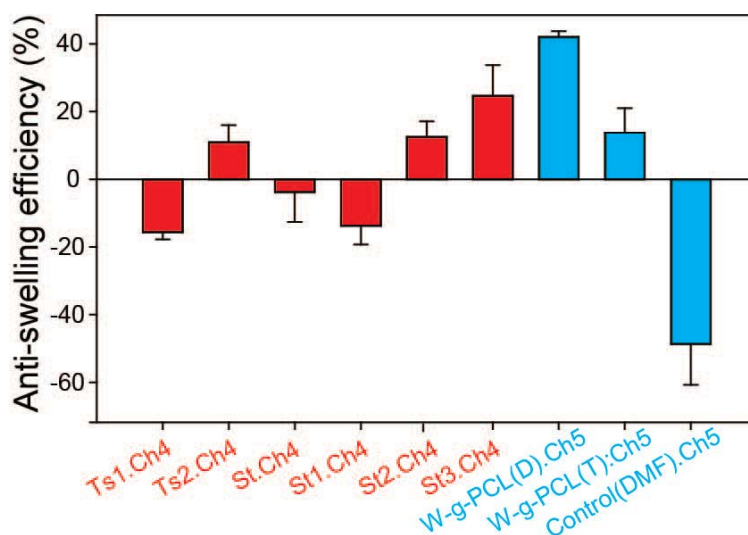
Figure 6-5. Anti-swelling efficieny values of treated samples after first immersion cycle in Chapter 2 and 3.

In the literature, acetylation has been reported to have around 55% ASE with around 15% WPG.[14] Furfurylation method suggests a 40% ASE and around 50% WPG.[115] Dimethylol dihydroxyl ethylene urea (DMDHEU) has typical ASE value in the range of 30-40% at 20% WPG.[116, 117] Anti-swelling efficiency of 40% of W-*g*-PCL(D) samples are even comparable to commercial methods (acetylation, furfurylation, DMDHEU treatment) because it shows such an improvement with low weight gain (around 17%).

Mechanical properties.

The goal of the novel modifications was to increase dimensional stability and durability of wood for certain applications. Since the mechanical properties play a crucial role for many applications the influence of the modifications on cell wall mechanics has been also studied by using nanoindentation.

The values of indentation modulus observed for reference cell walls in this thesis are similar to those reported for other spruce wood samples in the literature but hardness values are similar or lower than earlier works (Indentation modulus: 15-20 GPa, Hardness: 0,30-0,60 GPa).[118-120] The reason for the differences between reported values in this thesis as shown in **Figure 6-6** and former studies may be due to the natural variability of spruce wood samples. The difference of embedding material which was epoxy resin for earlier works and agar resin for our case may not cause severe differences as reported and well explained by Wagner et al 2014.[120]
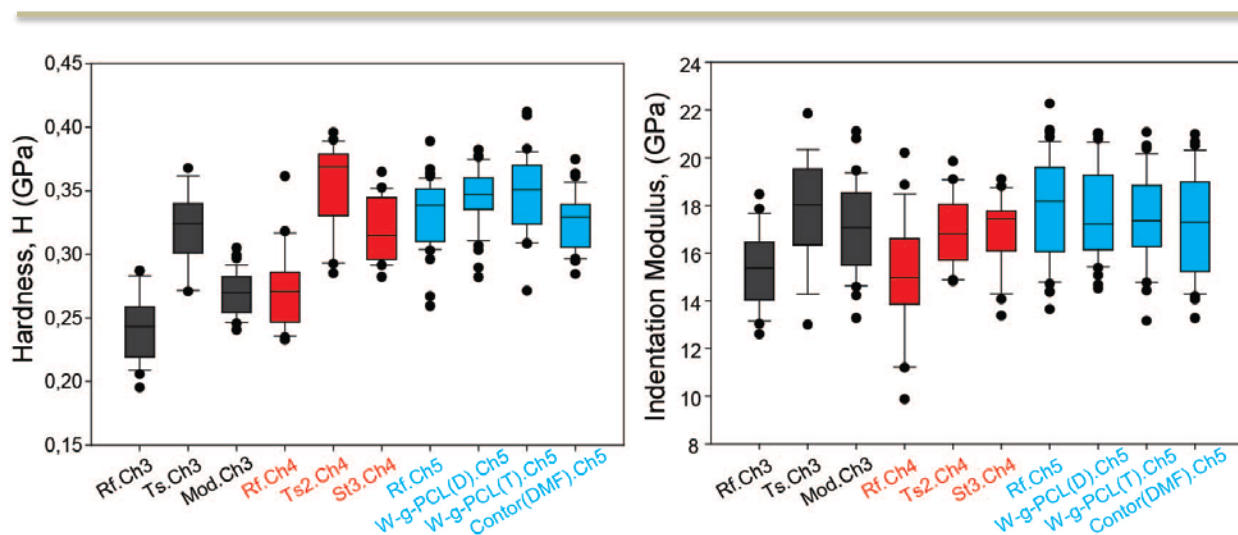
Figure 6-6. Left: Hardness and Right: Indentation modulus of modified cell walls in Chapter 1, 2, and 3.

In terms of improvement of mechanical properties among those modifications introduced in this thesis, polystyrene modification results in increased values. Both hardness and indentation modulus showed a significant ($P < 0.001$, U-test) increase of about 17% and 12% respectively (Chapter 4). For the flavonoid modification hardness and indentation modulus both showed a significant ($P < 0.001$, U-test) increase of about 10% from unmodified cell walls to flavonoid loaded cell walls (Chapter 3). Interestingly, in both modifications (Chapter 3-4) the tosylated (activated) samples show the highest hardness and indentation modulus. We suppose that this could be due to the diffusion of embedding material inside the cell walls during embedding process which also shows impact of tosylation. However, polycaprolactone modification provided no significant improvement of indentation modulus ($P >= 0.05$, U- test) and PCL grafted cell walls possess only a slight increase in hardness ($P < 0.05$, U-Test). The nanoindentation analysis essentially shows that all applied modification treatments did not reduce hardness and indentation modulus of the cell walls.

Conclusions

In this thesis three novel methods for chemical modification of wood were developed which are bio-inspired flavonoid impregnation, in-situ styrene polymerization and in-situ ε-caprolactone polymerization. Improvements in wood properties (dimensional stability and water repellency) are very dependent on inserting chemicals into the cell walls. From the beginning of this study, the aim was to target cell walls instead of the cell lumen, even for polymerization of vinyl monomer (e.g. styrene project) which has been known as a classical lumen modifier. That's why Nature's path of heartwood formation which provides durability to the tree by inserting phenolic substances into cell walls was taken as a source of inspiration.

The consequence of our studies is striking because the stated three methods not only considerably improve wood properties (e.g. dimensional stability, water repellency) but also may create an impact in the wood modification field and open a new page for further studies on use of hydrophobic molecules/monomers for wood modifications. A common feature of the three studies is the use of hydrophobic substances to modify cell walls. All three approaches have their own importance in different aspects. In the first project, the increased hydrophobicity by pre-treatment provided improved accessibility of the cell walls by aromatic flavonoids and enhanced stability of flavonoids in the cell wall. In the second project, a series of wood-polystyrene composites of spruce wood were produced with different degree of pre-treatments (no tosylation, low weight gain tosylation and high weight gain tosylation). It was observed that the diffusion of hydrophobic monomers into the cell walls have close correlation between degree and distribution of tosyl-groups. With this study it was demonstrated that the diffusion of hydrophobic monomers into the cell walls and their polymerization is possible and results in an efficient cell wall bulking which provides dimensional stability to the wood material. Such polymer inserted wood materials are highly desirable due to their long-service life and will help to promote the use of wood as a material from renewable resources with more reliable properties. The studies were finalized based on the experience from the first two projects, in a one step process of epsilon-caprolactone polymerization. We reported the first attempt of polyester grafting on wood cell wall polymers. The hydroxyl groups on cell wall polymers were used as macroinitiators for the ring opening polymerization of caprolactone. It was demonstrated that the choice of solvent with different swelling properties is critical for the amount of polymer which could be introduced in the cell wall for changing properties of final product. Most significant improvements in terms of water

repellency and dimensional stability were observed when treating samples with DMF which has excellent swelling potential of wood. We produced a novel fully biodegradable wood product with improved performance and with minimalized disposal problems.

All three methods were successful in improving both moisture uptake and dimensional stability. Especially polycaprolactone project promises for scale-up trials with its success on wood properties, proposing fully biodegradable wood material and having a one-step reaction. More arguments on industrialization potential of novel methods will be discussed in the outlook section.

In this thesis, confocal Raman imaging and Raman spectroscopy were extensively used to characterize chemically modified wood cell walls and were found to be an effective and easy spectroscopic technique. High resolution imaging (about 0.5 microns) helped us to localize and visualize inserted chemicals inside the cell walls. Detailed investigations by Raman spectroscopy revealed that even intermolecular interactions between inserted chemicals (e.g. flavonoids) and cell wall polymers in wood cell wall could be detected.

The three methods introduced in the thesis used mild reaction conditions (i.e. the wood retains its mechanical properties) and each study yielded new wood materials with limited weight gain and improved properties: both dimensional stability and hydrophobicity are increased.

Outlook

In order to commercialize these newly developed methods for utilization, further research is needed to optimize methods and to test success of modification for larger scales. The flavonoid project has rather limited application potential due to having a two-step procedure and relatively high costs of flavonoids, but the tosylation step is useful. Several advantages of tosylation were reported in this thesis, but tosyl chloride can be changed with another effective reactive reagent to decrease the price of the initial process. Also, flavonoids can be substituted by cheaper hydrophobic small molecules that do not have environmental risks.

The second project promises a better application potential due to water repellency ability of the polystyrene impregnated wood composites and low cost of polystyrene, although it is based on a two-step procedure. Water repellency is critical to increase the durability of wood material and affects essentially service-life. Up to now wood-polymer composites are produced by hot-pressing of dry-blends of wood particles/flour and polymers (around 50/50, w/w), however bulk wood was not considered to be modified with those polymers (e.g. PVC, PP, PE, styrene) at an industrial scale. This is because wood-polymer composites are much more effective in terms of water repellency and dimensional stability when high amount of polymers are blended with wood particles/flour. However bulk wood materials treated with polymers do not have improved dimensional stability without very large densification which is undesirable. With the introduced approach, use of bulk material and preparation of polymer impregnated wood materials with excellent properties becomes possible. Production of such improved bulk wood materials may be an alternative for current WPC products (panels, floorings, etc.), thus waste energy would be conserved due to the several processes to produce current WPCs (blending, extrusion, hot-pressing, etc.) and less polymer will be used which is critical for environmental aspects. The disposal problem of novel wood-polystyrene composites could be solved by grinding down and using it for the production of WPCs which makes the material more sustainable. As we mentioned above, the tosylation process can be changed with a cheaper or better reactive chemical which provides same or increased effectiveness. Also, polystyrene can be changed with other polymers of choice (PVC, PP, PE, etc.).

We found the best method convenient for commercialization among those three projects is polycaprolactone insertion into the cell walls because the method relies on a one step reaction which is highly feasible and favorable for industry and the products have excellent dimensional

stability as well as water repellency. In addition, the product is fully biodegradable means wood will have minimal disposal problems like untreated wood.

We used organic solvents (DMF or Pyridine) for all three methods. In the chemical industry, large amounts of organic solvents are used as a raw material for product syntheses or as reaction media for a range of products (paints, coatings, adhesives, etc.). In an ecological perspective use of solvents are not favorable due to possible toxic effects on humans at the production or service level. Fortunately, with increasing technology, recycling of solvents used in the processes becomes possible and closed-systems eliminate human contact to solvents. As discussed in the "chemistry of modifications" chapter, solvents like DMF are essential to swell wood cell walls if one uses hydrophobic chemicals which cannot swell cell walls. One solution may be use of green solvents such as ionic liquids which swell wood very well; however those solvents are very expensive which makes utilization unfeasible. In any case, solvent emission of the products should be investigated at some stage before industrial production to be sure that wood emits minimal or no DMF after processes. Indeed, additional mechanical, physical, and biodegradation tests need to be performed on larger test specimens in order to fully evaluate potential of these methods for potential end use applications.

Chapter 7. References for Chapter 1, 2, and 6

1. R. Ulber, K. Muffler, N. Tippkötter, T. Hirth and D. Sell, in *Renewable Raw Materials*, Wiley-VCH Verlag GmbH & Co. KGaA, 2011, pp. 1-5.

2. I. R. Noble and R. Dirzo, *Science*, 1997, 277, 522-525.

3. S. Higman, J. Mayers, S. Bass, N. Judd and R. Nussbaum, *The Sustainable Forestry Handbook: A Practical Guide for Tropical Forest*, Earthscan, 2005.

4. A. K. Petersen and B. Solberg, *Environmental Science & Policy*, 2002, 5, 169-182.

5. Forest Products Laboratory (U.S.), *Wood handbook : wood as an engineering material*, Centennial edn., The Laboratory, Madison, Wis., 2010.

6. R. Höfer, *Sustainable Solutions for Modern Economics*, Royal Society of Chemistry, Cambridge, UK, 2009.

7. T. H. Wegner and E. P. Jones, in *The Nanoscience and Technology of Renewable Biomaterials*, John Wiley & Sons, Ltd, 2009, pp. 1-41.

8. N. R. C. Board on Agriculture, *Wood in Our Future: The Role of Life-Cycle Analysis: Proceeding of a Symposium*, National Academy Press, Washington, D.C., 2009.

9. R. Bergman and S. Bowe, *Wood Fiber Sci*, 2008, 40, 448-458.

10. R. Bergman and S. Bowe, *Wood Fiber Sci*, 2010, 42, 67-78.

11. A. Dodoo, L. Gustavsson and R. Sathre, *Energy and Buildings*, 2011, 43, 1589-1597.

12. R. Sathre and J. O'Connor, *Environmental Science & Policy*, 2010, 13, 104-114.

13. D. Feldman, *Journal of Polymer Science: Polymer Letters Edition*, 1985, 23, 601-602.

14. C. A. S. Hill, *Wood modification : chemical, thermal and other processes*, John Wiley & Sons, Chichester, England ; Hoboken, NJ, 2006.

15. R. M. Rowell, *Handbook of wood chemistry and wood composites*, CRC Press, Boca Raton, Fla., 2005.

16. D. Fengel and G. Wegener, *Wood : chemistry, ultrastructure, reactions*, W. de Gruyter, Berlin ; New York, 1984.

17. R. M. Rowell and W. B. Banks, *Water repellency and dimensional stability of wood*, Forest Products Laboratory, Madison, WI: U.S., 1985.

18. S. Donath, H. Militz and C. Mai, *Wood Science and Technology*, 2004, 38, 555-566.

19. M. Deka and C. N. Saikia, *Bioresource Technology*, 2000, 73, 179-181.

20. R. R. Devi, I. Ali and T. K. Maji, *Bioresource Technology*, 2003, 88, 185-188.

21. S. N. Kartal, T. Yoshimura and Y. Imamura, *International Biodeterioration & Biodegradation*, 2004, 53, 111-117.

22. A. M. Taylor, B. L. Gartner and J. J. Morrell, *Wood Fiber Sci*, 2002, 34, 587-611.

23. W. E. Hillis, *Wood Science and Technology*, 1971, 5, 272-289.

24. R. K. Bamber, *Wood Science and Technology*, 1976, 10, 1-8.

25. B. B. Carrodus, *New Phytologist*, 1971, 70, 939-943.

26. V. Dellus, I. Mila, A. Scalbert, C. Menard, V. Michon and C. L. M. Herve du Penhoat, *Phytochemistry*, 1997, 45, 1573-1578.

27. N. Gierlinger, D. Jacques, M. Grabner, R. Wimmer, M. Schwanninger, P. Rozenberg and L. PÃ¢ques, *Trees - Structure and Function*, 2004, 18, 102-108.

28. F. H. Wadsworth and E. González, *Forest Ecology and Management*, 2008, 255, 320-323.

29. A. D. Kokutse, H. Baillères, A. Stokes and K. Kokou, *Forest Ecology and Management*, 2004, 189, 37-48.

30. R. Suzuki, Y. Matsushita, T. Imai, M. Sakurai, J. Henriques de Jesus, S. Ozaki, Z. Finger and K. Fukushima, *J Wood Sci*, 2008, 54, 174-178.

31. N. Hasler, D. Werth and R. Avissar, *J Climate*, 2009, 22, 1124-1141.

32. A. G. Cook, A. C. Janetos and W. T. Hinds, *Environ Conserv*, 1990, 17, 201-212.

33. R. A. Houghton, *Environ Sci Technol*, 1990, 24, 414-&.

34. K. v. Gadow, T. Pukkala and M. Tome, *Sustainable Forest Management*, Kluwer Academic Publishers, Noewell, MA, 2000.

35. F. H. Schweingruber, *Wood Structure and Environment*, Springer-Verlag, Berlin, Heidelberg, 2007.

36. J. R. Barnett and V. A. Bonham, *Biological Reviews*, 2004, 79, 461-472.

37. L. J. Gibson, *J R Soc Interface*, 2012, 9, 2749-2766.

38. L. Salmen and A. M. Olsson, *Iswpc - 9th International Symposium on Wood and Pulping Chemistry - Oral Presentations*, 1997, E61-E64.

39. C. Sanchez-Rodriguez, I. Rubio-Somoza, R. Sibout and S. Persson, *Trends Plant Sci.*, 2010, 15, 291-301.

40. A. J. Panshin and C. deZeeuw, *Textbook of Wood Technology*, 4 edn., McGraw-Hill, New York, 1980.

41. I. Burgert, J. Keckes, K. Fruhmann, P. Fratzl and S. E. Tschegg, *Plant Biology*, 2002, 4, 9-12.

42. I. Burgert, M. Eder, N. Gierlinger and P. Fratzl, *Planta*, 2007, 226, 981-987.

43. K. Kojiro, T. Miki, H. Sugimoto, M. Nakajima and K. Kanayama, *J Wood Sci*, 2010, 56, 107-111.

44. S. Dumitriu, *Polysaccharides : structural diversity and functional versatility*, 2nd edn., Marcel Dekker, New York, 2005.

45. T. E. Timell, *Wood Science and Technology*, 1967, 1, 45-70.

46. H. V. Scheller and P. Ulvskov, *Annual Review of Plant Biology*, 2010, 61, 263-289.

47. L. Salmén and I. Burgert, in *Holzforschung*, 2009, vol. 63, p. 121.

48. J. C. F. Walker, in *Primary Wood Processing*, ed. J. C. F. Walker, Springer, Dordrecht, The Netherlands, 2006, pp. 23-67.

49. R. M. Rowell, *Abstr Pap Am Chem S*, 1983, 185, 4-Cell.

50. M. Rowell Roger, in *The Chemistry of Solid Wood*, American Chemical Society, 1984, vol. 207, pp. 175-210.

51. H. Matsuda, *Wood Science and Technology*, 1987, 21, 75-88.

52. M. R. M. Farahani and F. Taghizadeh, *Bioresources*, 2010, 5, 2232-2238.

53. T.-Q. Yuan, S.-N. Sun, F. Xu and R.-C. Sun, *J Agr Food Chem*, 2010, 58, 11302-11310.

54. Y. Matsumoto, Y. Teramoto and Y. Nishio, *J Wood Chem Technol*, 2010, 30, 373-381.

55. H. Kishi, A. Fujita, H. Miyazaki, S. Matsuda and A. Murakami, *Journal of Applied Polymer Science*, 2006, 102, 2285-2292.

56. K. K. Pandey, M. Hughes and T. Vuorinen, *Bioresources*, 2010, 5, 598-615.

57. H. Tarkow, USDA Forest Service, Forest Products Laboratory, Madison, WI, 1945, p. 4.

58. H. Tarkow, USDA Forest Service, Forest Products Laboratory, Madison, WI, 1946, p. 9.

59. H. Tarkow, A. J. Stamm and E. C. O. Erickson, in *USDA Forest Service, Forest Products Laboratory*, Madison, WI, 1946, p. 29.

60. R. M. Rowell, *Wood Sci*, 1978, 10, 193-197.

61. G. Sebe and B. De Jeso, *Holzforschung*, 2000, 54, 474-480.

62. S. Kumar, *Wood Fiber Sci*, 1994, 26, 270-280.

63. J. Jokel, *Drev Vysk*, 1972, 17, 247-260.

64. A. J. Stamm and R. H. Baechler, *Forest Prod J*, 1960, 10, 22-26.

65. K. Sakai, M. Matsunaga, K. Minato and F. Nakatsubo, *J Wood Sci*, 1999, 45, 227-232.

66. M. Matsunaga, K. Sakai, H. Kamitakahara, K. Minato and F. Nakatsubo, *J Wood Sci*, 2000, 46, 253-257.

67. R. M. Rowell, *Adv Chem Ser*, 1984, 175-210.

68. S. Trey, S. Jafarzadeh and M. Johansson, *ACS Applied Materials & Interfaces*, 2012, 4, 1760-1769.

69. M. Tshabalala and L.-P. Sung, *J Coat Technol Res*, 2007, 4, 483-490.

70. B. Mahltig, C. Swaboda, A. Roessler and H. Bottcher, *J Mater Chem*, 2008, 18, 3180-3192.

71. S. Maggini, E. Feci, E. Cappelletto, F. Girardi, S. Palanti and R. Di Maggio, *ACS Applied Materials & Interfaces*, 2012, 4, 4871-4881.

72. G. Herzberg, *Molecular Spectra and Molecular Structure: II, Infrared and Raman Spectra of Polyatomic Molecules*, Van Nostrand Reinhold, New York, 1945.

73. N. Gierlinger, T. Keplinger, M. Harrington and M. Schwanninger, *Raman Imaging of Lignocellulosic Feedstock*, 2013.

74. E. Smith and G. Dent, *Modern Raman Spectroscopy - A practical Approach*, John Wiley & Sons Ltd, Manchester, 2005.

75. A. A. van Apeldoorn, H.-J. van Manen, J. M. Bezemer, J. D. de Bruijn, C. A. van Blitterswijk and C. Otto, *Journal of the American Chemical Society*, 2004, 126, 13226-13227.

76. J. Ma and D. Ben-Amotz, *Appl Spectrosc*, 1997, 51, 1845-1848.

77. I. Chourpa, P. Carpentier, P. Maingault, F. Fetissoff and P. Dubois, Biomedical Spectroscopy: Vibrational Spectroscopy and Other Novel Techniques, 2000.

78. S. M. Barnett, M. M. Carrabba, R. W. Bormett and A. Whitley, Biomedical Applications of Raman Spectroscopy, 1999.

79. J. A. Pezzuti, M. D. Morris, J. F. Bonadio and S. A. Goldstein, Three-Dimensional and Multidimensional Microscopy: Image Acquisition and Processing V, 1998.

80. T. Buchwald, M. Kozielski and M. Szybowicz, *Spectroscopy: An International Journal*, 2012, 27.

81. U. Agarwal, *Planta*, 2006, 224, 1141-1153.

82. N. Gierlinger, T. Keplinger and M. Harrington, *Nat. Protocols*, 2012, 7, 1694-1708.

83. M. A. Ermeydan, E. Cabane, A. Masic, J. Koetz and I. Burgert, *ACS Applied Materials & Interfaces*, 2012, 4, 5782-5789.

84. J. Konnerth and W. Gindl, *Holzforschung*, 2006, 60, 429-433.

85. F. A. Kamke and J. N. Lee, *Wood Fiber Sci*, 2007, 39, 205-220.

86. W. Gindl, H. S. Gupta, T. Schoberl, H. C. Lichtenegger and P. Fratzl, *Appl Phys a-Mater*, 2004, 79, 2069-2073.

87. A. C. Fischer-Cripps, *Nanoindentation*, Springer Science+Business Media, New York, 2004.

88. J. Konnerth, M. Eiser, A. Jäger, K. Bader Thomas, K. Hofstetter, J. Follrich, T. Ters, C. Hansmann and R. Wimmer, in *Holzforschung*, 2010, vol. 64, p. 447.

89. M. Matsunaga, E. Obataya, K. Minato and F. Nakatsubo, *J Wood Sci*, 2000, 46, 122-129.

90. W. E. Hillis, *Heartwood and tree exudates*, Springer-Verlag, Berlin, Germany, 1987.

91. G. Kleist and U. Schmitt, *Holz Roh Werkst*, 1999, 57, 93-95.

92. J. M. Harris, E. C. Struck, M. G. Case, M. S. Paley, M. Yalpani, J. M. Van Alstine and D. E. Brooks, *Journal of Polymer Science: Polymer Chemistry Edition*, 1984, 22, 341-352.

93. R. Bruckner, *Organic Mechanisms*, Springer, Berlin Heidelberg, 2010.

94. T. K. Timmons, J. A. Meyer and W. A. Cote, *Wood Sci*, 1971, 4, 13–24.

95. T. Furuno and T. Goto, *Mokuzai Gakkaishi*, 1979, 25, 488–495.

96. T. Nakagami and T. Yokota, *Mokuzai Gakkaishi*, 1983, 29, 240-247.

97. N. Shiraishi, M. Murata and T. Yokota, *Mokuzai Gakkaishi*, 1972, 18, 299-306.

98. G. I. Mantanis, R. A. Young and R. M. Rowell, *Holzforschung*, 1994, 48, 480-490.

99. R. M. Rowell, R. Simonson, S. Hess, D. V. Plackett, D. Cronshaw and E. Dunningham, *Wood Fiber Sci*, 1994, 26, 11-18.

100. E. Kurti, D. V. Heyd and R. S. Wylie, *Wood Science and Technology*, 2005, 39, 618-629.

101. N. Gierlinger, C. Hansmann, T. Roder, H. Sixta, W. Gindl and R. Wimmer, *Holzforschung*, 2005, 59, 210-213.

102. N. Gierlinger, T. Keplinger and M. Harrington, *Nat Protoc*, 2012, 7, 1694-1708.

103. S. Richter, J. Mussig and N. Gierlinger, *Planta*, 2011, 233, 763-772.

104. U. P. Agarwal and R. H. Atalla, *Planta*, 1986, 169, 325-332.

105. N. Gierlinger and M. Schwanninger, *Plant Physiol*, 2006, 140, 1246-1254.

106. N. Gierlinger and M. Schwanninger, *Spectrosc-Int J*, 2007, 21, 69-89.

107. N. Gierlinger, M. Schwanninger, A. Reinecke and I. Burgert, *Biomacromolecules*, 2006, 7, 2077-2081.

108. P. Larsson and R. Simonson, *Holz Roh Werkst*, 1994, 52, 83-86.

109. A. N. Papadopoulos and C. A. S. Hill, *Wood Science and Technology*, 2003, 37, 221-231.

110. P. D. Evans, A. F. A. Wallis and N. L. Owen, *Wood Science and Technology*, 2000, 34, 151-165.

111. H. Epmeier, M. Johansson, R. Kliger and M. Westin, *Holzforschung*, 2007, 61, 34-42.

112. H. Epmeier, M. Westin and A. Rapp, *Scand J Forest Res*, 2004, 19, 31-37.

113. R. Yasuda, K. Minato and M. Norimoto, *Wood Science and Technology*, 1994, 28, 209-218.

114. S. C. Cowin, *Journal of Applied Mechanics*, 1985, 52, 351-355.

115. B. Esteves, L. Nunes and H. Pereira, *European Journal of Wood and Wood Products*, 2011, 69, 521-525.

116. A. Dieste, A. Krause, S. Bollmus and H. Militz, *Holz als Roh- und Werkstoff*, 2008, 66, 281-287.

117. A. Krause, D. Jones, M. van der Zee and H. Militz, Prooceedings of the 1st European Conference on Wood Modification, 2003.

118. J. Konnerth, N. Gierlinger, J. Keckes and W. Gindl, *J Mater Sci*, 2009, 44, 4399-4406.

119. Y. F. Yin, L. Berglund and L. Salmen, *Biomacromolecules*, 2011, 12, 194-202.

120. L. Wagner, T. K. Bader and K. de Borst, *J Mater Sci*, 2014, 49, 94-102.

Acknowledgements

I want to start by thanking Prof. Dr. Ingo Burgert who provided the PhD position in Max Planck Institute of Colloids and Interfaces, welcomed me in his group in the end of 2010. He also continued to support my studies after he went to ETH Zurich with his great expertise in wood science. I want to thank Prof. Dr. Joachim Koetz who accepted me as a PhD candidate under his supervisory in Chemisrtry Department of Potsdam University. I'm also thankful to Prof. Peter Fratzl (MPIKG) who gave the opportunity to pursue my doctoral studies in his Biomaterials department. Furthermore, I would like to thank Dr. Etienne Cabane (ETH Zurich) for his extensive help during my studies. He is the key person who contributes a lot with his experience in polymer science. Also I would like to thank Dr. Admir Masic and Dr. Notburga Gierlinger for discussions on Raman imaging and spectroscopy.

Dr. Michaela Eder (MPIKG) is another key person in my PhD studies. She is the one who showed me how to use microtome and prepare samples for Raman investigations. Most importantly she was the one who motivated me during the last 3,5 years and special thanks to her for the discussion during thesis writing. I also want to thank our precious technicians Gabriela Wienskol and Susann Weichold for their effort and help for providing chemicals in the Lab, polishing embedded wood samples for nanoindentation, and some help for spectroscopic tools. I would like to thank in particular Dr. Dunlop for kindly reviewing this thesis prior to submission.

Finally, a big THANK goes to my precious wife, Meryem, who supported me all the time in this period and my son, Selim for the joy he brings into my life. A special thank goes to my mother and dad for their lifetime support for my education life.

Curriculum Vitae

Mahmut Ali ERMEYDAN

MAX-PLANCK-INSTITUTE OF COLLOIDS AND INTERFACES

Date and place of birth   4th December 1983 in Istanbul, Turkey

Personal contact   Suderoderstr. 32, 12347 Berlin, Germany
+049-157-8897132
mahmutermeydan@gmail.com

Professional contact   Max-Planck-Institute of Colloids and Interfaces
Biomaterials Department
Am Mühlenberg 1, 14476 Golm-Potsdam, Germany
+49(0)331/567-9426
mahmut.ermeydan@mpikg.mpg.de

Education:

2010 – 2014	PhD Candidate: Max Planck Institute of Colloids and Interfaces, Golm, Potsdam & ETH Zurich (Official Degree - Department of Chemistry at Potsdam University, Potsdam, Germany)
2006 – 2008	Master Degree, M.Sc.: Department of Chemistry at Gebze Institute of Technology (GIT), Kocaeli, Turkey
2001 – 2006	B.Sc.: Bilkent University, Faculty of Science, Department of Chemistry, Ankara, Turkey

Research Experiences & Experimental Skills:

PhD Period (10.2010-05.2014): With Prof. Dr. Ingo Burgert at ETH Zurich: Chemical and biomimetic modification of cell walls to improve dimensional stability and water repellency of bulk wood material by various polymerization processes (radical,ring opening) and their chemical and physical characterization. (Raman Microscopy and Spectroscopy, (E)SEM, DSC-TGA, ATR-FTIR, Nanoindentation).

Job Period (2009-2010): With Dr. Pharmacist Yıldız Özalp: Formulation and Process Development of oral dosage forms; tablets, capsules and solutions, validation of processes and interpretation of analysis (GC, HPLC, DSC). (Biofarma Pharmaceutical Ind. Co. Inc., R&D Department).

Master Research Period (2006-2008): With Assoc .Prof. Fabienne Dumoulin, Prof. Vefa Ahsen (Gebze Institute of Technology, Department of Chemistry): Starting from phthalonitrile derivatives, synthesis and characterization of symmetric, water-soluble, carbohydrate linked phthalocyanines which were prepared to test Photo Dynamic Therapy effect on in-vivo/in-vitro models. Synthesis and characterization of asymmetric, amphiphilic phthalocyanines (AB3 type) which were prepared to investigate electrochemical and photochemical properties by making Langmuir Blodgett films (NMR, MS, Elemental Analysis, UV-vis, FT-IR).

Summer Intern in Lyon, France (Spring 2008): With Dr. Dominique Lafont, (L'Université Claude Bernard, Lyon 1, France) (Spring 2008): With the scholarship by French Consulate; synthesis and characterization of carbohydrate linked phthalocyanines both with glycosylation and "click" (The Huisgen 1,3-dipolar cycloaddition) reactions (NMR, FT-IR).

Bachelor (2001-2006): With Prof. Margarita Kantcheva (Bilkent University, Turkey). 2005-2006 for 2 Semesters of Senior Project: Synthesis and characterization of WOx/ZrO2 catalysts by W(VI) peroxo precursor by Equilibrium Adsorption Method. (DRUV-vis, Photospectrometry, Raman, XRD, FT-IR in situ, EPR)

Conferences:

- JUNIOR EUROMAT 2012, FEMS, the Federation of European Materials Societies, Lousanne, Switzerland, 23-27 July, **2012**, Oral Presentation.
- ICPP-5, International Conference of Porphyrins and Phthalocyanines, Moskow, Russia, 5-12 July, **2008**, Poster Presentation.
- International Congress of Organic Chemistry, Erzurum, Turkey, 5-9 June, **2007**, Poster Presentation.

Publications:

1- **Mahmut Ali Ermeydan**, Etienne Cabane, Joachim Koetz, Ingo Burgert, Fully biodegradable modification of wood for improvement of dimensional stability and water absorption properties by poly(ϵ-caprolactone) grafting into the cell walls, Green Chemistry, **2014**, DOI: 10.1039/C4GC00194J.

2- **Mahmut Ali Ermeydan**, Etienne Cabane, Notburga Gierlinger, Joachim Koetz, Ingo Burgert, Improvement of wood material properties via in-situ polymerization of styrene into tosylated cell walls, RSC Advances, **2014**, 4, 12981-12988.

3- **Mahmut Ali Ermeydan**, Etienne Cabane, Admir Masic, Joachim Koetz, Ingo Burgert, Flavonoid Insertion into Cell Walls Improves Wood Properties, ACS Applied Materials and Interfaces, **2012**, 4 (11), pp 5782–5789 (*Cover Article*).

4- **Mahmut Ali Ermeydan**, Fabienne Dumoulin, Tamara V. Basova, Denis Bouchu, Vefa Ahsen and Dominique Lafont, Amphiphilic carbohydrate-phthalocyanine conjugates obtained by glycosylation or by azide-alkyne click reaction, New Journal of Chemistry, **2010**, 34, 1153–1162.

5- Yunus Zorlu, **Mahmut Ali Ermeydan**, Fabienne Dumoulin, Vefa Ahsen, Huguette Savoie and Ross W. Boyle, Glycerol and galactose substituted zinc phthalocyanines. Synthesis and photo dynamicactivity, Photochem. Photobiol. Sci., **2009**, 8, 312.

6- Ufuk Kumru, **Mahmut Ali Ermeydan**, Fabienne Dumoulin and Vefa Ahsen, Amphiphilic galactosylated phthalocyanines, J. Porphyrins Phthalocyanines **2008**, 12, 1090-1095.

Erklärung

Hiermit erkläre ich, dass ich die vorliegende Arbeit selbständig und unter Verwendung keiner anderen als den von mir angegebenen Quellen und Hilfsmitteln verfasst habe.

Ferner erkläre ich, dass ich bisher weder an der Universität Potsdam noch anderweitig versucht habe, eine Dissertation einzureichen oder mich einer Doktorprüfung zu unterziehen.

Erklärung